Development of New Flame Retardant and Heat Stabilized Polyamides

Vom Fachbereich Chemie
der Technischen Universität Darmstadt

zur Erlangung des Grades

Doctor rerum naturalium
(Dr. rer. nat.)

Dissertation

von

Dipl.-Chem. Kim Loretta Garth

Erstgutachter: Prof. Dr. Matthias Rehahn
Zweitgutachter: Prof. Dr. Rudolf Pfaendner

Darmstadt 2019

Tag der Einreichung: 16. September 2019

Tag der mündlichen Prüfung: 11. November 2019

This thesis is a result of the work carried out at the Fraunhofer LBF under the supervision of Prof. Dr. Matthias Rehahn from March 2015 to March 2018.

Acknowledgments

Zunächst möchte ich mich bei Prof. Dr. Matthias Rehahn dafür bedanken, dass ich meine Promotion am Fraunhofer LBF durchführen konnte.

Weiterhin bedanke ich mich bei Prof. Dr. Manfred Döring für seine gute Betreuung während dieser Arbeit und sein Vertrauen in mich, sowie seinen konstanten Antrieb.

Ein großes Dankeschön geht auch an meine Projektpartner von der BASF Dr. Roland Krämer, Dr. Michael Roth und Dr. Carsten Thomas für die hervorragende Zusammenarbeit, die produktiven Projekttreffen und guten Ideen zum Voranbringen meiner Arbeit. Bei meinen Besuchen in Ludwigshafen habe ich mich immer sehr willkommen und integriert gefühlt. Danke auch für ein immer offenes Ohr und nicht zuletzt für die Finanzierung dieser Arbeit.

Jochen Kammerer von der BASF möchte ich danken für die professionelle Verarbeitung meiner hergestellten Additive und die ausgezeichnete Dokumentation von Versuchsdaten.

Meinem Tischnachbarn Dr. Michael Ciesielski vom Fraunhofer LBF möchte ich danken für seine fachliche Kompetenz und seine vielen hilfreichen Tipps und Tricks im Labor, durch die meine Arbeit weiter voran gebracht wurden.

Auch bedanken möchte ich mich bei Lara Greiner vom Fraunhofer LBF für die gewissenhafte Durchführung meiner Pyrolyse-GC/MS Messungen.

Natürlich möchte ich mich auch bei meinen anderen Kollegen vom Fraunhofer LBF bedanken für die vielen fachlichen und persönlichen Gespräche, die lustigen und entspannten Pausen und die zahlreichen Erinnerungen. Explizit möchte ich hier Christian Schmidt, Jens Reuter und Jacob Sag nennen für alle Kaffeepausen, die spaßigen und aufbauenden Gespräche und ihre tatkräftige Unterstützung bei anfallenden Arbeiten. Die Zeit am Fraunhofer LBF hat mir sehr gut gefallen und ich werde viele meiner Kollegen vermissen.

Zuletzt möchte ich mich natürlich noch bei meiner Familie bedanken, die mich während meines gesamten Studiums und meiner Promotionszeit immer unterstützt haben, wo es nur ging. Sei es finanziell oder emotional, ich wurde immer aufgefangen.

In the frame of this work, the following publications and scientific contributions were produced:

Publications:

G. Kim, K. Christoph, F. Olaf and D. Manfred, Synthesis of a new phosphorylated ethylamine, thereon based phosphonamidates and their application as flame retardants, *Heteroatom Chemistry*, 2017, 28, e21407.

Kim Garth, Manfred Döring, Roland Kraemer, Michael Roth, Carsten Thomas, Novel phospinate-containing zinc polyacrylate and its utilization as flame retardant for polyamides, *Journal of Applied Polymer Science*, 2019, 136, 47586.

Poster:

K. Garth, C. Klinkowski, B. Burk and M. Döring, Phosphorylated Ethylamine and Thereon Based Flame Retardants, *15th European Meeting on Fire Retardancy and Protection of Materials*, Germany, Berlin, 2015.

Table of Contents

Table of Abbreviations

$(PhO)_2PO$	diphenyl phosphite
AHP	aluminum hypophosphite
AIBN	Azobisisobutyronitrile
APCI	atmospheric pressure chemical ionization
APP	ammonium polyphosphate
Bis-MPA	2,2-*bis*(hydroxymethyl)propionic acid
br	broad
calcd.	calculated
conc.	concentrated
d	duplet
DBF	Dibenzofuran
DBU	1,8-diazabicyclo[5,4,0]undec-7-ene
DCM	dichloromethane
DMAc	*N*,*N*-Dimethylacetamide
DOP-Cl	6-Chloro-6H-dibenzo[c,e][1,2]oxaphosphinine
DOPO	9,10-dihydro-9-oxa-10-phospha-phenanthrene-10-oxide
DPE	dipentaerythritol
DSC	Differential scanning calorimetry
E&E	Electrical and electronics
EI	electron ionization
ESI	electrospray ionization
EWG	Electron-withdrawing group
FR	flame retardant
HCl	Hydrochloric acid
HMF	5-hydroxymethylfurfural
LDA	Lithium diisopropylamide
LOI	limiting oxygen index
m	medium (IR), multiplet (NMR)
MALDI-TOF	matrix-assisted laser desorption/ionization time-of-flight mass spectrometry
MPP	melamine polyphosphate
MS	mass spectrometry
n.c.	not classified
NCS	*N*-chlorosuccinimide
OHV	Hydroxyl value

PA	Polyamide
PBT	persistent, bioaccumulative and toxic
PE	Pentaerythritol
PET	Polyethylene terephthalate
Ph_2PO	diphenylphosphine oxide
p-TSA	*p*-toluenesulfonic acid
PVC	Poly(vinyl chloride)
py-GC/MS	pyrolysis - gas chromatography/mass spectroscopy
q	quartet
s	singlet
sat.	saturated
sol.	solution
SPDCP	3,9-dichloro-2,4,8,10-tetraoxa-3,9-diphosphaspiro[5,5]undecane 3,9-dioxide
st	strong
t	triplet
t_1	First afterburn time
t_2	Second afterburn time
T_g	Glass transition temperature
TGA	Thermogravimetric analysis
THF	Tetrahydrofuran
T_m	Melting point
TMP	Trimethylolpropane
VN	viscosity number
w	weak
ZDA	zinc diacrylate

Abstract

This work is concerned with the synthesis and application of novel polymeric flame retardants for polyamides based on phosphorus functionalities. The flame retardants are primarily formed using the reactive P–H bond to form monomers that then can be polymerized. One promising approach was the Phospha-Michael addition of 9,10-dihydro-9-oxa-10-phospha-phenanthrene-10-oxide (DOPO) with zinc diacrylate in order to combine different flame retardancy mechanisms. A polymer and a low-molecular weight complex were synthesized for comparison. Interestingly, the phosphorus moiety, which usually acts in a gas-phase mechanism in the case of DOPO, acted mainly in the condensed phase for the resulting substances. Both products were incorporated into polyamides in varying concentrations and with different synergists. A drop in melt viscosity during compounding was observed and the effect was investigated. The flame retardant properties of the tested materials were a V-2 rating due to dripping and thus not sufficient except for one sample for which a UL94 V-1 rating was reached.

In a second topic, this work deals with the combination of heat stabilization with flame retardancy in a one-molecule approach. Three different tactics were pursued. First, phosphorylated polyols (P-Polyols) were generated. Therefore, different phosphorus-containing diols were synthesized as precursors and then fused with polyols in a solvent-free melt reaction. The produced P-Polyols where incorporated into polyamides as a flame retardant synergist in different concentrations together with diethyl phosphinate aluminum (DEPAL) in order to find a concentration at which some amount of DEPAL can be replaced with the new flame retardant/heat stabilizer combination. Also, the heat stabilization effect in polyamide was tested for one of the P-Polyols in comparison with a phosphorus-free reference polyol. The results showed that the new P-Polyol works as a heat stabilizer but is not as efficient as the reference. Also, it was found that both the reference and the self-synthesized substance only work in glass fiber-reinforced polyamide. However, P-Polyols seem to be a promising approach.

Another tactic for the combination of heat stabilizer and flame retardant was the copolymerization of different hydroxyl- and phosphorus-containing acrylates and acrylamides. A variety of homopolymers and copolymers were synthesized and compared with respect to thermal stability and residue. It was expected that a higher amount of residue will lead to better heat stability. To test the feasibility of this approach, two non-phosphorus-containing polyacrylamides with different amounts of hydroxyl units were incorporated into polyamide 6 and were tested for heat stabilization. Both polymers showed insufficient stabilization behavior and thus this approach was not pursued further.

As a last approach the Pudovik reaction of DOPO with the bio-based aldehydes acrolein and hydroxymethylfurfural was conducted. This reaction generated α-hydroxyphosphinates with which polymerization via radical polymerization and polycondensation was attempted. However, neither polymerization was successful. Different functionalizations were performed on the DOPO-acrolein adduct in order to make it stable enough to incorporate in polyamides as a flame retardant. However, non of these functionizations yielded a sufficiently thermally stable product.

Zusammenfassung

Diese Arbeit beschäftigt sich mit der Synthese und Anwendung neuer, polymerer Flammschutzmittel für Polyamide auf der Basis von Phosphoreinheiten. Es wurden hauptsächlich Phosphoreinheiten mit einer reaktiven P–H-Bindung genutzt um Monomere zu formen, die dann polymerisiert werden können. In einem vielversprechenden Ansatz wurde die Phospha-Michael Addition von 9,10-Dihydro-9-oxa-10-phospha-phenanthren-10-oxid (DOPO) an Zinkdiacrylat durchgeführt um verschiedene Flammschutzmechanismen miteinander zu verbinden. Auf dieser Reaktion basierend wurden ein Polymer und ein niedermolekularer Komplex als Vergleich dargestellt. Interessanterweise wirkt die Phosphoreinheit in dieser chemischen Umgebung als Flammschutzmittel hauptsächlich in der Festphase, obwohl DOPO sich normalerweise eher gasphasenaktiv verhält. Beide Produkte wurden mit unterschiedlichen Konzentrationen und Synergisten in Polyamide eingearbeitet. Währenddessen kam es zu einem Abfall der Schmelzeviskosität, welcher weitergehend untersucht wurde. Die Flammschutzeigenschaften der erstellten Compounds waren wegen Abtropfen mit einer V-2 Wertung nicht ausreichend bis auf eine Probe, welche eine UL94 V-1 Wertung erreichte.

Als zweites Thema behandelt diese Arbeit die Kombination von Flammschutzmittel und Hitzestabilisator in einem Molekül. Es wurde nach drei verschiedenen Ansätzen verfahren. Als Erstes wurden phosphorylierte Polyole (P-Polyole) hergestellt, wofür zunächst verschiedene phosphorhaltige Diole synthetisiert wurden, die anschließend mit verschiedenen Poylolen in lösungsmittelfreien Schmelzereaktionen zusammengeführt wurden. Die so dargestellten P-Polyole wurden daraufhin als Flammschutzsynergist in verschiedenen Konzentrationen zusammen mit Aluminiumdiethylphosphinat (DEPAL) in Polyamide eingearbeitet, um eine Konzentration zu finden, bei der eine gewisse Menge DEPAL durch die neue Flammschutzmittel/Hitzestabilisatorkombination ersetzt werden kann. Auch wurde die Wirksamkeit als Hitzestabilisator für Eines der P-Polyole im Vergleich mit einem Referenzpolyol ohne Phosphor getestet. Dabei stellte sich heraus, dass das neue P-Polyol zwar als Hitzestabilisator wirkt, allerdings nicht so effektiv ist wie die Referenzsubstanz. Außerdem wurde festgestellt, dass sowohl die selbst hergestellte Substanz, als auch die Referenz nur in glasfaserverstärktem Polyamid als Hitzestabilisator wirken. Trotz alledem scheinen die P-Polyole einen vielversprechenden Ansatz zu geben.

Ein weiterer Ansatz zur Kombination von Flammschutzmitteln und Hitzestabilisatoren war die Copolymerisation von verschiedenen hydroxyl- und phosphorhaltigen Acrylaten und Acrylamiden. Mehrere Homo- und Copolymere wurden synthetisiert und ihre thermische Stabilität sowie der verbleibende Rückstand untereinander verglichen, da für eine höhere Rückstandsmenge eine bessere Hitzestabilisierung erwartet wurde. Um die Wirksamkeit dieses Ansatzes zu prüfen, wurden dann zunächst zwei phosphorfreie Polyacrylamide mit unterschiedlicher Hydroxylanzahl in Polyamid 6 eingearbeitet und auf ihre Hitzestabilisierung getestet. Beide Polyacrylamide zeigten unzureichende Stabilisierungseigenschaften, weswegen dieser Ansatz nicht weiter verfolgt wurde.

Zuletzt wurde noch die Pudovik Reaktion von DOPO mit den biobasierten Aldehyden Acrolein und Hydroxymethylfurfural durchgeführt. Durch diese Reaktion wurden α-Hydroxyphosphinate generiert, welche dann versucht wurden mittels radikaler Polymerisation bzw. Polykondensation zu polymerisieren. In beiden Fällen funktionierten die Polymerisationen nicht, weshalb daraufhin die weiteren vorhandenen funktionellen Gruppen des DOPO-Acrolein Addukts genutzt wurden um Flammschutzmittel zu produzieren, die thermisch stabil genug für die Einarbeitung in Polyamide sind. Diese Funktionalisierungen führten allerdings nicht zu der gewünschten Stabilität.

1. Introduction

Today polymer materials surround us everywhere in our daily life. They are used excessively due to their tunable properties that can provide the right tool for nearly every situation, which is why the plastics market continues growing. An important class of polymers is engineering plastics that are used for special applications, where superior mechanical and/or thermal properties are required, compared to the more cost-efficient commodity plastics, like polypropylene or polystyrene. One type of engineering plastic is polyamide (PA). Due to their excellent overall properties, PAs can be used for a lot of different applications. In 2006, PA 6 and 66 possessed 33 % of the global demand of engineering plastics, which corresponds to 2.6 million t (Figure 1),[1] while until 2015 the global production nearly tripled to over 7 million t.[2]

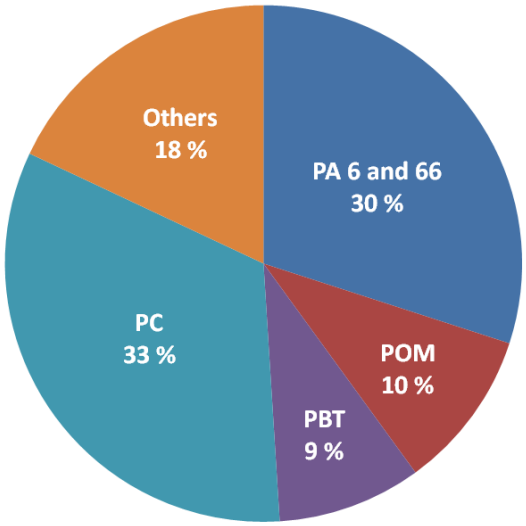

Figure 1: Global demand of engineering plastics in 2006.[1] POM: Polyoxymethylene; PBT: Polybutylene terephthalate; PC: Polycarbonate.

The main usage of PAs is as fibers or films, but in 2015 46 % of the worldwide consumption of PA 6 and 66 were used for PA compounds as well.[2] In Europe, PAs are mostly applied in the automotive sector (38 %),[2] what is due to a reduction of weight compared to metal and thus a reduction in fuel demand.[3] But the electrical and electronics (E&E) industry also seizes a large part with 21 % (Figure 2).[2]

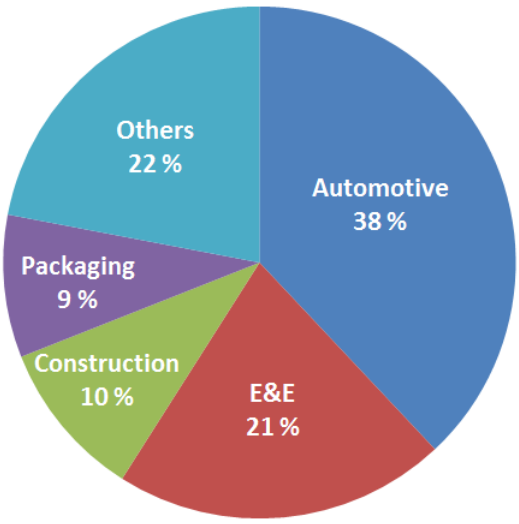

Figure 2: Demand of polyamide for different industrial sectors in Europe in 2014.[2]

Despite their excellent properties, most polymers are based on carbon and hydrogen and are thus easily flammable. Fires are still a major threat not only for the personal life but mainly in a financial matter. In 2015, there were 343 fire related deaths in Germany and a financial damage of 1.295 billion euros was caused.[4, 5] Flame retardants (FRs) can enhance the time for humans to escape and fire fighters to arrive by a crucial margin and thus significantly lower the risk for life and property. In the best possible scenario they should be able to induce an extinguishing behavior so that the fire is stopped completely. The main reasons for fire hazards in Germany in 2017 are summarized in Figure 3.[6]

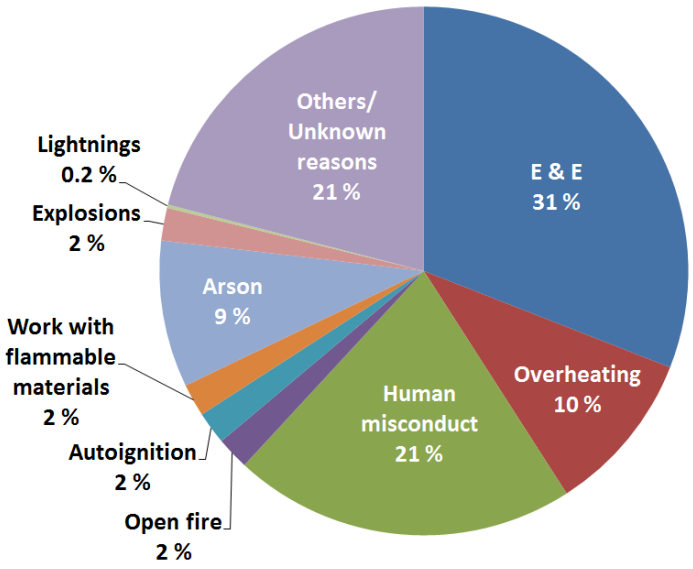

Figure 3: Reasons for fires in Germany in 2017.[6]

As can be seen, the main sector, where fires are a threat, is the E&E industry. Since PAs are often used for E&E applications, it is highly necessary to develop fame-protected solutions for this specific purpose. One possibility to do so is the utilization of halogenated FRs, like decabromodiphenyl ether in combination with antimony oxide.[7] However, halogen-containing FRs are more and more undesired or even banned by the European chemical regulation REACH (**R**egistration, **E**valuation, **A**uthorization and restriction of **CH**emicals) due to toxicity and environmental issues.[8-10] Firstly, molecular halogenated flame retardants, like brominated biphenyls or diphenylether, are often **p**ersistent, **b**ioaccumalative and **t**oxic (PBT). Secondly, they are able to form toxic decomposition products through thermal degradation. Alongside inorganic substances, like aluminum or magnesium hydroxide, phosphorus-containing FRs often offer an environmentally friendly alternative and thus are of great interest for research and application.[11-16]

Another criterion that especially PAs have to fulfill is a high heat resistance. Since they are often applied in the automotive sector, e.g. in under-the-hood applications, they need to be able to endure high temperatures over a long period of time. The thermo-oxidative degradation proceeds via oxygen induced radical processes. Therefore, so-called heat stabilizers have to be applied that can protect the polymer over time. Often, special antioxidants as for example copper halides are utilized.[17] However, to expand the application areas it is interesting to develop new heat stabilizers for specific needs. Also, in industries there is always a demand for more efficient or environmentally-friendly alternatives.

2. Background

2.1. Polyamides

Polyamide (PA) is an essential class of polymers. They are named after the amide bonds in their backbone that are majorly responsible for their good properties regarding mechanical and thermal properties due to an ordered chemical structure.[18, 19] There are aliphatic, aromatic (Aramids) and semi-aromatic PAs, depending on the carbonaceous units of the main chain, and they are usually linear thermoplastics.[18] Since the most applied PAs are aliphatic nylons, this work will focus on them. There are two different structures of PAs, the so-called AB-PA and the AABB-PA depending on their monomer composition.[19] Their general structures can be seen in Figure 4.

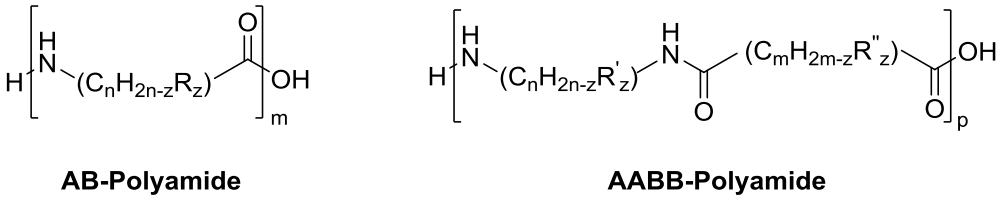

Figure 4: General structures of the AB- and the AABB-PA.

The most important representatives of these types are PA 6 and PA 66. The numbers correspond to the number of carbon atoms of the respective monomer unit in the main chain, whereas for the AABB-PA the diamine is taken into account first, followed by the diacid. PA 66, synthesized from adipic acid and hexamethylenediamine, was invented by Carothers of DuPont in 1935.[20, 21] Inspired by the research of Carothers, Schlack of IG Farben then patented PA 6 in 1938, which is based on ε-caprolactam.[21, 22] Since the two PAs are based on different synthesis methods, the two separate patents were even possible.

Initially, Carothers synthesized AABB-PAs via step-growth polycondensation of diamines and diacids (Figure 5).[23]

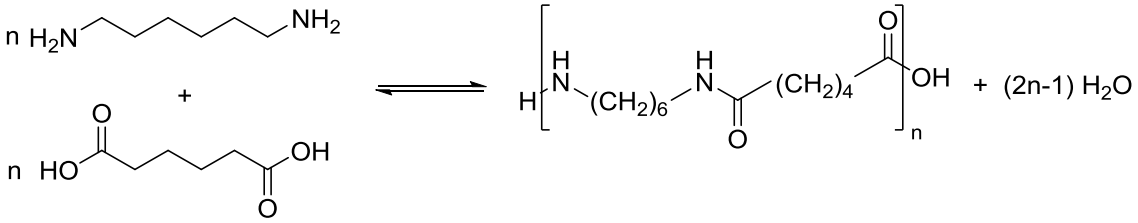

Figure 5: Polycondensation of adipic acid and hexamethylenediamine towards PA 66. [23]

As is typical for a step-growth polymerization, the key for reaching high molecular weights and conversion is the stoichiometric application of the individual monomers. Therefore, industrially later on the AABB-PAs were generated from aqueous solutions of their salts under high pressure and a temperature beyond the melting point of the synthesized polyamide for immediate processing. In the case of PA 66, the so-called “Nylon salt” hexamethylene diammonium adipate (Figure 6) is utilized.[24-27] This has the merit that a stoichiometry of 1:1 is automatically applied.

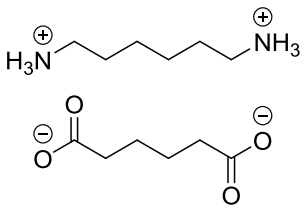

Figure 6: The “Nylon salt” hexamethylene diammonium adipate.

Another way to avoid stoichiometric weighing is the Schotten-Baumann reaction, which is conducted on the boundary surface of an aqueous diamine solution and the acid chloride of the diacid in carbon tetrachloride.[27] The polymer is removed from the boundary surface so that fresh monomers can diffuse to the surface and the stoichiometry is guaranteed.[27] This method is applied industrially if the monomers are decomposing below the melting temperature of the polymer.[28]

The AB-PAs are usually synthesized via ring-opening polymerization of the corresponding lactams, which in contrast to the polymerization for the AABB-type is a chain-growth reaction. As mentioned earlier, ε-caprolactam is used as monomer for PA 6. In a continuous procedure, the monomer and small amounts of water (0.3 –5 %) are heated to 240 °C.[27] The water will hydrolytically open the ring of the caprolactam and thus start the chain reaction (Figure 7). The molten polymer is gained as product that can be purified by the removal of residual monomers via vacuum.

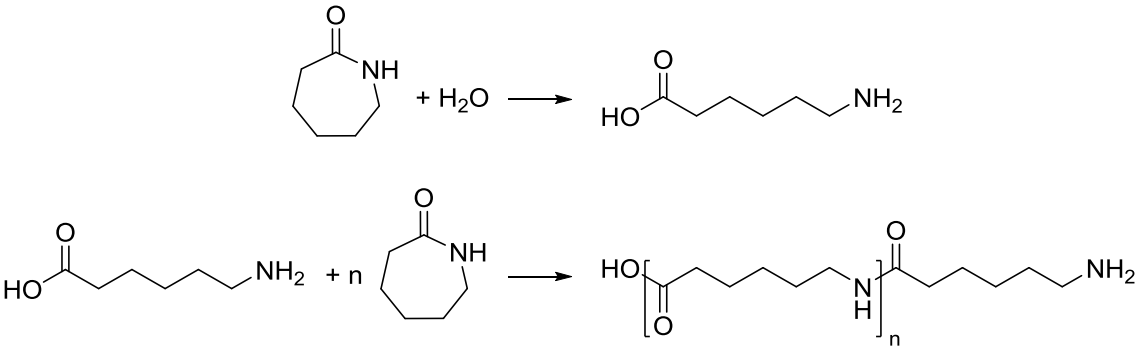

Figure 7: Hydrolytically chain-growth polymerization of ε-caprolactam towards PA 6.[27]

The reaction can also be initiated by bases for an anionic ring-opening polymerization that works at 120 °C and only takes a few minutes to form a polymer in an exothermal reaction and thus is mainly used for mold casting processes.[27] The initiation step of this process is shown in Figure 8.[27] It can be accelerated by the addition of acid chlorides, anhydrides or isocyanates.[27]

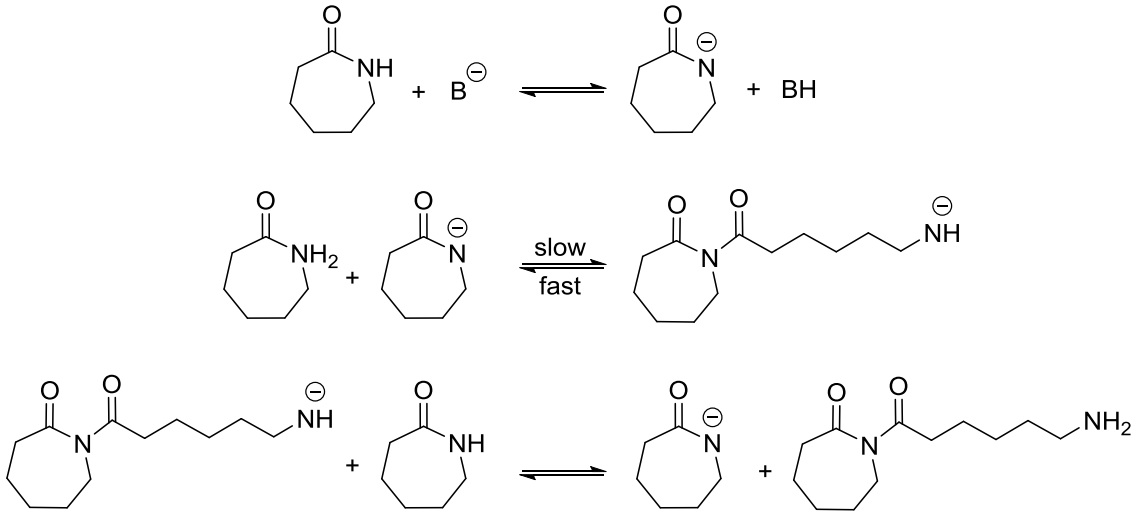

Figure 8: Initiation step of the base (B) catalyzed ring-opening polymerization of ε-caprolactam.[27]

The properties of PAs are mostly determined by their amide bonds. Like most engineering polymers, they possess amorphous regions, though due hydrogen bonding of the amide groups ordered regions of crystallinity appear (Figure 9). These crystalline regions, which is corresponding to the amide frequency of the main chain, do have a high influence on the melting point (T_m) of the semi-crystalline polymers as can be seen in Table 1.[18] The T_m of PA 66 is significantly higher than the one of PA 6 due to a center of symmetry for the AABB-type compared to the AB-type. This makes

hydrogen bonding between the chains easier leading to more crystalline domains and thus resulting in a higher T_m.[3] Overall, the melting temperatures of PAs are quite high making them interesting for high-temperature applications.

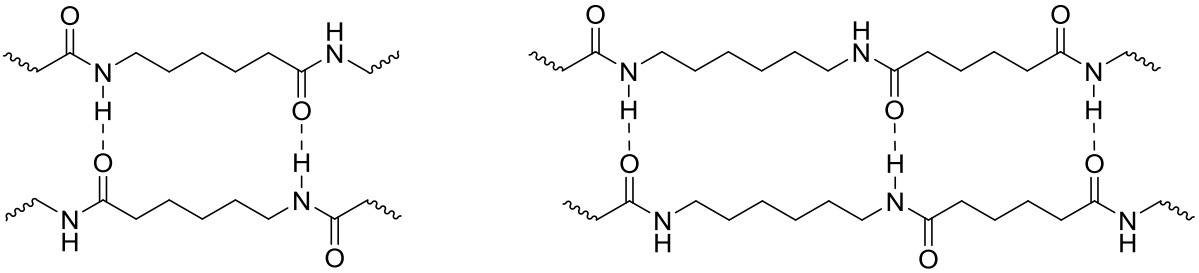

Figure 9: Hydrogen bonding in the crystalline regions of PA 6 and PA 66.

Table 1: Melting points (T_m) of different polyamides in correlation with the amide bond frequency of the main chain.[18]

Polyamide	Amide frequency / %	T_m / °C
PA 6	14.3	225
PA 11	8.3	183
PA 12	7.7	180
PA 22	4.3	145
PA 66	14.3	265
PA 46	16.7	295[29]
PA 86	12.5	250[29]
PA 612	10.0	212[3]

Although the amide bonds also help to immobilize the chain in the amorphous regions, the glass transition temperature (T_g) is not heavily influenced by the amide frequency, leading to a T_g in the range of 40-50 °C for AB-PAs and 40-80 °C for the AABB-type.[18]

The crystalline domains also help for their solubility behavior making PAs fairly resistant against typical organic solvents as well as oils or fats.[19] However, the higher the amide frequency the higher is also the water absorption what causes a variation of their physical properties and potential hydrolysis during compounding.[3, 19] For PA 6 and PA 66 the water absorption is at 10 and 8.5 %, while it is only 1.5 and 2.7 % for PA 12 and PA 612, respectively.[19] Nylons can be used as electrical insulators, however, the water absorption can affect these properties, so they are not suited for every application.[3] The mechanical properties are also reliant on the crystalline domains as well as on the water content during measurement. The higher their amide frequency and the crystallinity, the higher is also their tensile strength as well as their E-modulus, but the impact strength and elongation is decreased.[3, 19] However, water absorbance does change these values considerably due to a reduced T_g.[3, 19] Often, PAs are filled with reinforcing agents such as glass fibers to enhance their mechanical properties for specific applications. These fillers do increase stiffness and strength considerably but make the PA more brittle. Anyways, the mechanical integrity of these compounds persists almost up to the melting point of the specific PA.[3]

2.2. Thermal Degradation an Combustion Behavior of Polyamides

The thermal degradation of PA 6 is mostly based on chain scission at the relatively weak C–N bonds. This can be either the C(O)–NH amide bond or the *N*-alkylamide bond leading to different volatile products (Figure 10).

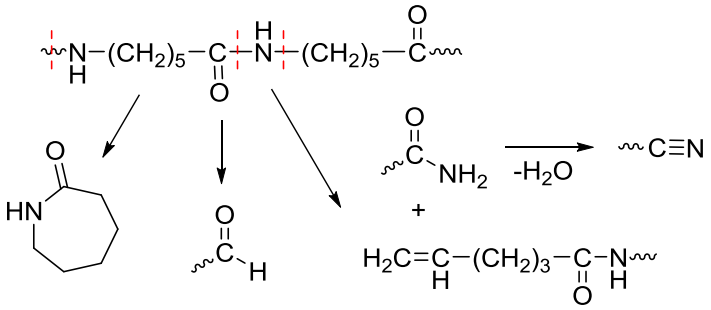

Figure 10: Various thermal scission processes of PA 6.[30, 31]

The main decomposition product found by coupled pyrolysis - gas chromatography/mass spectroscopy (py-GC/MS) is ε-caprolactam.[31] At lower temperatures, the amide bond seems to be the weak point, especially in the presence of water, while at higher temperatures the scission of the *N*-alkylamide bond or β-CH_2–CH_2 bonds is also possible. The so produced fragments can further decompose to yield various minor gaseous hydrocarbons, CO, CO_2, water and NH_3.[32] The organic gaseous products deliver the fuel for keeping the flame alive. At 550 °C, a stable char of about 5 wt% remains that can be accounted to crosslinked and branched structures generated by reactions of carboxylic acid or amine end groups with CO or NH functionalities (Figure 11).[30, 33] Also, via IR-spectroscopy nitrile and vinyl groups were found in the remaining char.[33]

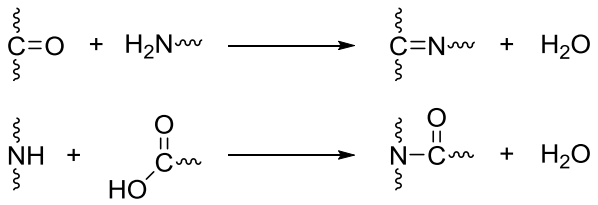

Figure 11: Thermal crosslinking of PA 6.[30]

For PA 66 there are many different opinions about the main bond scission reaction in research. Steppan *et al.* gave a brief overview of possible reactions.[34] What can be agreed on is that the main gaseous decomposition products are CO_2, H_2O and NH_3. Cyclopentanone seems to be developed as a terminal group in the process either under scission of the amide bond or as a cyclization of the chain-end (Figure 12).[30, 35] The cyclopentanone group can then evolve either as a gaseous product under CO_2 elimination or be transformed to an imine which can happen inter- or intramolecular (Figure 13).[36, 37]

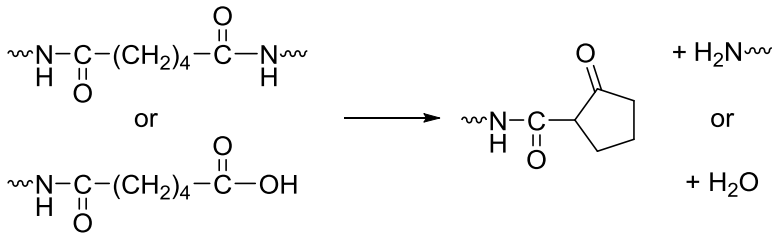

Figure 12: Generation of a cyclopentanone end group in PA 66.[30, 35]

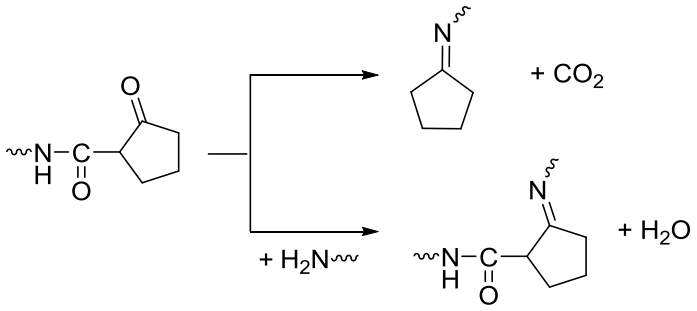

Figure 13: Intra- and intermolecular imine transformation.[36, 37]

Similar to PA 6 (Figure 10, right path) nitriles and vinyl chain ends can emerge during decomposition and also carbodiimides are present due to isocyanates (Figure 14).[35]

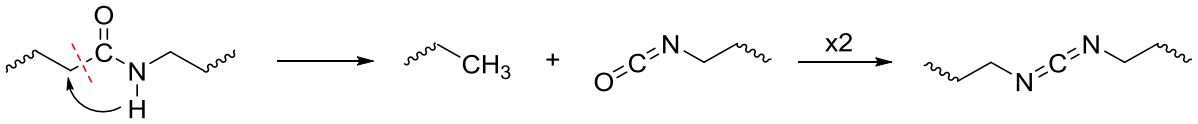

Figure 14: Isocyanate and carbodiimide generation.[35]

For PA 66 a char yield of 8 wt% is gained at 550 °C.[35] Gelation can occur via different mechanisms, either analog to PA 6 (Figure 11)[38], over the formed imine end groups[36] or through the isocyanate groups[35].

Both PA 6 and 66 are highly flammable above their decomposition temperatures of 350 °C[39, 40] (measured in inert atmosphere and air), respectively, due to the release of volatile organic fragments during decomposition. The condensed phase of the polyamide is decreasing in viscosity because of chain scission, what allows the formed melt to drip burning droplets, if possible.[41] Often, this dripping leads to extinguishing of the bulk material but it can cause a new source of fire at the landing site of the droplet.[41]

2.3. Flame Retardancy Mechanisms

2.3.1. Gas- versus Condensed-phase Mechanism

For a steady burning process, several requirements have to be met.[42] An ignition source (flame, heat source, etc.) needs to be applied to start the process. Due to this initial heat, the burning material starts decomposing to set free vaporizable molecules. For polymers, this process is called pyrolysis. The volatiles are transported to the gas phase where they mix with oxygen to form a flammable mixture. The burning process itself produces heat energy which is again used for pyrolysis and thus a steady combustion process is established (Figure 15).

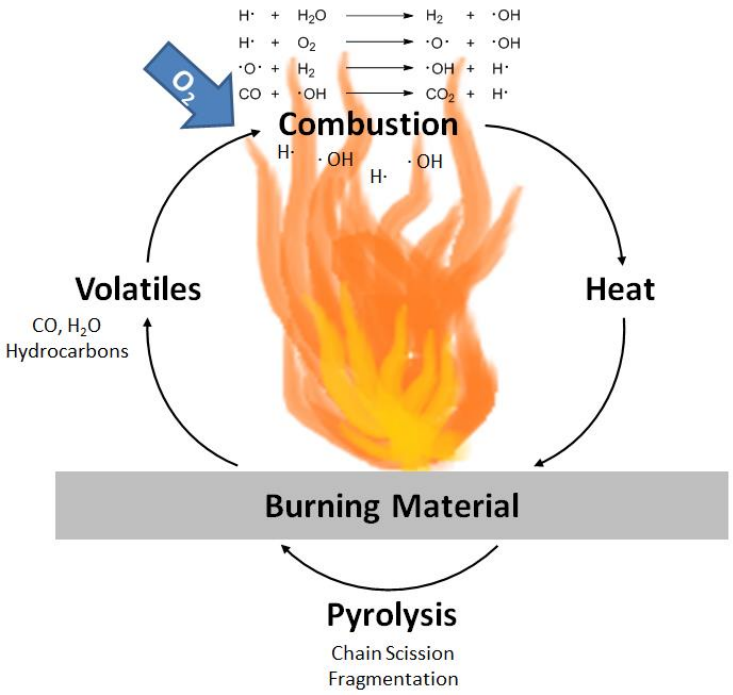

Figure 15: Scheme of the combustion process.[43]

To inhibit the fire cycle, different strategies can be chosen depending on the type and form of burning polymer and the application. Deployed flame retardants can either act in condensed or in gas phase or even in a combination thereof. During combustion, exothermic reactions take place that keep the burning process going (Figure 16).[43, 44] Highly reactive ·H- and ·OH-radicals are being produced that can react with hydrocarbons and volatile fragments, such as CO.[43, 44] The carbon radicals are being oxidized towards CO_2 in radical chain reactions whereas the reaction of CO with a hydroxyl radical generates the most heat energy and reproduces a hydrogen radical.[43, 44]

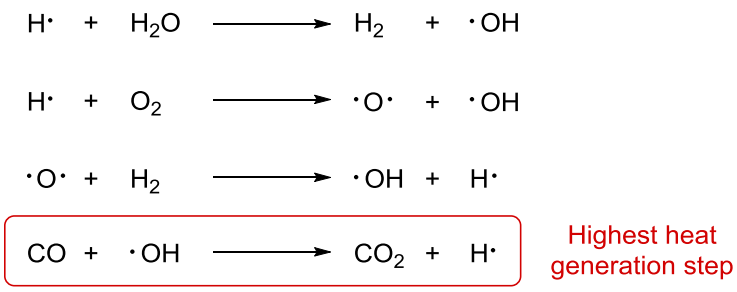

Figure 16: Selection of different radical reactions proceeding in the flame.[43, 44]

Gas-phase activity is based on the inhibition of these radical reactions due to radical scavenging. The reactive species ·H and ·OH are replaced by less reactive radicals. Halogen-containing FRs usually proceed via gas-phase mechanism. They set free hydrogen halides which then allow a radical transfer from the ·H- or ·OH-radicals towards the less reactive halogen radical (Figure 17).[45] Metal oxides, like MgO or SnO, can further enhance the gas-phase activity due to a radical recombination mechanism through which reactive hydrogen radicals can be recombined towards molecular hydrogen or water utilizing metal hydroxides as intermediates.[46]

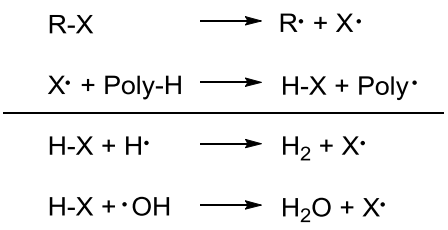

Figure 17: Gas-phase mechanism for halogen-containing FRs.[45] X: halogen atom; R: organic rest; Poly: polymer chain.

In the condensed phase there are several ways of flame retardancy mechanisms. The FRs can either interact with the polymer matrix during pyrolysis or they can act on their own. Via interaction with the matrix, the FR can promote the formation of char, which is the remaining residue after such reaction. One example of interaction with the condensed phase would be the dehydration of oxygen-containing polymers via phosphoric acids, which is further described in chapter 2.3.2.[45] Another way is the promotion of crosslinking and thus char formation during the pyrolysis. Usually, crosslinked polymers, like epoxy-resins, do produce a higher amount of char than linear ones. The newly formed covalent bonds can help to bind monomer units that occur from depolymerization during decomposition and would otherwise fuel the burning process.[45] A condensed-phase mechanism that is more based on the FRs than on the polymeric matrix is the so-called intumescence, which describes the formation of a foamy, expanded char layer that shields the remaining material from heat and oxygen. An intumescent formulation consists of three different compounds: an acid source, a char forming agent[47] and a blowing agent.[45, 48] At first, the acid source, which can be polyphosphoric acid for example, reacts with a char forming agent, like pentaerythritol, in a carbonization reaction.[48, 49] Then the blowing agent, e.g. melamine, decomposes yielding gaseous products, mostly nitrogen and NH_3 that cause the char layer to swell immensely.[45, 48, 49] The acid source and the blowing agent can be combined in one molecule by the application of polyphosphate salts, such as melamine polyphosphate (MPP).[45] It is also possible to protect polymeric material by endothermic reactions of the FR in the condensed phase because then more energy will be necessary during the pyrolysis. Inorganic FRs, like aluminum or magnesium hydroxide, often proceed via this mechanism.[45] During heating, they react towards the corresponding oxides, setting free water that is able to dilute the reactive molecules and oxygen in the gas phase.[45] However, a large amount (50-65 wt%) of these FRs usually need to be applied, what drastically changes the mechanical properties of the material.[45, 50]

Of course, FRs need to be designed based on the structure of the polymer matrix and can be combined to efficient formulations that act in both gas and condensed phase. In the following chapter, phosphorus-containing FRs will be specified as they are the main focus of this work.

2.3.2. Phosphorus-based Flame Retardants

Phosphorus-based FRs can act through various ways. In the condensed phase, they form polyphosphoric acid. Through this formation the char yield can be enhanced via dehydration of hydroxyl groups and even intumescent layers can be formed with the right additive mixture. In gas phase, they act through radical scavenging of the more reactive hydroxyl and hydrogen radicals. They can also combine gas- and condensed-phase mechanisms. Which way is chosen, is not only dependent on the P-containing additive itself but also on the chemical environment during pyrolysis and thus on the polymer matrix and other additives and synergists.[51, 52] An overview over some important reactions is given in Figure 18.

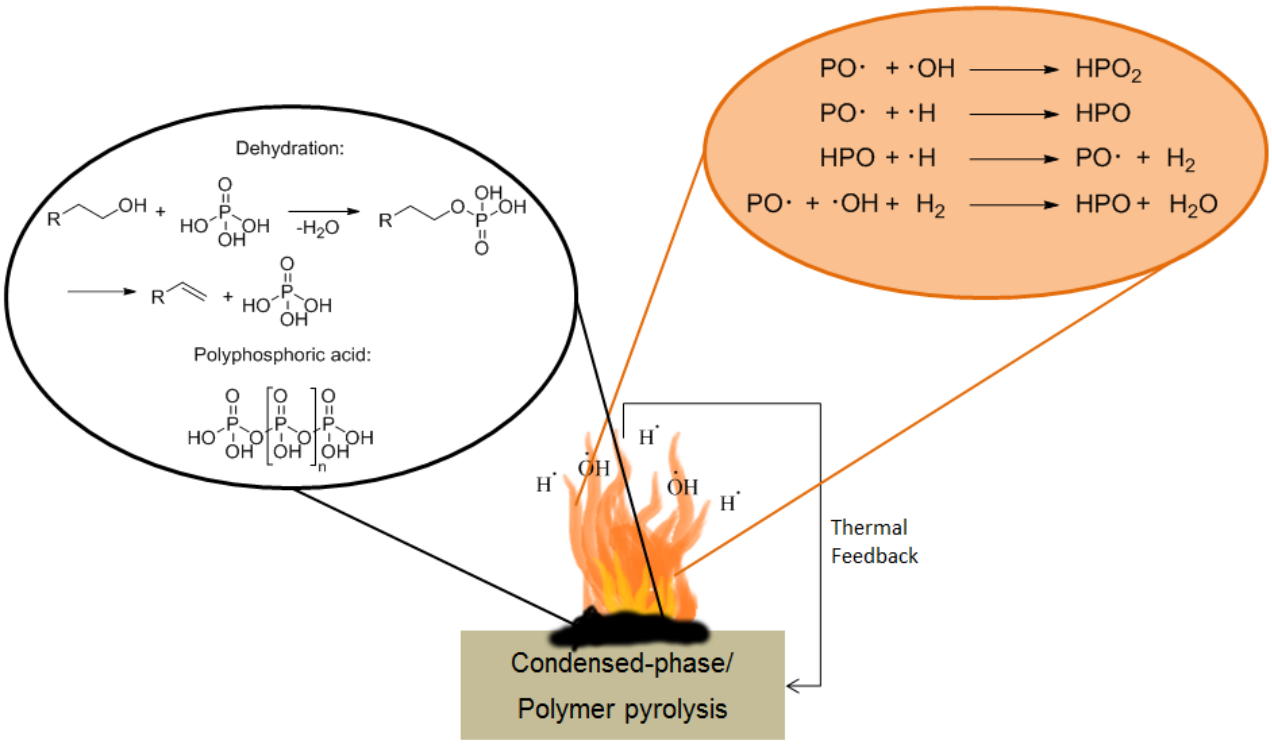

Figure 18: Flame retardant reactions of phosphorus-containing compounds in condensed and gas phase.

Their condensed-phase mechanism tends to have a higher efficiency in oxygen-containing polymers because they have a high susceptibility to dehydration. Due to this dehydration, a protective char layer is formed that protects the polymer from oxidation and acts as physical and heat barrier.[45, 53-55] This layer is promoted by the formation of polyphosphoric acid that acts like a coating on the char.[55] If the polymer does not possess any hydroxyl functionalities, a char forming agent, like a polyol such as pentaerythritol (PE), can be added. If additionally a blowing agent, like melamine, is applied, phosphorus systems can also create intumescent layers that protect the polymer in a better way.[48, 53, 55] As a rule of the thumb it can be said that whether a condensed- or gas-phase mechanism is preferably conducted is depending on the chemical environment around the phosphorus atom. A condensed-phase mechanism is preferred in an oxygen-rich environment, while in a carbon-rich environment the gas-phase mechanism is favored. Thus, phosphates are dominantly acting in a condensed-phase mechanism.[51]

In gas phase, phosphorus-containing FRs act in a very similar way to halogen-containing ones through radical scavenging. The highly reactive hydroxyl- and hydrogen-radicals are trapped by less reactive species, like PO·, HPO_2, PO_2· or HPO, which can be identified via pyrolysis gas chromatography coupled with mass spectrometry.[53, 54, 56] PO radicals can especially effectively undermine the branching reaction of H· + O_2 → ·OH + ·O· by radical combination reactions, as can be seen in Figure 18, and thus the PO radical is considered to be the most important species.[55] Due to their carbon-rich environment, phosphine oxides are more likely to react in a gas-phase mechanism.[51]

There are several phosphorus-based FRs for PAs. A few often used are shown in Figure 19. The most efficient is red phosphorus, an allotrope of elemental phosphorus. Between 6 and 9 wt% are sufficient in glass fiber (GF)-reinforced and non-reinforced PA 66 due to the high phosphorus content.[57] Since it can generate toxic phosphine and it is flammable in its powdered form, it should be stabilized prior compounding by coating or preformulation into a masterbatch.[7] Despite its effectiveness, the red color of the finished compounds and the hazards during handling of the pure phosphorus limits its usage to certain applications.[7] In polyamides it acts in condensed phase, where it is oxidized to phosphoric acid leading to the formation of polyphosphoric acid.[47, 58]

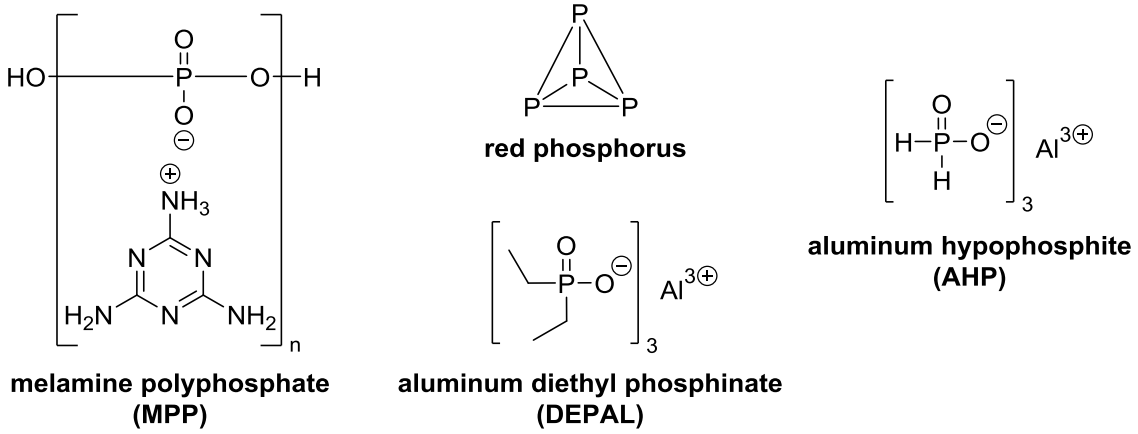

Figure 19: Structures of some phosphorous FRs for aliphatic PAs.

Another often used FR is MPP. It acts via condensed-phase mechanism in an intumescent fashion by carbonification with useful matrices.[59] Also it releases melamine into the gas phase, if applied in PAs.[59] However, loadings of more than 20 wt% in GF-reinforced nylons need to be added if MPP is applied alone and only with over 25 wt% good flame retardancy is reached.[59, 60] To lower the overall amount of FR needed, MPP can be applied in synergistic mixtures.[59, 61]

Additives that combine P-containing anions with metal ions also seem beneficial to enhance flame retardancy in different polymer systems. *Tris*-(**die**thyl **p**hosphinate) **al**uminum (DEPAL), for example, shows good flame retardant properties in different PAs.[7, 62, 63] GF-reinforced PA 6 needs 20 wt% of DEPAL, while PA 66 requires only 18 wt% for a good fire protection.[7, 64] These amounts can even be lowered in combination with nitrogen-containing synergists, like MPP or melamine cyanurate.[59, 65, 66] If DEPAL is applied in PAs without a synergist it acts mainly via gas-phase mechanism releasing phosphinic acid and vaporized DEPAL into the gas phase, that break down further into the active phosphorus species and ethane, while most of the aluminum remains in the condensed phase as aluminum phosphate.[59] In combination with MPP, DEPAL does not vaporize but diethylphosphinic acid, phosphinic acid and melamine are released into the gas phase, whereas aluminum phosphates again are being formed in the condensed phase leading to a combined gas- and condensed-phase mechanism.[59]

Aluminum hypophosphite (AHP) is another metal salt of phosphorus-containing anions that is used as FR for PAs. For non-reinforced PA 6 12 wt% have to be applied for a decent FR performance, while for GF-reinforced PA 6 the necessary amount was higher with up to 18 wt%.[67] AHP can release PH_3, formed by a disproportionation reaction, to the gas phase, which can be easily oxidized in the flame, and leaves aluminum phosphate in the condensed phase under release of water.[68, 69]

It is also possible to incorporate phosphorus units into a polymer structure that is then blended with matrix polymer for the flame retardant protection. This does prevent the FR from blooming and migration during application.[70-72] Furthermore, the mechanical properties of the matrix system are often less influenced by those polymeric additives.[71, 72] However, it is important to keep their miscibility in mind since, as is typical for polymer blends, they can suffer from phase-separation and a homogeneous mixture of the FR with the polymer is necessary for a good protection.[71, 72]

2.3.3. Characterization and Classification of Flame Retardants

There are multiple methods for the characterization of the effectiveness of FRs. Two often applied methods are the determination of the limiting oxygen index (LOI), which is the minimum concentration of oxygen in a nitrogen/oxygen mixture under which the combustion of a material is

supported, and the cone calorimetry, from which a variety of parameters, like the heat release rate or the smoke production rate, can be obtained.

For E&E applications, the most important tests are the indirect flame glow wire test, in which a wire is heated to a pre-determined temperature and is then applied to a specimen with a set force for a specified time period, and the direct flame UL94 test, in which a direct flame is applied to a test specimen in horizontal or vertical application.[73] The UL94 vertical burning test (UL94 V) test is a common method in research and industries because it allows a quick classification of the material with rather small amounts (Figure 20). The test was developed by *Underwriters Laboratories* and was adopted in Germany as DIN standard IEC/DIN EN 60695-11-10.[74] It is a standardized method in which a flame of defined energy (50 W) and height (20 mm) is applied to a test specimen, which has the dimensions 125 mm (length) x 13 mm (width). The thickness of the specimen is variable between the values 0.8, 1.6 or 3.2 mm. The burner is placed 10 mm underneath the sample for 10 s. After that period the burner is removed from the sample and the first afterburn time (t_1) until the sample extinguishes is recorded. Immediately after extinguishing, the flame is applied to the sample again for 10 s and the second afterburn time (t_2) is taken. 300 mm underneath the burner cotton wool is placed to examine if any droplets that may drip from the sample are burning. To categorize the samples, a set of five specimens should be tested. The tested material can be classified into three categories V-0, V-1 or V-2. The criteria for each class are listed in Table 2. If the specimens do not pass the test they are called “not classified” (n.c.). Non-reinforced PAs do usually already give a V-2 rating due to melt dripping of burning material which results in extinguishing of the flame.[3, 75]

Table 2: Classification criteria for the UL94 test after IEC/DIN EN 60695-11-10.

Afterburn time of one specimen (t_1/t_2)	≤ 10 s	≤ 30 s	≤ 30 s
Total afterburn time of a set of five specimens	≤ 50 s	≤ 250 s	≤ 250 s
Total afterburn time of one specimen (t_1 + t_2)	≤ 30 s	≤ 60 s	≤ 60 s
Flaming droplets allowed?	No	No	Yes
Total burning of the specimen to the holding allowed?	No	No	No
FR classification	**V-0**	**V-1**	**V-2**

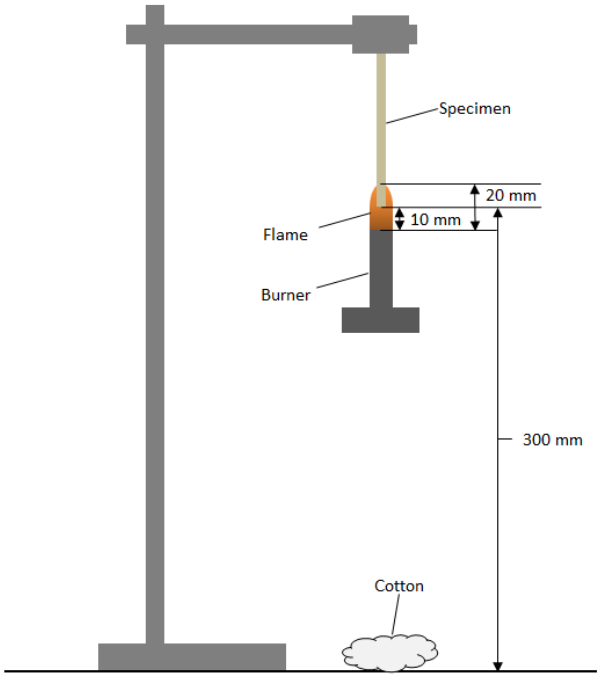

Figure 20: Schematic drawing of the UL94 V burning test.

Other important parameters about the thermal degradation of a polymer can be gained by thermogravimetric analysis (TGA). In a TGA experiment the sample is heated under nitrogen or synthetic air with a defined heating rate and its mass is recorded over the temperature. After the measurement, the amount of residue and the decomposition temperature can be determined. These are interesting parameters not only for the application of the finished compound but also for the pure FR since it should be able to withstand the compounding temperature while also start acting as FR close to the decomposition temperature of the matrix polymer.

The flame retardancy and thermal results in this work will mostly be based on TGA and UL94 V tests, since it deals with PAs that are often applied in the E&E sector (Figure 2) and E&E applications are the main reason for fires in Germany (Figure 3).

2.4. Chemistry of P–H Bond-containing Compounds

Organophosphorus compounds can be divided into different classes. The P atom in those compounds can occur tri- or tetra-coordinated with the usual oxidation states being tri- or pentavalent. Since in this work mostly tetra-coordinated phosphorus compounds with P–H bonds are applied, the focus of this chapter will be on the specific chemistry of those species. They can also be further classified by the number of P–C or P–H bonds compared to the number of P–O bonds. An overview over those classes is given in Figure 21. Depending on the number of R that equals H, phosphinates can be sub-divided into hypophosphites, if R' and R" equal H, or H-phosphinates, if only R" is a hydrogen atom.

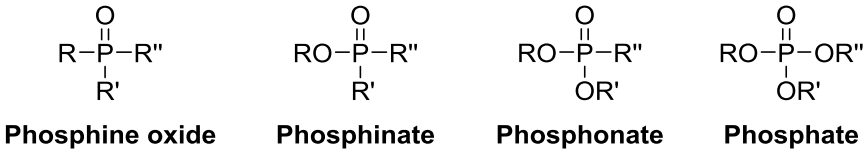

Figure 21: Classes of tetravalent organophosphorus compounds. R, R' and R'' equal organic rests or H.

The chemistry of P–H bond-containing tetra-coordinated compounds is influenced by their ability to tautomerize between its tri- and tetra-coordinated forms, what is shown exemplarily for H-phosphinates in Figure 22.[76-78] The reactivity of hypophosphites is usually higher than for H-phosphinates because the tautomerization towards **B** is hindered by the addition of donating R groups. If more electron-withdrawing groups are applied as R', the tautomeric form **B** is better stabilized. That being said though, the equilibrium is still heavily favored towards tautomer **A** for the most part. One exception is pure phosphine oxide H_3PO which is not stable under standard conditions and tautomerizes towards phosphinous acid H_2POH.[79] However, both forms disproportionate towards phosphine and hypophosphorous acid.[80]

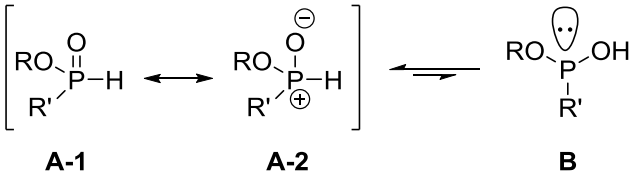

Figure 22: Tautomerization of phosphinates. R and R' equals H or any organic rest.[76]

Although the tri-coordinated species are often applied due to their high reactivity, their utilization also bears drawbacks, like their hydrolysis susceptibility and spontaneous oxidation if stored under air. This is the major advantage of the P–H moiety-containing tetravalent compounds since they are chemically stable against oxidation and are thus convenient to handle but due to their tautomerization can act as electrophilic or nucleophilic center if the right reaction conditions are applied. Owing to their tautomerization, P–H compounds do possess a slight acidity but it is rather

weak compared to the P–OH acidity of phosphoric or phosphonic acids. The grade of P–H acidity, though, is very dependent on the substituents.[81]

The ester groups of phosphinates, phosphonates and phosphates can undergo hydrolysis and transesterification. However, phosphates are relatively inert to hydrolysis unless the reaction is catalyzed.[82, 83] Both reactions are catalyzed by acids, like acetic acid, and bases, like tertiary amines or alkali alcoholates.[81, 84] Transesterification can be utilized for the generation of new compounds[85] and it can also occur without any catalyst[84] what makes it a possible side reaction for P–H compounds. The base-catalyzed mechanism of hydrolysis is suggested to proceed via the tri-coordinated species, as can be seen exemplary for H-phosphonates in Figure 23.[81, 86] The sterically hindrance of the substituents plays a critical role for the hydrolytic stability.[81, 83] Similar to carbon larger substituents can hinder nucleophiles from approaching the phosphorus atom, however, since phosphorus has a larger atom ratio than carbon this effect is not as pronounced as for substitution reactions at the carbon atom.[81] Due to this hydrolytic instability it is beneficial to carry out reactions under water-free conditions if no hydrolysis is desired.

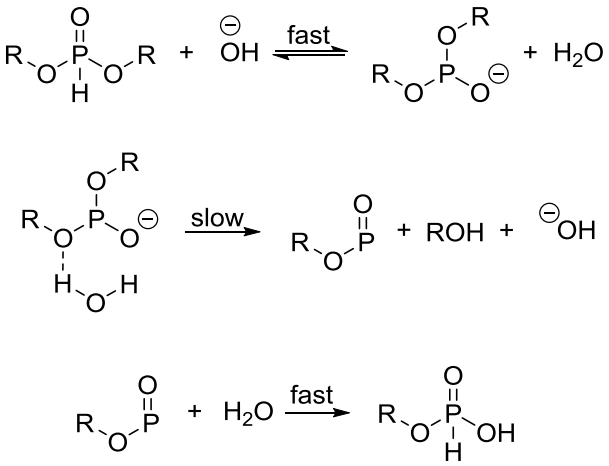

Figure 23: Base-catalyzed hydrolysis mechanism of H-phosphonates.[81, 86]

In the following four chapters some of the key reactions of tetra-coordinated P–H compounds are briefly discussed.

2.4.1. Pudovik Reaction

The Pudovik reaction is usually referred to as the addition of P–H-bond-containing moieties to carbonyl or imine bonds towards α-hydroxy- or α-aminophosphonates (Figure 24). This reaction is often base catalyzed but may even work without any catalyst.[87] Its proposed mechanism is also shown in Figure 24.

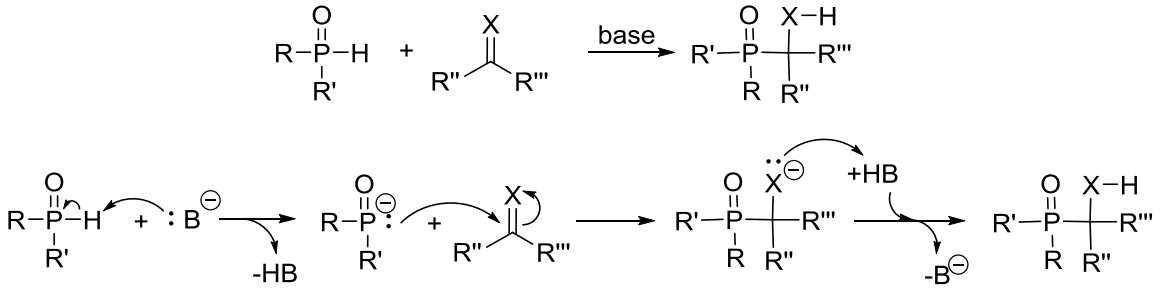

Figure 24: Scheme and mechanism of the Pudovik reaction. X stands for O or N–H. R, R′, R′′ and R′′′ may be any organic rest. B is a base.

It has the merit of yielding a functional group (N–H or O–H) that can be used in further reactions. Also, as is typical for addition reactions, it proceeds in an atom-efficient way, meaning that every atom of the starting compounds is used to form the new product and thus no by-products are generated. The Kabachnik-Fields reaction uses the Pudovik reaction as key step. It is a multicomponent reaction of a P–H compound with a carbonyl and an amine towards α-aminophophonates. Depending on the different substrates it can either first form an imine from the carbonyl and the imine compound, which then reacts with the P–H compound in a Pudovik reaction, or the P–H compound first reacts with the carbonyl in a Pudovik reaction and then with the amine.[88]

2.4.2. Phospha-Michael Addition

The Phospha-Michael addition describes the nucleophile addition of a phosphorous nucleophile with an acceptor-substituted alkene or alkyne to form a P–C bond, usually under basic conditions. Thus it has a broad spectrum of starting materials and product variety. A brief overview was given by Enders *et al.* in 2006.[89] Due to the huge number of different P-containing starting materials, in this work, the field will be narrowed down to P(O)H-containing nucleophiles (Figure 18).

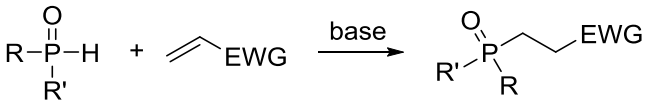

Figure 25: Scheme of the Phospa-Michael addition of a P(O)H-containing nucleophile and an activated alkene. R and R' may be any organic rest and EWG is an electron-withdrawing group.

Up to now, little effort was made to explore the mechanism of the reaction.[90] For phosphinates, different investigations have been performed regarding the selectivity of the reaction between a 1,2-(Pudovik type) and a 1,4-addition to unsaturated carbonyls.[89] Without basic conditions, the 1,4-product is the thermodynamically more stable product, while the 1,2-addition (Pudovik product) is favored kinetically at room temperature.[91] Unsaturated aldehydes were shown to exclusively react in a 1,2-type addition when a lithium-containing base, such as lithium diisopropylamine (LDA), is used.[92]

2.4.3. Oxidation

P–H bonds can also be oxidized towards their corresponding P–OH acid (Figure 26). Therefore usual oxidation agents can be applied. One common way is the application of hydrogen peroxide.[93-97] Another possibility is the use of potassium permanganate for which the reaction rate is dependent on the pH value.[88, 98] The reaction with chlorine leads to the corresponding acid chloride.[88]

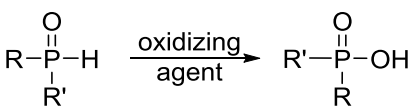

Figure 26: Oxidation reaction of P–H compounds. R and R' may be any organic rest.

2.4.4. Atherton-Todd Reaction

The Atherton-Todd reaction was first examined in 1945[99] and is one of the key tools of organophosphorus chemistry. A detailed review on the reaction and its mechanism was given by

Jaffrès *et al.* in 2014.[100] The reaction describes an oxidative nucleophilic substitution reaction of an amine or an alcohol and a pentavalent P–H bond utilizing carbon tetrachloride and a base to convert the P–H bond into the corresponding phosphorus-containing ester or amidate. Although the mechanism of the reaction was studied intensively, not all details are fully established. However, after studying the literature Jaffrès *et al.* suggested the mechanism shown in Figure 27.[100]

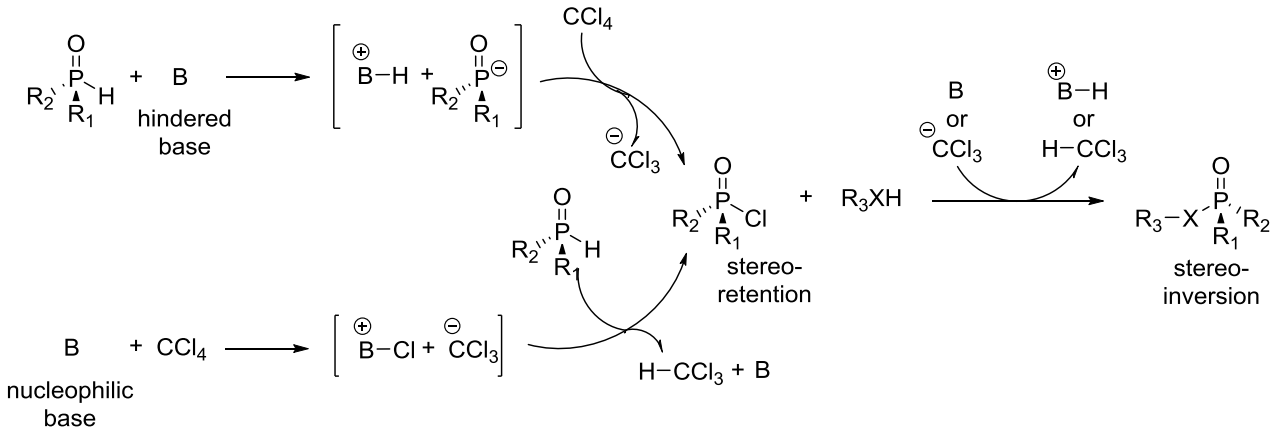

Figure 27: Mechanism of the Atherton-Todd reaction as proposed by Jaffrès *et al.*[100] X stands for O or N–H. R_1, R_2 and R_3 may be any organic rest. B is a base.

Based on studies of Steinberg[101] and Krutikov[102] *et al.*, they proposed that during the first reaction step the mechanism depends on the base. If a more nucleophilic base is applied, it will first react with carbon tetrachloride, while a sterically hindered base like trimethylamine will most likely abstract the hydrogen atom from the phosphorus. However, it was agreed upon that the corresponding chlorinated phosphorus compound is formed as an intermediate[103] under retention of stereoisomerism[104-107] after the first step. The second step of the reaction does follow under stereoinversion.[104-107] Due to the formation of chloroform during the reaction, it is usually also carried out in chloroform as solvent. Although being a versatile tool, the Atherton-Todd reaction has its drawbacks, like the toxicity of carbon tetrachloride. Therefore, the Atherton-Todd reaction is under constant development, e.g. regarding the exchange of the chlorinating agent.[108, 109]

2.4.5. Different P–H Compounds and their flame retardancy mechanisms

There are plenty of different P–H compounds that can be used for various applications. Figure 28 shows the chosen compounds that were applied in this work. Despite the phenyl groups lowering the phosphorus content and thus raise the additive amount needed for efficient flame protection, they often offer an enhanced thermal stability of the FR due to possible delocalization of emerging radicals.[110] This makes them especially interesting for engineering plastics, like PA, where high processing temperatures are required.

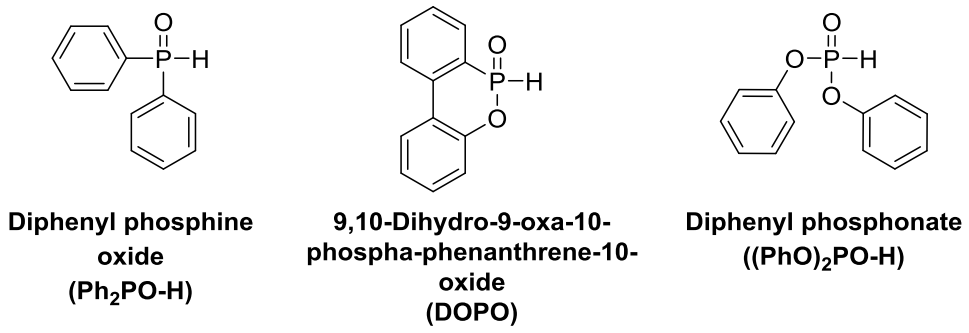

Figure 28: P–H compounds used in this work.

With its high thermal stability and flame retardant efficiency 9,10-dihydro-9-oxa-10-phospha-phenanthrene-10-oxide (DOPO) does play an important role in the development of new FRs for various systems.[111-114] It was developed by Saito company (Figure 29).[115] For its synthesis 2-phenylphenol and excess PCl_3 are used to form a phenol ester. A catalyst, like $ZnCl_2$, is applied at an increased temperature and the excess PCl_3 is removed via distillation to create the trivalent 6-chloro-6H-dibenzo[*c,e*][1,2]oxaphosphinine (DOP-Cl). It is possible to isolate DOP-Cl as an intermediate from this process to use it as a basic compound for the synthesis of DOP-containing FRs. For the synthesis of DOPO, DOP-Cl is then hydrolyzed to form a ring-opened DOPO, which can be heated to eliminate water and perform a ring closure. The last step is reversible, causing DOPO to undergo addition if exposed to water.[116, 117]

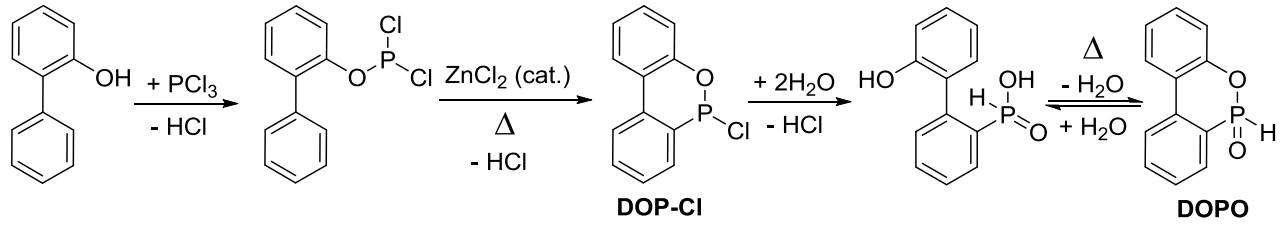

Figure 29: Synthesis of DOPO after the Saito method.[115]

As a flame retardant, DOPO acts mainly in a gas-phase mechanism with PO· radicals scavenging radicals with higher reactivity from the flame, but it can also act in both gas- and condensed phase.[111, 113, 118] In the flame, DOPO first cleaves the P–H bond forming H· and DOPO· radical, which then decomposes into PO· and extremely stable dibenzofuran (DBF) what is the driving force of this reaction. In Figure 30 the main decomposition reactions in the gas phase are shown as well as various radical scavenging reactions inside the flame with the corresponding calculated reaction energies.

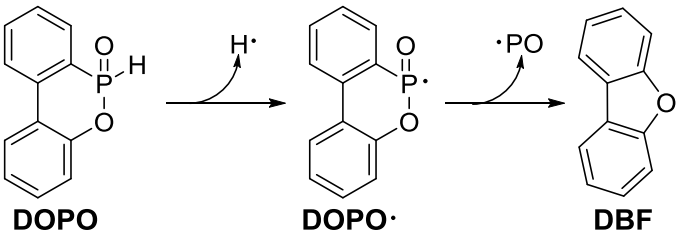

DOPO	⟶	DBF	+	HPO		163.9 kJ/mol
DOPO	⟶	H·	+	DOPO·		354.2 kJ/mol
HPO	⟶	H·	+	·PO		278.8 kJ/mol
DOPO·	⟶	DBF	+	·PO		88.6 kJ/mol
DOPO + H·	⟶	DOPO·	+	H_2		-105.1 kJ/mol
DOPO + ·OH	⟶	DOPO·	+	H_2O		-148.8 kJ/mol
DOPO + H·	⟶	·PO	+	H_2	+ DBF	-16.5 kJ/mol
DOPO + ·OH	⟶	·PO	+	H_2O	+ DBF	-60.3 kJ/mol

Figure 30: Proposed gas-phase mechanism of DOPO with the calculated reaction energies (calculated with density functional theory).[16, 118, 119]

Like other H-phosphinates, in solution DOPO is present in a tautomeric equilibrium where it can either exist in its tetra- (**A**) or tri- (**B**) coordinated form (Figure 31).[77, 114] The equilibrium is

heavily sided to form **A** due to the stability towards oxygen, but utilizing the right reagents it can be shifted to form **B** and thus react as a nucleophile as well as an electrophile. This opens up a broad spectrum of reactions like additions, oxidations and substitution reactions.

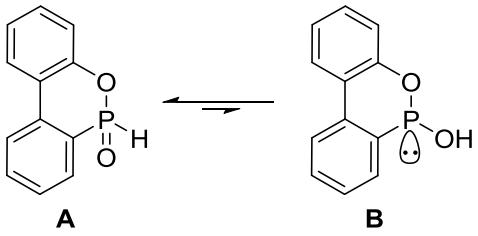

Figure 31: Tautomeric forms **A** and **B** of DOPO.[114]

Due to this versatile reactivity, DOPO bears a lot of potential in the development of new FRs. It can either be incorporated into a polymer chain, for example by addition to a monomeric unit followed by copolymerization with an unmodified monomer[97, 119], or derivatized, e.g. via substitution of halogenated compounds, to yield FR additives.[114] However, free DOPO can act as an acidic catalyst for ester or amide cleavage or even as an oxidizing agent at higher temperatures since it is only thermally stable up to 210 °C and starts decomposing.[120] This makes pure DOPO a poor additive for engineering plastics because of possible acidic cleavage of the polymer during the melting process and thus DOPO must be further functionalized prior application.[121]

Ph_2PO-H can also be prepared from PCl_3 which is utilized in a Friedel-Crafts reaction with benzene (Figure 32).[122] The resulting diphenyl chlorophosphine is then hydrolyzed to yield the desired product.[122]

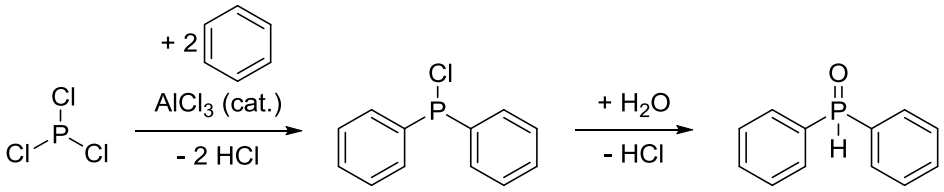

Figure 32: Synthesis of Ph_2PO via Friedel-Crafts reaction followed by hydrolysis.[122]

Based on TGA results and analyses of gaseous decomposition products of a Ph_2PO-substituted polyethylene terephthalate (PET), it is assumed that the molecule partially goes into gas phase[123] and, besides the PO· radical, yields to the products shown in Figure 33.[124] Overall, it is agreed on a gas-phase mechanism.

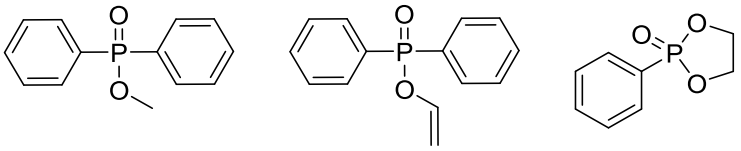

Figure 33: Decomposition products of a Ph_2PO-substituted PET.[124]

The conventional method for the preparation of $(PhO)_2PO$-H also utilizes PCl_3, however, there is a growing demand for healthier alternatives regarding the synthesis of H-phosphonates without the use of chlorinated agents. Montchamp *et al.* described the synthesis of $(PhO)_2PO$-H from phosphinic acid with a Ni/SiO_2 or even without any catalyst,[125] which yielded in a patent for the generation of H-phosphonates[126] (Figure 34). Their proposed mechanism leads over tri-coordinated intermediates.[125]

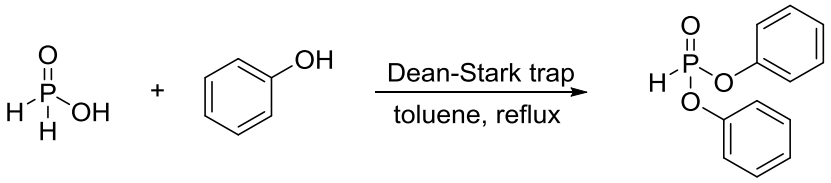

Figure 34: Synthesis scheme for $(PhO)_2PO$ from phosphinic acid via Dean-Stark trap.[125, 126]

As stated earlier, the H-phosphonates can undergo hydrolysis and transesterification what makes it necessary to work in water-free conditions. As a phosphonate it usually mainly acts in the condensed phase.[51, 52] Similar to DOPO, Ph_2PO-H and $(PhO)_2PO$-H should be utilized as derivatives if applied to thermoplastic polymers, like PA.

2.5. Heat Stabilization of Polyamides

Slow thermal degradation due to aging is a problem in several elevated temperature applications, e.g. in the automotive sector, for aliphatic polyamides. The thermal aging process is similar to the thermal degradation discussed in chapter 2.2 but due to the constant exposure to oxygen, it is dominated by several oxidative steps. The main reactions of this thermo-oxidative degradation in polyamides are shown in Figure 35.[30] The oxidation predominantly takes place at the methylene group close to the nitrogen of the amide bond via H-abstraction.[127, 128]

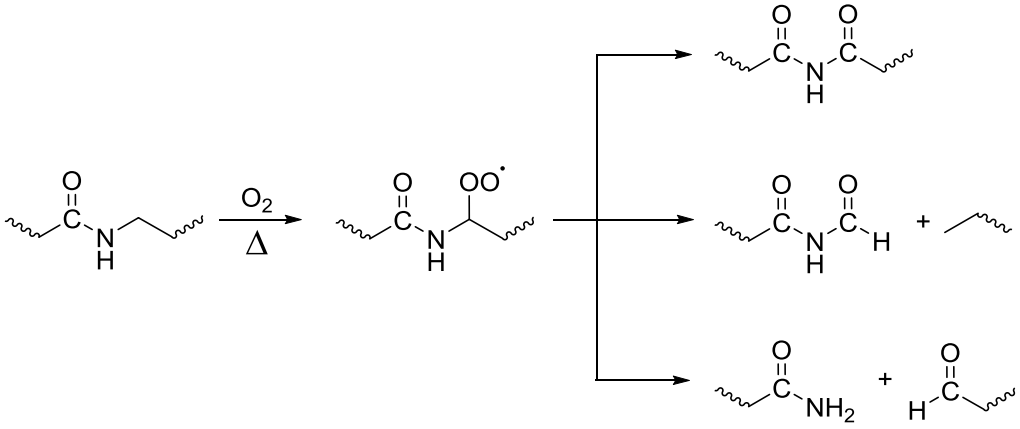

Figure 35: Main reactions of the themo-oxidative degradation of aliphatic polyamides.[30]

During this long-term process, the polyamide undergoes yellowing owing to crosslinking reactions towards conjugated structures of azomethines in similar reactions as described in chapter 2.2.[129]

A common way of protecting polyamide from thermo-oxidative decomposition is the addition of antioxidants, like metal halides,[17] secondary aromatic amines, hindered phenols or hindered aliphatic amines.[130, 131] Since metal halides are applied the most, they herein will be described in further detail. The most efficient metal salt for the heat stabilization of polyamides is copper(I)iodide, especially in combination with potassium iodide (Figure 36).[132-134] The Cu^+ ion can interact with the peroxide formed of the polyamide via oxidation and thus generate Cu^{2+}.[134] In combination with halogen ions the peroxides can be decomposed towards alcohols. Resulting water can react together with a Cu^+ ion and the so formed halogen molecule to copper(II)hydroxide while regenerating halogen ions.[134] The Cu^{2+} ion is able to scavenge occurring radicals in the polyamide due to chain scission via electron-transfer and thus recover the Cu^+ ion.[134] Owing to the regenerative processes only small amounts of the stabilizing salts are necessary, e.g. 0.04/0.26 wt% of a CuI/KI combination in PA 66 to retain 70 % stress at break after 500 h aging time at 210 °C.[135]

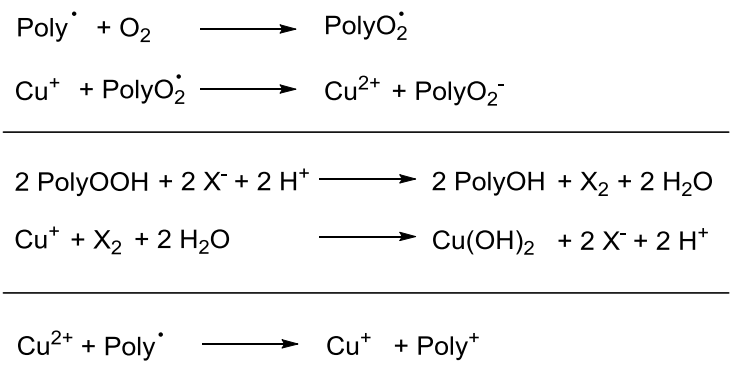

Figure 36: Stabilization reactions of copper salts inside a polyamide (Poly) in combination with halogen atoms (X) as well as the recovery of Cu(I) from Cu(II) ions.[134]

In recent patents, another approach on the stabilization of polyamides aroused which offers new, efficient heat stabilization for polyamides.[135-141] In this approach, either the combination of common stabilizers with[139-141], or the stand alone use of polyhydric alcohols[135, 136, 138] (polyols) is performed. In both cases, the mechanical properties of the chosen GF-reinforced polyamide after thermal aging are significantly improved with the use of 1-5 wt% of, for example, dipentaerythritol (DPE) or polypentaerythritol (Charmor PP100), over the common stabilizing systems. The stabilizing mechanism of these polyols has not been in the focus of research so far and thus no proposed mechanism is known up to now. However, for poly(vinyl chloride) (PVC) the addition of pentaerythritol (PE) and other polyols is known to thermally stabilize the polymer.[142-145] It is claimed that the polyol may either crosslink the generated polymer fragments[143] or coordinate via hydrogen-bonds onto the chlorine atom in the PVC chain shielding the chlorine from dehydrochlorination to some degree.[142, 145] In the case of polyamides, H-bonding of the hydroxyl groups to the labile amide group as well as crosslinking of generated radicals in the chains could also be the reason of the proper heat stabilization. Similar to the SHIELD technology for polyamides invented by DuPont[146, 147], a crosslinking reaction would first start at the surface of the specimen resulting in a protective char layer that stops the oxygen from accessing further into the material (Figure 37).

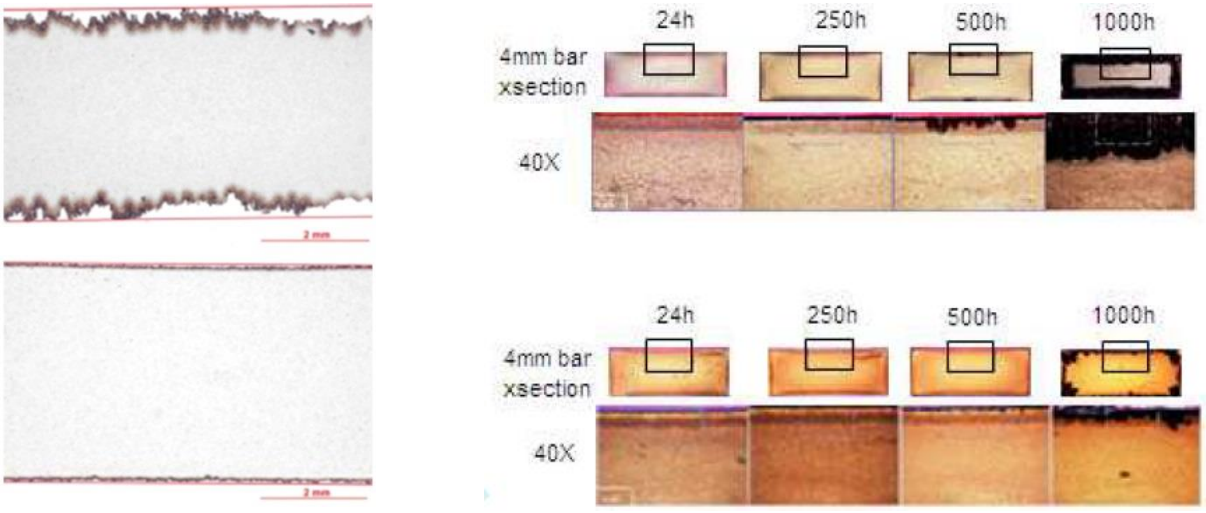

Figure 37: Microtome sections of aged PA 66 tensile bars. Left: The top shows conventionally stabilized PA 66 after 1000 h at 210 °C while the bottom was stabilized with DuPont™ SHIELD technology.[146] Right: The top shows conventionally stabilized PA 66 after 24, 250, 500 and 1000 h at 210 °C while the bottom was stabilized with DuPont™ SHIELD technology and aged at 230 °C.[147]

However, the proposed mechanism for the stabilization effect of polyols is far from verified and its proof will not be part of this work.

3. Aim of this work

The first goal of this thesis was the development of novel phosphorus-containing FRs and their application in polyamides 6 and 66. Therefore, a monomer should be synthesized that combines different FR acting mechanisms through the possession of a metal ion, phosphorus and a functionality that can be polymerized afterwards. The newly synthesized compounds should then be tested for their flame retardancy in polyamides with and without glass fibers and in combination with different synergists.

Another goal was the combination of flame retardancy with heat stabilization in one polymer. This should be reached via the combination of different phosphorus moieties with hydroxyl groups. Three different approaches should be explored. For the first approach, phosphorus-containing diol precursors should be synthesized that are then merged with polyols to yield phosphorylated molecules with a high hydroxyl number. Afterwards, those substances should be tested for both their performance as heat stabilizers and as FR synergist. In a second approach, copolymerizations of hydroxyl- and phosphorus-containing acrylates and acrylamides should be performed and it should be tested whether this approach is feasible for heat stabilization in PAs. The last approach on that regard was the Pudovik reaction of phosphorus compounds with bio based molecules. In this type of reaction a P–H bond is added onto an aldehyde resulting in a hydroxyl group. Therefore, a desired functionality can be created while other functional groups still can be used for further functionalization or polymerization.

Throughout the whole work it was taken care of that the conducted reactions are atom-efficient and in compliance with “green chemistry”.

4. Results and Discussion

In the following chapters the results of this work will be presented.

As stated in chapter 2.3.2, the combination of metal and phosphorus can be beneficial for flame retardancy. Thus, in the first part of this section a novel approach towards P-containing polymeric FRs was the combination of metal-containing acrylates with DOPO as a phosphorus compound. The key reaction was the stoichiometric Phospha-Michael addition of DOPO to one acrylate group while one acrylate group stays unconverted for radical polymerization. The flame retardant efficiency of the DOPO-containing polymeric zinc acrylate (DOPO-propionate)Zn(acrylate) (**1**) in PA 6 and 66 was compared to an also new low-molecular-weight complex Zn(DOPO-propionate)$_2$ (**3**) as well as the non-phosphorus-containing poly(zinc diacrylate) (**4**).

Afterwards three different attempts on the combination of flame retardancy and heat stabilization in one molecule or polymer are presented. Similar to a commercially-available polymeric polyol stabilizer, condensations of phosphorus-containing polyols, non-phosphorus-containing polyols and a hydroxyl-containing acid were performed to create oligomer polyol structures with phosphorus. Different phosphorus species were utilized and their performance as flame retardant synergists and heat stabilizers for PA 6 was evaluated.

In chapter 4.2.4 the copolymerizations of different DOPO-containing acrylates and acrylamides with hydroxyl-containing acrylates and acrylamides is described. Their thermal stabilities were compared and phosphorus-free, hydroxyl-containing polyacrylamides were tested as proof of concept for heat stabilization in PA 6.

The last approach was the Pudovik reaction of DOPO with acrolein and hydroxylmethylfurfural. Despite no polymerization of the products could be reached, novel compounds were synthesized that were further functionalized. The thermal stabilities of those compounds were too low for the incorporation into polyamides and thus for testing their heat stabilization effect or flame retardancy, but they might be interesting for the employment in other polymers or as reactive FRs.

4.1. DOPO-containing Metal Carboxylates

4.1.1. Polyacrylates containing P-based Zinc Carboxylates

For a combination of the merits of the phosphorus-containing salts and of polymer FRs, several approaches on this matter were taken in literature. An organic approach on metal-containing polymeric phosphinates was patented by Sicken *et al.,* in which an ethylene bridged polymer was synthesized from phosphinic acid and acetylene and the corresponding salts thereof were prepared.[148, 149] Another approach was performed by Wang *et al.*, who used zinc- or copper-doped poly(vinyl phosphonate) as a flame-retardant coating for natural fibers.[150] A coordination polymer, containing zinc and DOPO, that was examined previously in our research group, is *bis*(dibenzo[*c,e*][*1,2*]oxaphosphinin-6-olate 6-oxide) zinc (Zn(DOPO-O)$_2$)$_n$.[151]

In this thesis, the idea was to utilize P–H compounds and multi-functional metal acrylates. Zinc diacrylate (ZDA) was chosen because phosphorus-containing zinc salts, like *bis*-(diethyl phosphinate) zinc (DEPZN), are known to work well in engineering plastics.[62, 65, 152, 153] DOPO was chosen as P–H compound due to the merits stated in chapter 2.4.5.

For the synthesis of (DOPO-propionate)Zn(acrylate) (**1**) two different approaches were conducted. The first route (Route **A** towards **1-A**) was the Phospha-Michael addition of DOPO to ZDA.

Therefore, ZDA and one equivalent of DOPO were dissolved in *N,N*-dimethylacetamide (DMAc) and heated up to 90 °C (Figure 38). For the second approach (Route **B** towards **1-B**), diethylzinc was used (Figure 39) because if correct stoichiometry is applied there should only be ethane as a side product and thus fewer impurities. In a first step, DOPO-propionic acid (**2**) was synthesized according to literature by Phospha-Michael addition of DOPO to acrylic acid.[154] It was then dissolved in DMAc and a diethylzinc solution was added at 0 °C in a stoichiometric amount. Then one equivalent of acrylic acid was added to yield compound **1-B**.

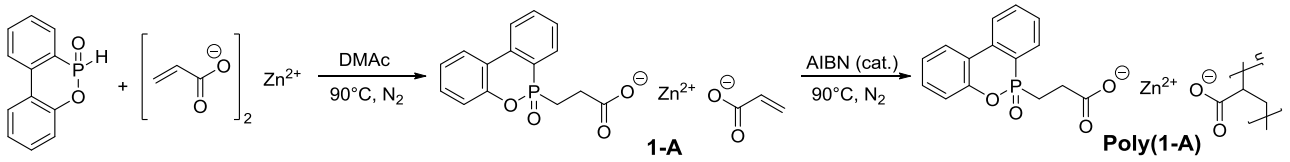

Figure 38: Zinc diacrylate route (Route **A**) for the synthesis of **1-A**.

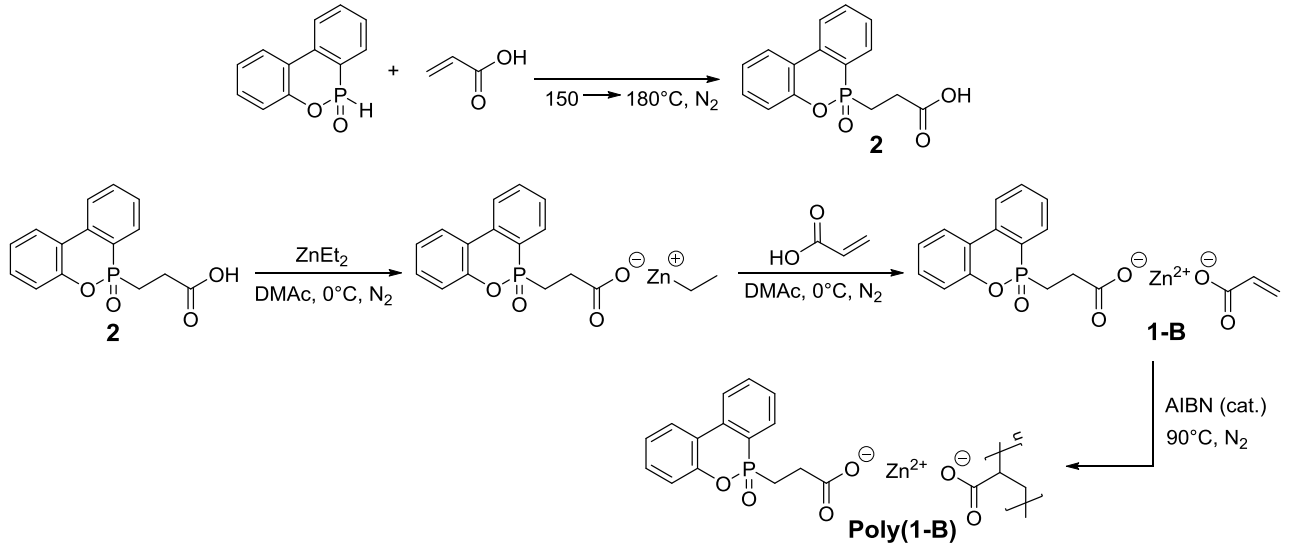

Figure 39: Diethylzinc route (Route **B**) for the synthesis of **1-B**.

When trying to isolate each product from the reaction solution by precipitation with another solvent an insoluble solid occurred, that was not further analyzed for its structure. Thus, the polymerization was conducted in the reaction solution without prior isolation of the monomer in a one-pot synthesis with azobisisobutyronitrile (AIBN) as radical initiator. The created polymer was washed with dry solvents afterwards.

Pyrolysis - gas chromatography/mass spectroscopy (py-GC/MS) of the washed and dried polymers at 200 °C revealed that despite drying the samples thoroughly, residual DMAc remained in the sample and a significant amount of water is taken up, even if the substance is applied only shortly to air after drying. To analyze if there was a negative influence of water on **Poly(1-A)** it was washed with water rigorously and a ^{31}P-spectrum of the washing solution was taken, which showed that phosphorus compounds were removed from the product by the washing step. To quantify the loss of phosphorus, elemental analysis of the washed as well as the dried **Poly(1-A)** was conducted. The phosphorus content was identified to be 3.51 % less than in the untreated sample (P-content: 6.48 wt%). Due to its deliquescence, **Poly(1)** was hence synthesized and handled under moisture-free conditions.

It is well known that complexes can exist in equilibrium like the one shown in equation 1. This equilibrium is examined, for example, for ethylzinc carboxylates.[155]

$$\text{A-Zn-A} + \text{B-Zn-B} \rightleftharpoons 2\ \text{A-Zn-B} \qquad (1)$$

Thus, compound **1** should exist statistically distributed over the three structures ZDA, a di-(DOPO-propionate)-substituted zinc complex, Zn(DOPO-propionate)$_2$ (**3**), and the desired structure **1**. To analyze this structural behavior for component **1-A**, compound **3** was synthesized. For its synthesis both routes also were tested utilizing ZDA and diethylzinc. Interestingly, even if two equivalents of DOPO were applied in the Phospha-Michael addition to ZDA only the mono-substituted product **1-A** occurred and more impurities were generated instead of the di-substituted complex **3**. This shows that the Phospha-Michael addition towards **1-A** works selectively for the mono-adduct and no statistically distribution is received. Thus, only the diethylzinc route was further conducted for the synthesis of **3** (Figure 40).

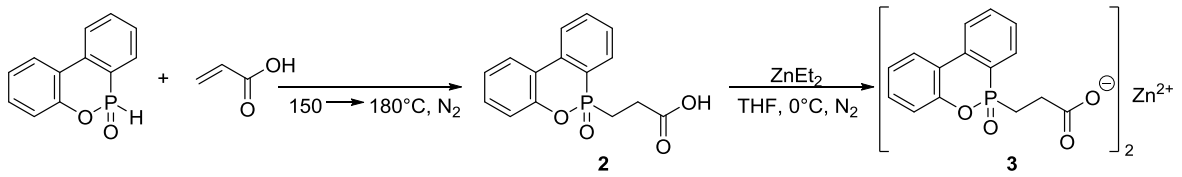

Figure 40: Diethylzinc route for the synthesis of **3**.

Diffusion-ordered spectroscopy (DOSY) was performed on the monomer solution of **1-A** in DMAc (Figure 41) as well as on complex **3** (Figure 42) and ZDA (Figure 43) in comparison for further examination of the equilibrium. All signals of **1-A** align at the same diffusion constant D of $6.13 \cdot 10^{-6}$ m^2 s^{-1} and thus at one hydrodynamic radius. This shows that both carboxylate functionalities of the acrylate and the DOPO-propionate are bound to the zinc ion and thus that the desired structure of the molecule was formed. The equilibrium fully favors the mixed A-Zn-B side in the monomer solution. It also shows that both DMAc and deuterated dimethylsulfoxide (DMSO-d_6) possess strong dipolar interactions with **1-A** and possibly even coordination since the solvent signals also align with the monomer signals. This strong interaction also explains the difficulty of drying the polymer. This result differs from the DOSY spectra of component **3** and zinc acrylate where all solvent signals possess different diffusion constants than the examined structure.

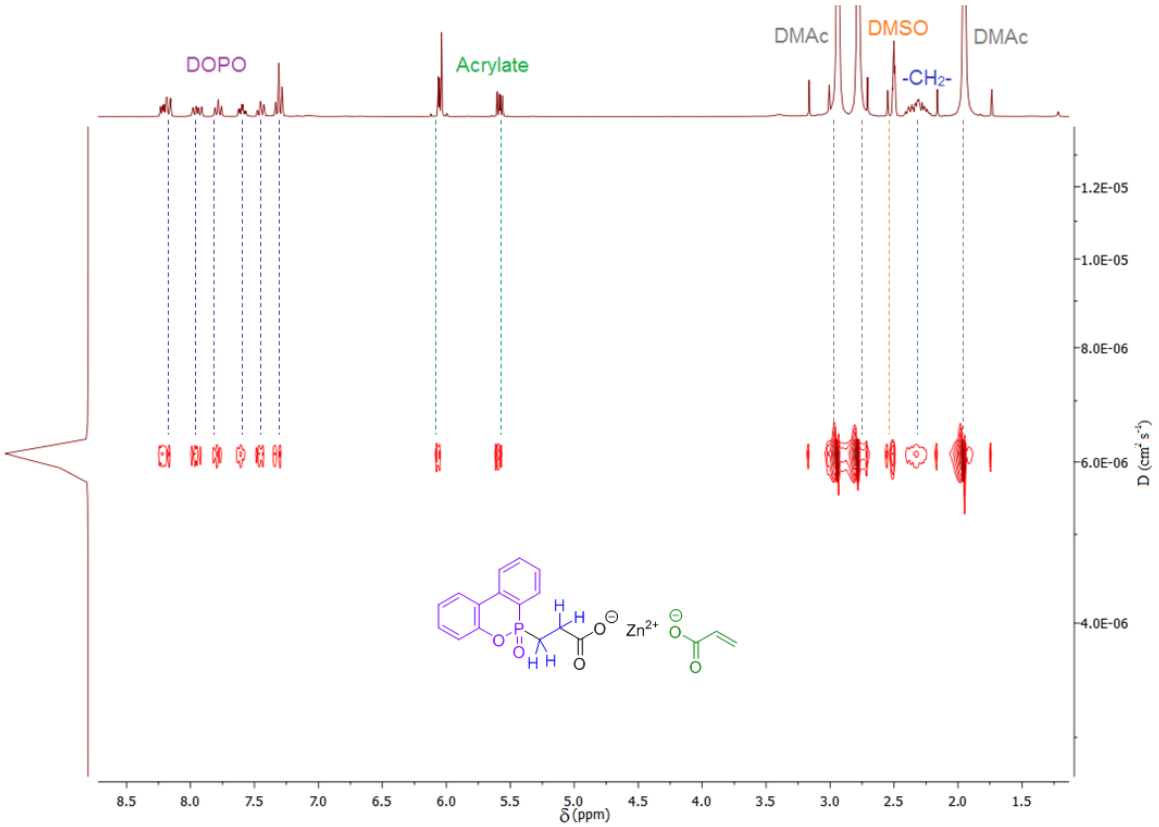

Figure 41: DOSY spectrum of component **1-A** in the reaction solution and DMSO-d_6.

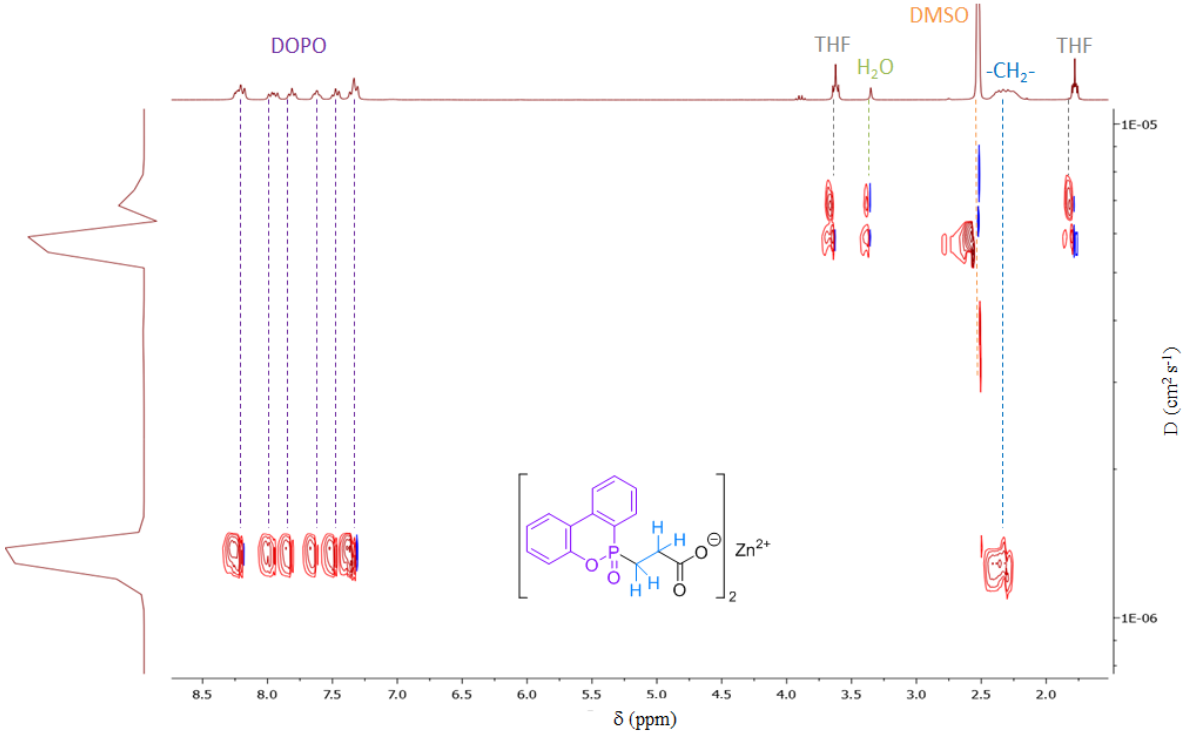

Figure 42: DOSY spectrum of **3** in DMSO-d_6.

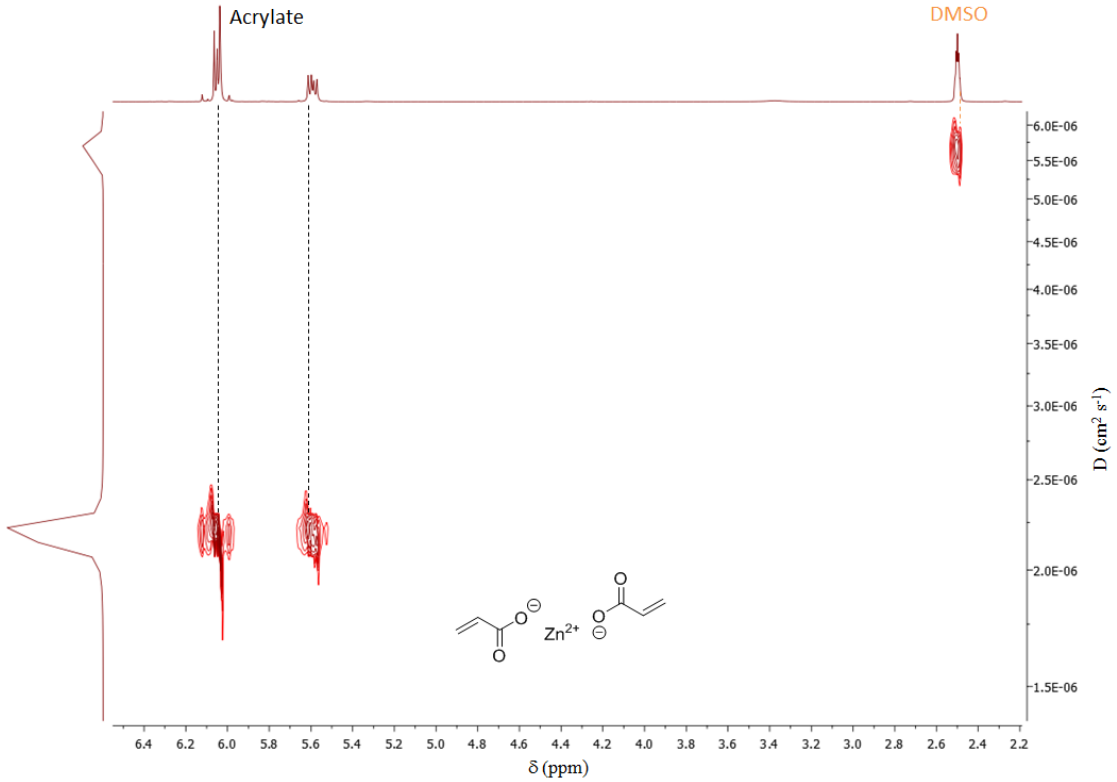

Figure 43: DOSY spectrum of **ZDA** in DMSO-d_6.

The thermal stability of the dried polymers from both routes (**Poly(1-A)** and **Poly(1-B)**) was determined via TGA and the results were compared (Figure 44). Despite **Poly(1-A)** is starting to decompose at nearly the same temperature compared to **Poly(1-B)**, a significantly larger amount of residue is created (55.7 wt% at 650 °C).

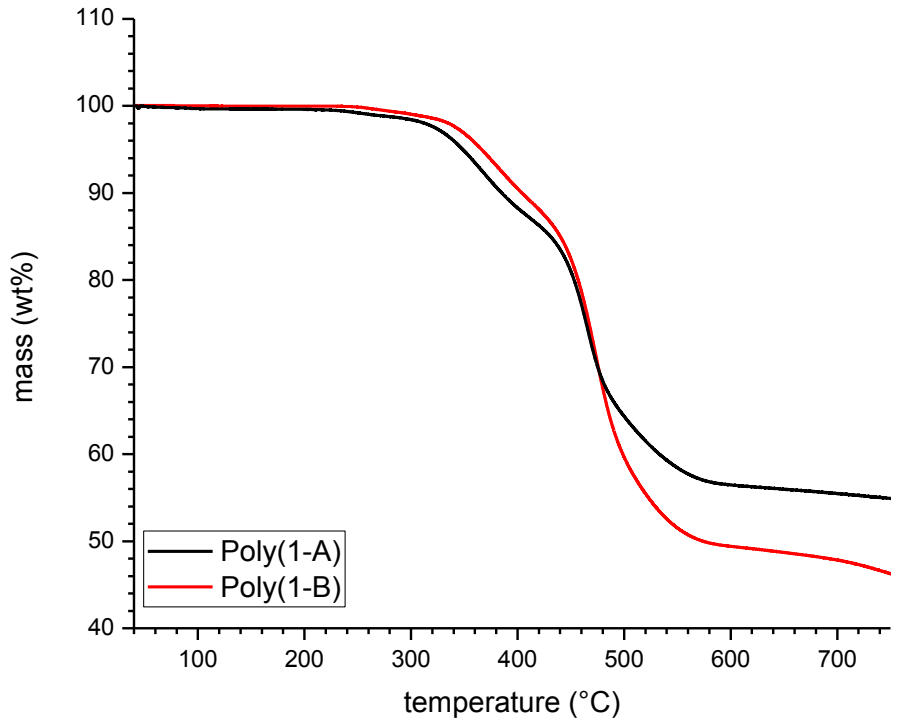

Figure 44: TGA of **Poly(1)** synthesized via route A (**Poly(1-A)**, black) and via route B (**Poly(1-B)**, red).

To further examine this matter, elemental analyses of the products from both routes were compared (Table 3). **Poly(1-B)** gave a huge discrepancy between calculated and experimental values. This indicates that, during the synthesis of **1-B**, the statistical mixture between zinc complex **3**, ZDA and the desired product **1-B** was created. During polymerization, ZDA is causing crosslinking of **Poly(1-B)**, while the soluble complex **3** is filtrated off from the precipitated polymer which results in a decreased phosphorus and carbon content and thus a higher zinc content. A similar trend in the elemental analysis is followed for **Poly(1-A)** but the difference in zinc and phosphorus content is substantially lower than for **Poly(1-B)** showing again that the statistical mixture is not favored and that a more pure product can be synthesized via route A. The decreased phosphorus content is also the explanation for the difference in the amount of residue. For **Poly(1-B)** the zinc content is higher but the amount of residue is lower and thus the phosphorus has to be responsible for the bigger residue of **Poly(1-A)**. An elemental analysis of the residue of **Poly(1-A)** at 650 °C showed an increased phosphorus content of 12.66 wt%. This indicates that, for this particular polymer, DOPO not only acts in gas but also in condensed phase. Henceforward, route A towards the novel compound **1-A** was followed for all further experiments utilizing the Phospha-Michael addition of DOPO to ZDA.

Table 3: Results of the elemental analyses of compounds **Poly(1-A)** and **Poly(1-B)**. Values in brackets are the calculated ones for one repeating unit of the polymer **Poly(1)**.

Compound	wt% C (calculated)	wt% H (calculated)	wt% P (calculated)	wt% Zn (calculated)
Poly(1-A)	49.10 (51.03)	3.80 (3.57)	6.48 (7.31)	16.58 (15.43)
Difference	-1.93	+0.23	-0.83	+1.15
Poly(1-B)	46.72 (51.03)	3.64 (3.57)	4.96 (7.31)	18.26 (15.43)
Difference	-4.31	+0.07	-2.35	+2.83

In order to compare another metal ion with the polymeric zinc salt **Poly(1-A)**, magnesium diacrylate was chosen as starting compound. However, it has a lower solubility than ZDA in DMAc as well as other solvents. Thus, when trying to use the same reaction conditions as for ZDA no reaction occurred. Due to the low solubility and the associated problems with the reaction, this approach was not further pursued.

ZDA was polymerized in DMAc using AIBN as radical starter to yield a non-phosphorus containing polyacrylate as a reference (**4**). Thermogravimetric analyses (TGA) of all three synthesized additives under nitrogen and air were conducted in order to examine their thermal decomposition behavior and to analyze their deployment as possible FRs for engineering plastics (Figure 45).

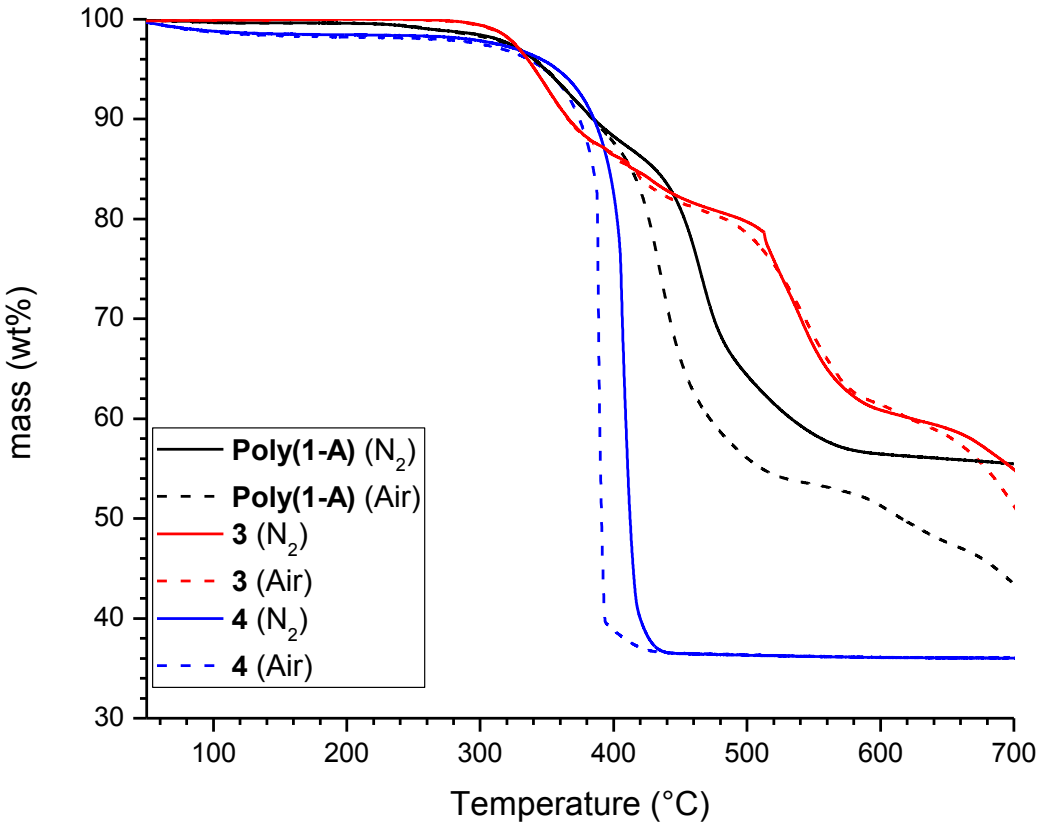

Figure 45: TGA curves of **Poly(1-A)**, **3** and **4**. Dashed lines correspond to measurements under air and solid lines under nitrogen.

Despite tempering **4** with the TGA at 225°C for 90 min a small amount of water (1.4 wt% in N_2 and 1.7 wt% in air) still remained. This underlines the hygroscopic nature of the substance. Skorsepa *et al.* examined the decomposition of zinc propionate via TGA and IR spectroscopy and stated that it leaves zinc oxide as solid residue and carbon dioxide and pentan-3-one as its volatile products.[156] Polymer **4** behaves in a similar fashion.[157] As can be seen in Table 4 its residue at 650 °C measured under air or nitrogen is close to the calculated amount of zinc oxide that should remain. Despite the fact that DOPO usually mainly acts in gas phase, both DOPO-containing compounds possess a drastically enlarged residue compared to **4**. This leads to the conclusion that in case of the phosphorus-containing compounds **Poly(1-A)** and **3** the remaining residue is not only ZnO. To check if the phosphorus component is responsible for the larger residue, the phosphorus content of the residue of **Poly(1-A)** and **3** was determined. Therefore, both compounds were heated to 650 °C in the TGA and the temperature was held isothermal for 20 min. The residue was examined photometrical for the phosphorus content. As stated earlier, the residue of **Poly(1-A)** contains

12.66 % of phosphorus while the phosphorus content of the residue of **3** was determined to be 17.11 %. With the amount of phosphorus known in the untreated substances **Poly(1-A)** and **3**, the percentage of phosphorus passing into the gas phase can be calculated. For **Poly(1-A)** 13.4 % phosphorus turn into the gas phase, while for **3** it is only 11.0 %. This shows that for both phosphorus-containing compounds, the phosphorus is strongly involved in the formation of the residue. A similar effect of the zinc coordination polymer $(Zn(DOPO\text{-}O)_2)_n$[151] was observed earlier, which also leaves a large amount of residue (>60 wt% at 700 °C)[117] and leads towards a partially aromatic network in PA 66 in combination with melamine poly(aluminium phosphate)[158]. This undermines the assumption that DOPO is acting not only in gas but mainly in condensed phase for the herein described substances. All compounds behave similarly under air as under nitrogen, only **Poly(1-A)** seems to undergo an oxidative step at temperatures above 600 °C and thus its decomposition is accelerated under air. The thermal decomposition temperatures of all three substances are above 300 °C and hence high enough for the incorporation into engineering plastics.

Table 4: Decomposition temperatures and char yields of components **Poly(1-A)**, **3** and **4** measured under nitrogen and air.

	Component	$T_{2wt\%}$ / °C	$T_{5wt\%}$ / °C	Residue at 650 °C / wt%	wt% ZnO (calculated)
N_2	**Poly(1-A)**	312.9	345.9	54.4	19.2
	3	324.0	342.0	59.1	12.7
	4	336.9 [a]	369.2 [a]	36.2	39.2
Air	**Poly(1-A)**	309.5	349.8	47.1	19.2
	3	322.9	341.1	58.3	12.7
	4	332.4[a]	360.7[a]	36.2	39.2

[a]: Values are adjusted by the percentage according to the water removal (1.4 wt% in N_2 and 1.7 wt% in air)

4.1.2. Polyacrylate containing P-based zinc carboxylate as Flame Retardant for Polyamides

The synthesized substances **Poly(1-A)**, **3** and **4** were tested as FRs for PA 6 and PA 66 in various blends. The compound mixtures shown in Table 5 were used for extrusion and injection molding of UL94 specimen. Only half a specimen of mixture **d** and no specimen for mixture **s** could be obtained.

Table 5: Compounding mixtures for the UL94 specimens. Given values are in wt%.

Specimen	PA 6 (B27)	PA 66 (A24)	PA 6/GF30 (B3EG6)	PA 66/GF30 (A3EG6)	Poly(1-A)	3	4	MPP	DEPAL
a	0	90	0	0	10	0	0	0	0
b	90	0	0	0	0	10	0	0	0
c	0	90	0	0	0	10	0	0	0
d[1]	0	90	0	0	0	0	10	0	0
e	0	90	0	0	0	0	0	0	10
f	82	0	0	0	6	0	0	12	0
g	0	82	0	0	6	0	0	12	0
h	82	0	0	0	0	0	6	12	0
i	0	82	0	0	0	0	6	12	0
j	0	0	82	0	12	0	0	6	0
k	0	0	0	82	12	0	0	6	0
l	0	0	82	0	0	12	0	6	0
m	0	0	0	82	0	12	0	6	0
n	0	0	82	0	6	0	0	12	0
o	0	0	0	82	6	0	0	12	0
p	0	0	82	0	0	6	0	12	0
q	0	0	0	82	0	6	0	12	0
r	0	0	82	0	0	0	6	12	0
s[2]	0	0	0	82	0	0	6	12	0
t	0	0	82	0	0	0	0	0	18
u	0	0	0	82	0	0	0	0	18

[1]Half a specimen obtained. [2]: no specimen obtained.

During compounding of **3** into PA 6 and 66, a depression of the shaft force and gas formation inside the melt vessel was observed what indicates an accelerated decomposition of the polymer. The same trend is followed for compound **Poly(1-A)**. To validate these observations viscosity numbers (VN) were recorded for specimen **f** – **u**, which are shown in Table 6.

Table 6: Viscosity numbers of specimen f to u.

Specimen	VN / $cm^3 \cdot g^{-1}$	Specimen	VN / $cm^3 \cdot g^{-1}$
PA 6 (B27)*	150	**PA 66 (A24)***	124
f	150	**g**	98
h	180	**i**	118
PA 6 (B3EG6)*	140	**PA 66 (A3EG6)***	145
j	106	**k**	93
l	117	**m**	86
n	128	**o**	101
p	111	**q**	95
r	187	**s**	-
t	150	**u**	149

*: Values taken from the material data sheets.

The VNs for the reference specimens **t** and **u**, containing only DEPAL, do not differ significantly from the pure polyamides. All components comprising complex **3** (**l**, **m**, **p**, **q**) do drop in the VN considerably. This decay is larger for PA 66 than for PA 6 what is due to the higher extrusion

temperature for PA 66. The specimens containing **Poly(1-A)** (**f**, **g**, **j**, **k**, **n**, **o**) do show the same trend except for sample **f**, which did retain the VN of pure PA 6. Compounds with incorporated **4** (**h**, **i**, **r**) possess a substantially increased viscosity number in PA 6 due to the cross-linked structure of the additive. They do, however, have slightly decreased values in PA 66, what is also related to the higher compounding temperature.

These results may be explained when comparing the decomposition temperatures of the different additives (Table 4). Both DOPO-containing components start decomposing between 310 and 320 °C, while **4** is stable up to slightly higher temperatures. When looking at the TGA derivatives (Figure 46), **3** is decomposing faster around 300 °C than **4** and **Poly(1-A)** even shows a small degradation step prior 300 °C. This step lies within the extrusion temperature range of both PA 6 and PA 66 and thus should be the cause of the degradation during the extrusion process.

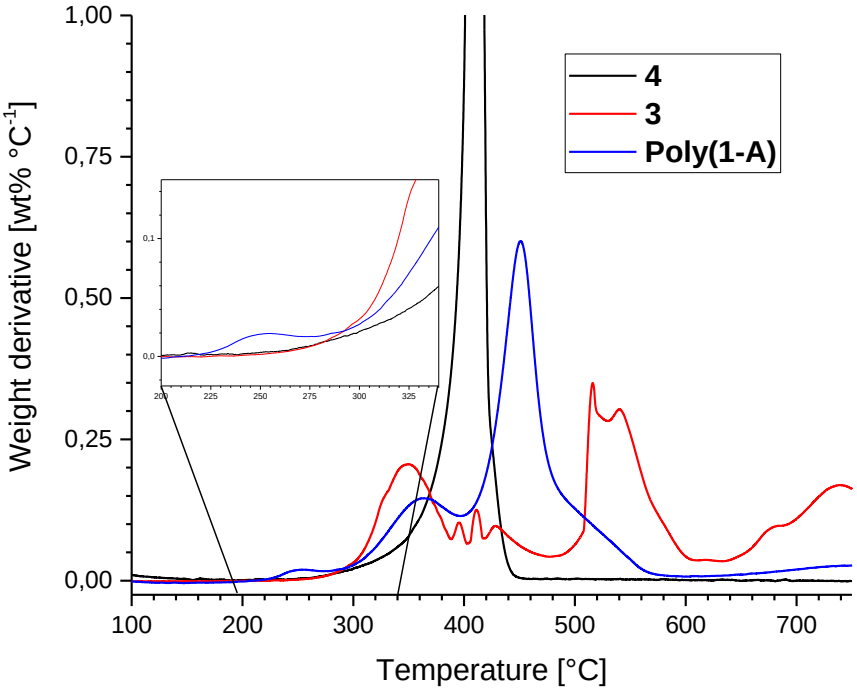

Figure 46: Weight derivatives of the TGA curves of **3** (red), **Poly(1-A)** (blue) and **4** (black).

To validate that theory, a py-GC/MS experiment of **Poly(1-A)** at 300 °C was performed to determine the pyrolysis products of this first decomposition step (Figure 47). Despite severe drying of **Poly(1-A)** (180 °C in vacuum while stirring for several days), the main decomposition product was still residual DMAc and due to the hygroscopic nature of the substance water was found too. Also, o-hydroxybiphenyl, a decomposition product of DOPO, as well as intact DOPO were assigned to the mass spectra of peaks 4 and 5 gathered from the gas phase. It is possible that the released DOPO acts as an acid for the degradation of the polyamide[120] and thus is the reason for the viscosity drop and the gas formation inside the melt vessel. CO_2 is released during decomposition of the propionate group.

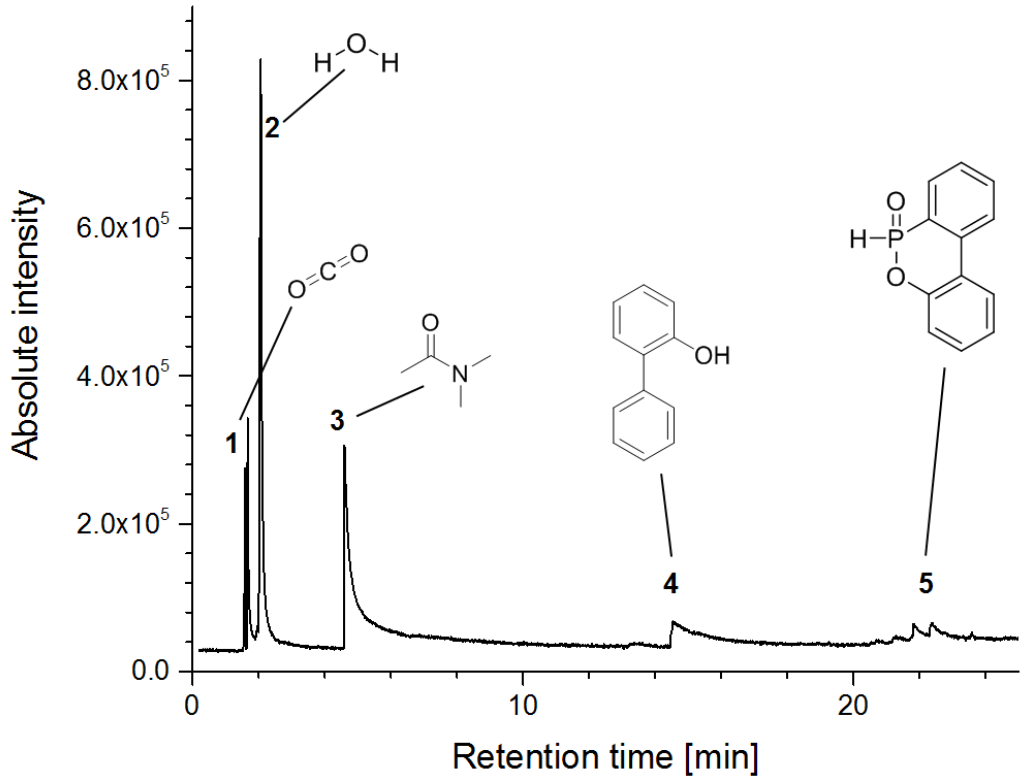

Figure 47: Py-GC/MS spectrum of **Poly(1-A)**.

UL94 tests of all specimens were performed and the results are shown in Table 7. Specimens **a** to **e**, that contain non-reinforced PA 6 or PA 66 and 10 wt% of the respective FR additive, did all yield in V-2 ratings, except for reference sample **e** which gave a V-0 rating. The excessive dripping causes the samples to only reach a V-2 rating although the afterburn times are rather short, especially for the phosphorus-containing samples. In order to prevent dripping, glass fiber (GF)-reinforced specimens were tested[7] and blending with MPP was performed[113, 119]. Another reason for the compounding with mixtures of MPP in combination with the novel substances, is a possible synergistic effect since MPP is also known for a synergistic effect with DEPAL in GF-reinforced PA 6.[59] Against expectations,[41] both measures did not impede the generation of flaming droplets, except for sample **o**, that hence achieved a V-1 rating. Interestingly, this specimen, containing only 6 wt% of **Poly(1-A)** and 12 wt% MPP, reached a better rating than sample **k** with 12 wt% **Poly(1-A)** and 6 wt% MPP. This indicates that if **Poly(1-A)** is applied, a small amount is more efficient since the effect of accelerated decomposition and thus the dripping of the material is more impactful than its FR activity. This observation is also contrary from the usually applied ratio of DEPAL/MPP which is 2:1 for achieving the best FR efficiency.[153, 159] Compounds containing the non-phosphorus **poly(ZDA) 4** (specimen **d**, **h**, **i**, **r**) do possess overall longer afterburn times than the phosphorus-containing specimen what causes them to pass with V-2 or even fail the test. Overall, the new synthesized substances **Poly(1-A)** and **3** did not yield in a sufficient flame retardancy for PA 6 and 66 due to acceleration of the decomposition of the PA.

Table 7: UL94 test results and TGA data for blends **a** to **z**.

Specimen	UL94 classification	First afterburn time / s	Second afterburn time / s	Flaming droplets
a	V-2	4	1	Yes
b[1]	V-2	3	2	Yes
c	V-2	1	2	Yes
d	V-2	25	6	Yes
e	V-0	3	4	No
f	n.c.	11	42	Yes
g	V-2	14	6	Yes
h	n.c.	> 71	-	Yes
i	V-2	11	28	Yes
j	V-2	15	4	Yes
k	V-2	15	4	Yes
l	V-2	12	4	Yes
m	V-2	17	4	Yes
n	V-2	16	8	Yes
o	V-1	22	2	No
p	V-2	7	3	Yes
q	n.c.	16	42	Yes
r	n.c.	> 39	-	Yes
t	V-0	8	8	No
u	V-0	1	4	No

[1]: UL94 rating is based on half a specimen.

In summary, it can be stated that a new phosphorus- and zinc-containing polyacrylate and its analog molecular coordination compound were successfully synthesized. The structures of monomer **1-A** and complex **3** were revealed by DOSY spectroscopy. Their thermal decomposition behavior was examined by TGA and elemental analysis, what showed that the usually gas-phase active DOPO in this chemical compound acts mainly in the condensed phase as a high amount of residue remains after the TGA measurements, which still contained high amounts of phosphorus. All compounds proved to be stable enough for the incorporation into PA 6 and PA 66 as FR additives. During the extrusion process, a drop in melt viscosity indicated the decomposition of the PAs. Thus, py-GC/MS at 300 °C was performed on **Poly(1-A)** which showed early decomposition products as a possible reason for the degradation during compounding. UL94 measurements were performed on all compounded samples. The highest achieved rating was V-1 for a mixture of GF-reinforced (30 wt%) PA 66 with 6 wt% **Poly(1-A)** and 12 wt% MPP. All other specimens containing the newly synthesized species' suffered from severe dripping.

4.2. Combination of Flame Retardancy with the Heat Stabilizing Effect of Polyols

Several approaches were taken on the idea of the combination of the effect of phosphorus on flame retardancy with the heat stabilization effect of polyols in one molecule. This combination of phosphorus with aliphatic alcohols should be beneficial for flame retardancy because of the ability of polyols to act as char forming agents in combination with possible formed acid and thus support a condensed-phase mechanism.[47-49] If the supposed SHIELD mechanism for heat stabilization, mentioned in chapter 2.5, is correct as heat stabilizing mechanism for polyols, a fast generated char layer via cross-linking could also be beneficial to heat stabilization of PAs. Thus, the combination of polyol and phosphorus might support both purposes.

The first approach was to generate a molecule similar to the commercially-available Charmor PP100 (mentioned in chapter 2.5). According to its datasheet, Charmor PP100 is claimed to be a polypentaerythritol with a large hydroxyl number of $1000 - 1100\ mg \cdot g^{-1}$ and a melting point between 160 and 180 °C.[1] It is used as a carbon source in intumescent systems,[137, 160] however, it also fits the criteria of polyhydric alcohols as heat stabilizer in several patents[135-141]. The new synthesized molecule should thus also contain a large number of OH-groups for the stabilizing effect but also possess phosphorus units to perform as FR. In chapter 4.2.1, the synthesis of P-containing diols is described which will work as precursor molecules. These diols will then be merged with further hydroxyl-containing molecules, as presented in chapter 4.2.2, to yield molecules with high hydroxyl values. The resulting flame retardancy and heat stabilization tests in PA are illustrated in chapter 4.2.3.

A second approach regarding the copolymerization of OH-containing acrylates or acrylamides with P-containing ones was shown in chapter 4.2.4. The P-containing acrylates and acrylamides were synthesized via Atherton-Todd reaction and an *in-situ* copolymerization with **Poly(1-A)** was performed as well. The resulting polymers were compared for their thermal stabilities and partially tested in PA for their heat stabilization effect as presented in chapter 0.

The last approach, shown in chapter 4.2.7, was the Pudovik reaction of DOPO with acrolein or 5-hydroxymethylfurfural. The reaction products were then tested for their polymerizability or further functionalization. However, the resulting molecules were not suitable for the incorporation in PAs.

4.2.1. Synthesis of P-containing Diols as Precursors

As precursor molecules for phosphorus-based polyols different phosphorus-containing diols were synthesized. Usually, P-containing diols can be used as, for example, reactive FRs in polyurethanes or polyesters[161-163] or as FRs bound onto natural fiber[164]. To compare the effect of different phosphorus classes OH-containing phosphinates, phosphonates and phosphates were generated. DOPO was combined with pentaerythritol (PE) and trimethylolpropane (TMP). To get a defined ratio of OH-groups to phosphorus units two OH-groups of each PE and TMP were protected with benzaldehyde or acetone, respectively. The remaining OH-groups were modified with DOPO by the nucleophilic substitution of 6-chloro-6H-dibenzo[*c,e*][1,2]oxaphosphinine (DOP-Cl) followed by oxidation of P(III) to P(V). Afterwards, the protective group was separated again to yield the respective diol (Figure 48). The synthesis of the PE derivative **DiDOPO-PE** was performed earlier over this route in our group by Patrick Müller.[165]

[1] Product data sheet of Charmor PP100 from: https://www.perstorp.com/products/charmor_pp100 (Last opened: 15/05/2018).

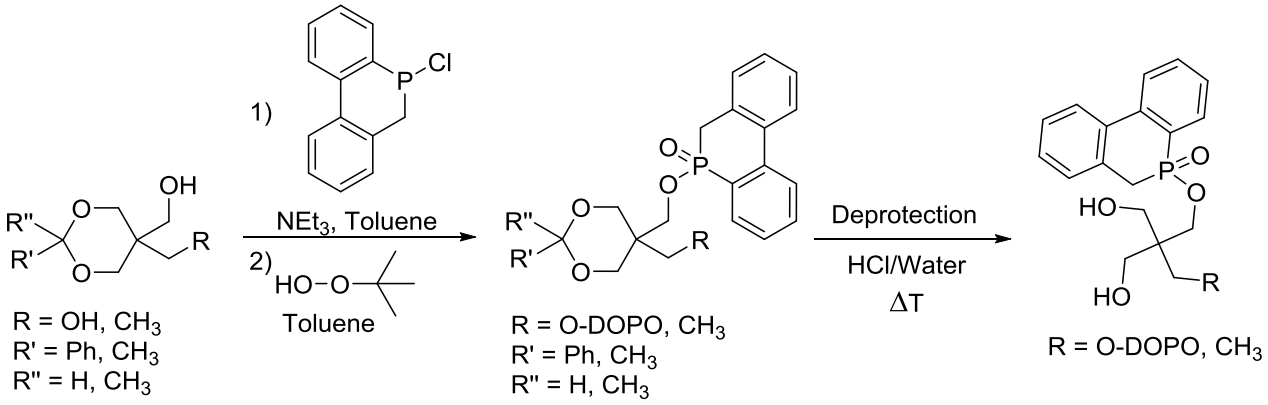

Figure 48: Synthesis of **DiDOPO-PE** and **DOPO-TMP** via protective groups.

Bad yields of the deprotection step and the use of protection groups make this type of synthesis not atom-efficient in compliance with "green chemistry".[166, 167] Thus, another route developed in our research group by Christian Schmiedl[168] for the synthesis of **DOPO-TMP** was approached where no solvent and no catalyst need to be applied. Therefore, TMP was molten at 100 °C and 6-chlorodibenzo[c,e][1,2]oxaphosphinine 6-oxide (DOPO-Cl) was added over 2 h in small doses (Figure 49). This reaction has the advantage that it is a one-step synthesis with only gaseous hydrochloric acid as side product. Potentially this could be a route towards an Atherton-Todd product without the usage of toxic carbon tetrachloride. However, previous work on multi-functional alcohols used in an Atherton-Todd reaction showed that the Atherton-Todd reaction does not yield in selective mono-substituted products, but in a product mixture.[116]

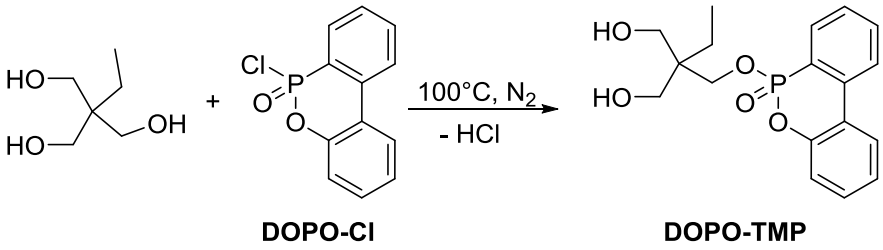

Figure 49: Synthesis of **DOPO-TMP** in substance with DOPO-Cl.

Because of the high melting point of PE (T_m = 260.5 °C), this method is not applicable in this case. After purification via washing with saturated (sat.) sodium hydrogen carbonate and water a 90 % pure product (determined via ^{31}P-NMR) was gained, which is pure enough for the follow-up reactions. The side-products result from partial multi-substitution of the residual OH-groups (Figure 50). The product may be purified by column chromatography (MeOH:$CHCl_3$ / 1:9) to yield the pure mono-substituted **DOPO-TMP**.

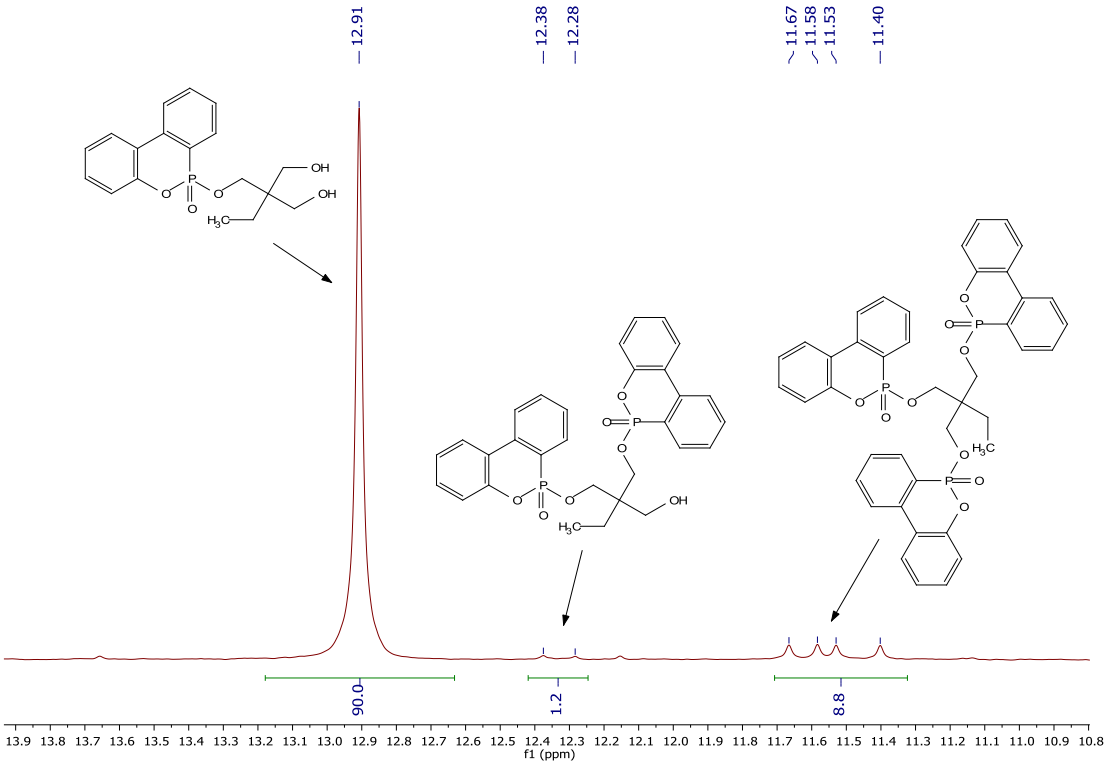

Figure 50: ^{31}P-NMR of **DOPO-TMP** via substitution reaction with DOPO-Cl in $CDCl_3$.

The thermal stabilities of **DOPO-TMP** synthesized via the defined method using protective groups (**DOPO-TMP-d**) and via substitution reaction (**DOPO-TMP**) were compared in order to check if there was a difference due to the side products (Figure 51). The curves nearly possess the same progression, char yield and decomposition point what points to an identical decomposition process. The side products of the substitution procedure do not seem to influence the thermal behavior. Thus, it can be concluded that no purification step via column chromatography is necessary for sequential reactions.

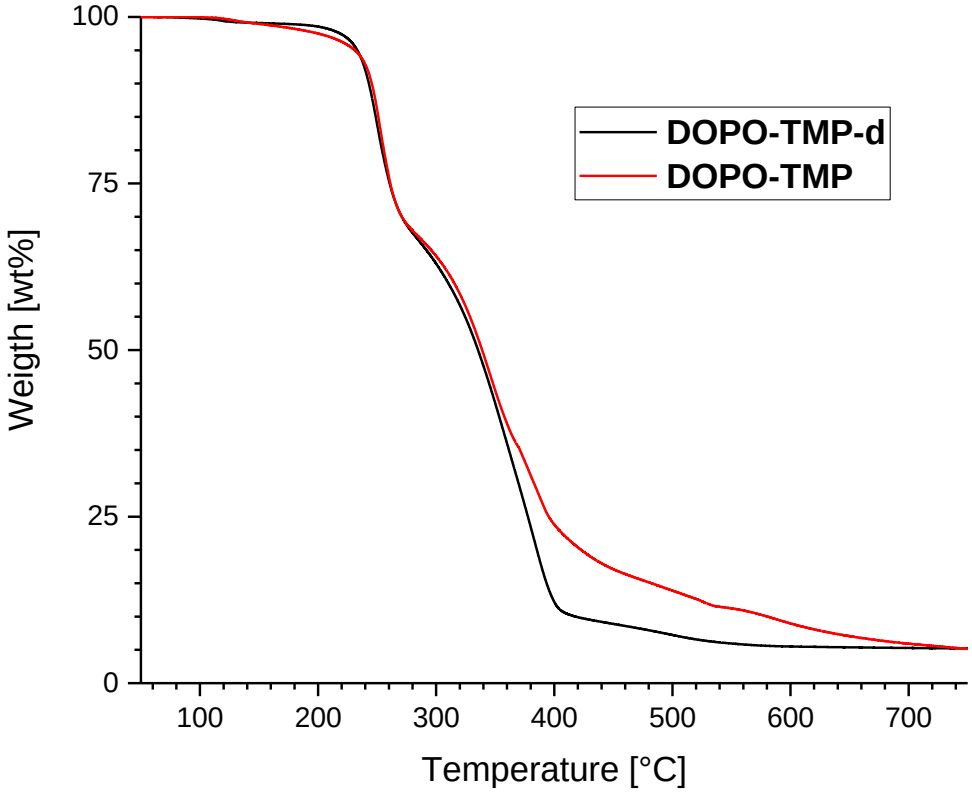

Figure 51: TGA curves of **DOPO-TMP-d** (black) and **DOPO-TMP** (red) measured under nitrogen.

With the same synthesis method like **DOPO-TMP** the diphenyl phosphinate (**Ph_2PO-TMP**) and phosphate (**$(PhO)_2$PO-TMP**) of TMP were synthesized (Figure 52). The phosphinate **Ph_2PO-TMP** had a purity of 87 % (Figure 53) with the other 13 % being the Ph_2PO-di-substituted TMP confirmed by mass spectroscopy. The phosphate **$(PhO)_2$PO-TMP** was 84 % mono-substituted (Figure 54) and the side products were not only $(PhO)_2$PO-di-substituted TMP but also, due to acid-catalyzed transesterification, 5-ethyl-5-(hydroxymethyl)-2-phenoxy-1,3,2-dioxaphosphinane oxide, which was as well confirmed by mass spectroscopy.

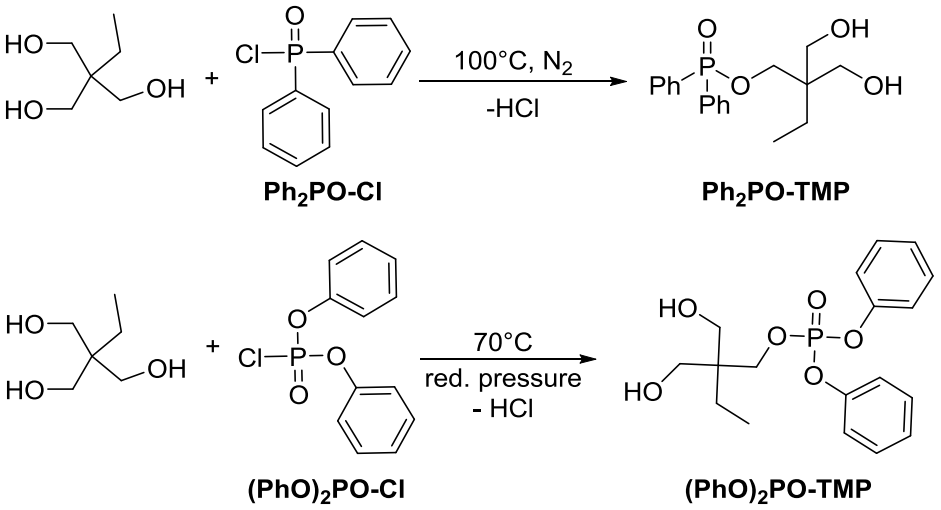

Figure 52: Syntheses of **Ph_2PO-TMP** (top) and **$(PhO)_2$PO-TMP** (bottom).

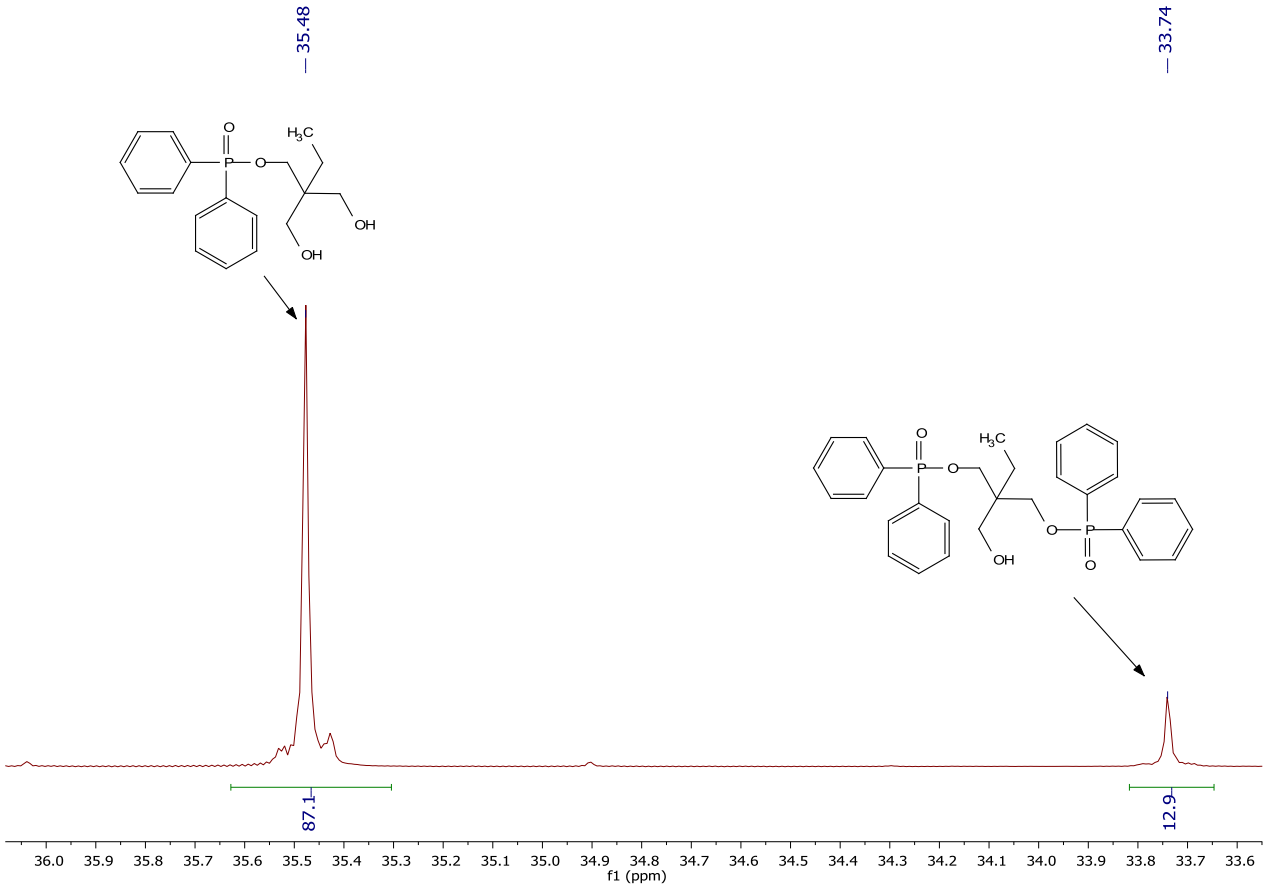

Figure 53: ^{31}P-NMR of **Ph_2PO-TMP** via substitution reaction with Ph_2PO-Cl in $CDCl_3$.

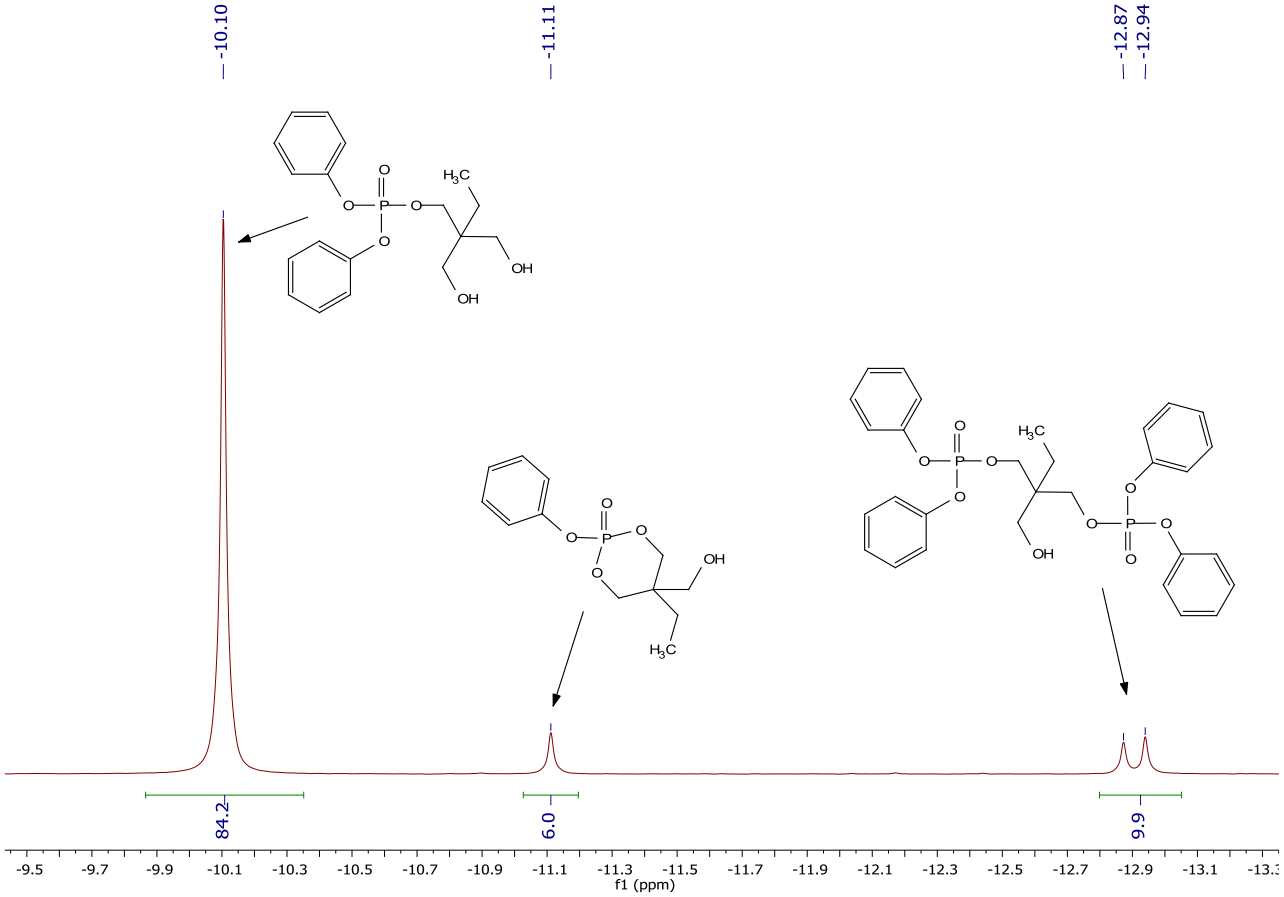

Figure 54: ^{31}P-NMR of **$(PhO)_2PO$-TMP** via substitution reaction with $(PhO)_2PO$-Cl in $CDCl_3$.

When comparing the thermal stabilities of the phosphinate to the phosphonate and the phosphate, the first noticeable thing is its low decomposition temperature of $T_{2\%}$ = 101.6 °C (Table 8, Figure 55). The first decomposition step comprises 15.5 wt%. As expected, the phosphate **$(PhO)_2$PO-TMP** possesses the highest char yield, followed by the phosphonate **DOPO-TMP**. Nearly no char is left from the phosphinate which is expected to be exclusively gas-phase active. An enlarged char yield should support the heat stabilization from the shielding effect. Also, a condensed-phase flame retardancy mechanism of phosphorus units is usually supported by polyols, such as DPE, that provide the necessary oxygen for the dehydration leaving only carbonaceous residue for the char formation. Thus, if looking only at the thermal information, **$(PhO)_2$PO-TMP** is expected to yield the best results regarding combined heat stabilization and flame retardancy.

Table 8: Thermal decomposition temperatures and char yields at 650 °C of **Ph_2PO-TMP** (black), **DOPO-TMP** (red) and **$(PhO)_2$PO-TMP** (blue) measured under nitrogen.

Sample	$T_{2\%}$ / °C	Residue at 650°C / wt%
Ph_2PO-TMP	101.6	0.5
DOPO-TMP	189.0	7.1
$(PhO)_2$PO-TMP	183.4	14.3

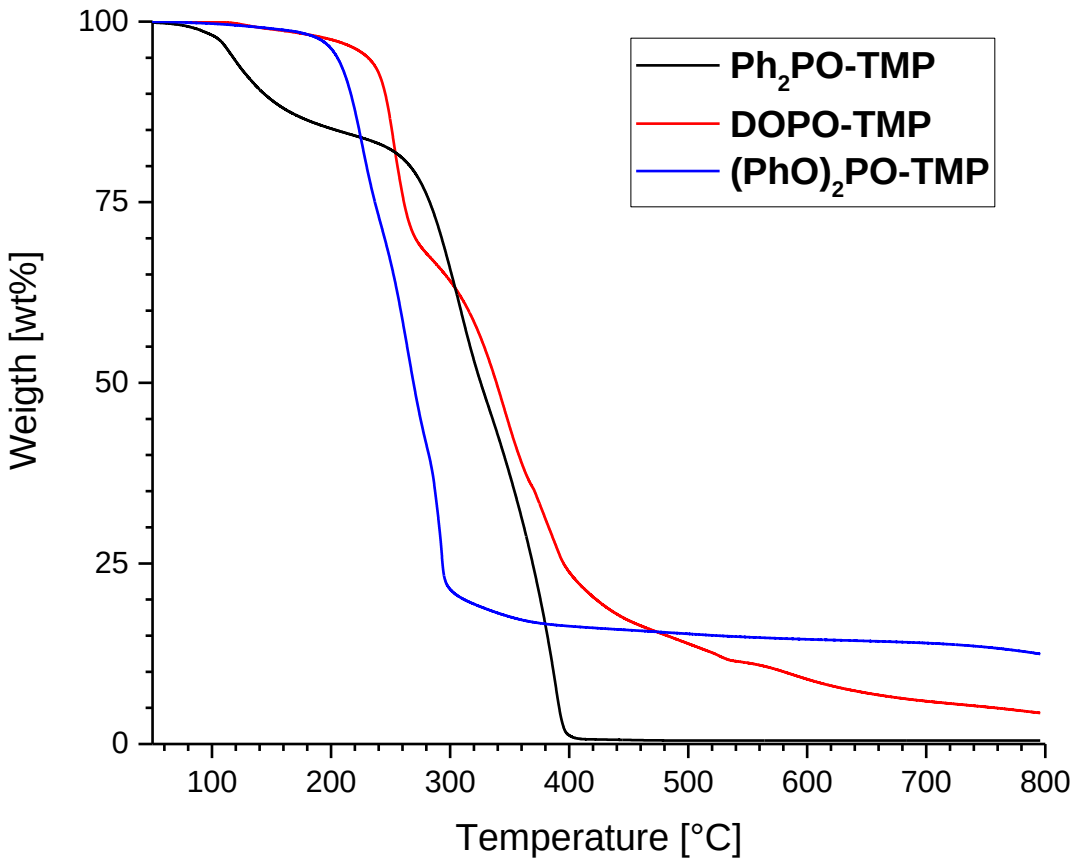

Figure 55: TGA comparison of **Ph_2PO-TMP** (black), **DOPO-TMP** (red) and **$(PhO)_2$PO-TMP** (blue).

The first decomposition step of **Ph_2PO-TMP** was analyzed by DSC followed by NMR of the residue (Figure 56). The ^{1}H-NMR spectra are nearly identical what suggests that no decomposition of the product occurs during the first mass loss but it is only partially volatized. Thus, it can be acted on

the assumption that **Ph_2PO-TMP** can be processed up to temperatures of 200 °C and still retain its chemical structure.

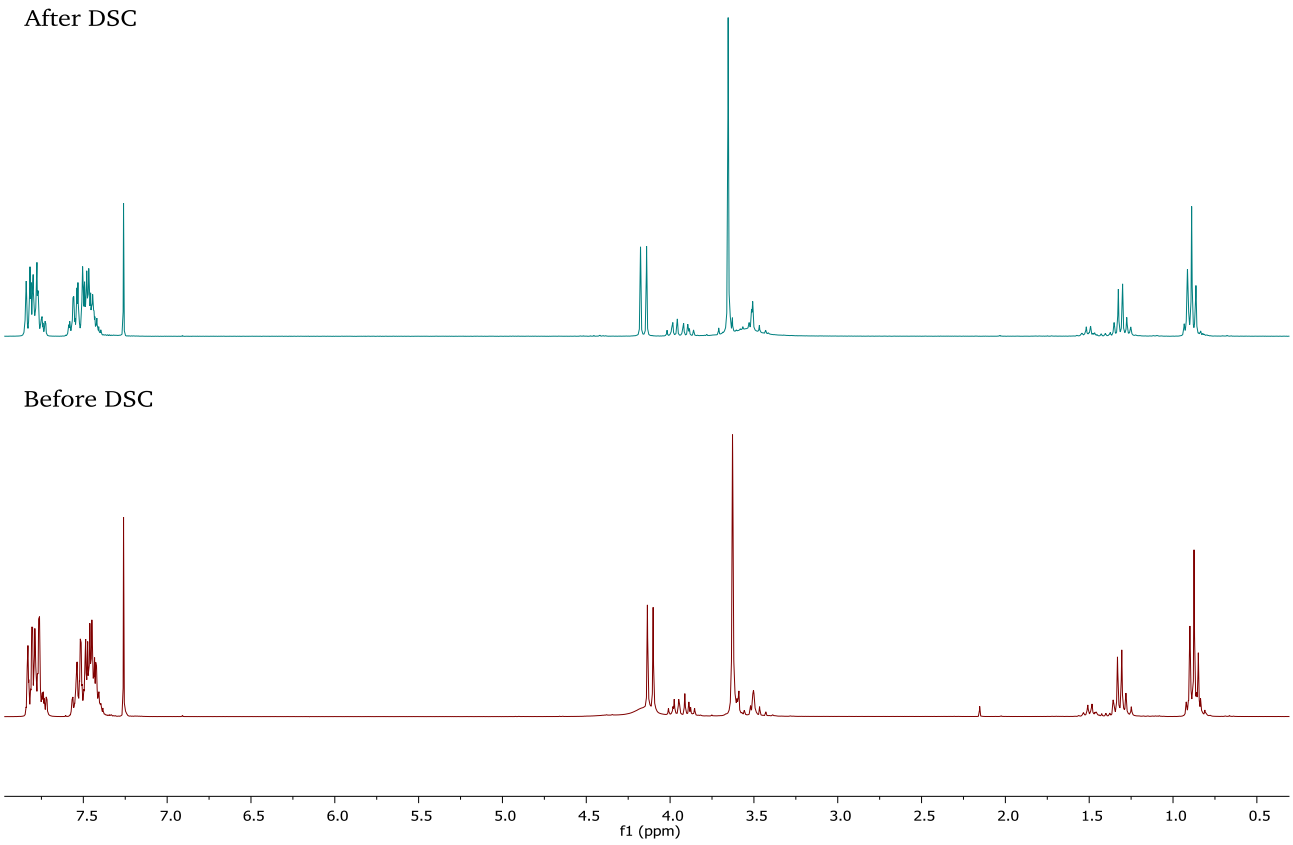

Figure 56: ^{1}H-NMR spectra of **Ph_2PO-TMP** in $CDCl_3$ before and after two DSC cycles from -50 to 200 °C.

4.2.2. Preparation of P-containing Aliphatic Polyol based Heat Stabilizers

Charmor PP100 was analyzed for its structure and properties via different analytic techniques (NMR, IR, DSC, TGA, MALDI-MS, GPC, HPLC/ESI-MS). Based on the mass spectroscopy results, it is a pentaerythritol-based polyester that was condensed with adipic acid (Figure 57). This is backed up by the IR spectrum that matches the spectrum of PE with the addition of a strong C=O valency vibration at 1713 cm^{-1}. The GPC results show an M_w of 1280 g mol^{-1} with a dispersity of 3.4.

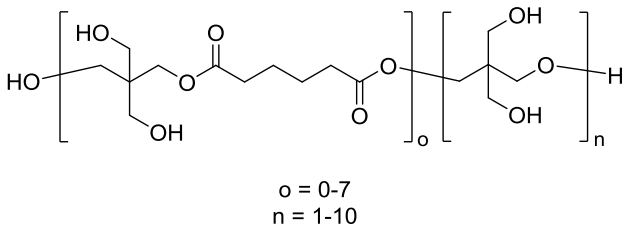

Figure 57: Proposed structure of **Charmor PP100** based on mass spectrometry.

In a patent by Ogemark *et al.*[169], they give a synthesis procedure for polyol-based co-stabilizers for poly(vinyl chloride) (PVC) with a similar chemical structure to **Charmor PP100** (Figure 58). In this procedure, 2,2-*bis*(hydroxymethyl)propionic acid (Bis-MPA) and PE were molten together with *p*-toluenesulfonic acid (p-TSA) at 180 °C. The hot melt was then neutralized with calcium hydroxide and filtered to remove formed calcium sulphonates. The resulting product was cooled down and

pulverized. Afterwards, it was fused with one weight equivalent of dipentaerythritol (DPE) at 220 °C to form a homogeneous blend.

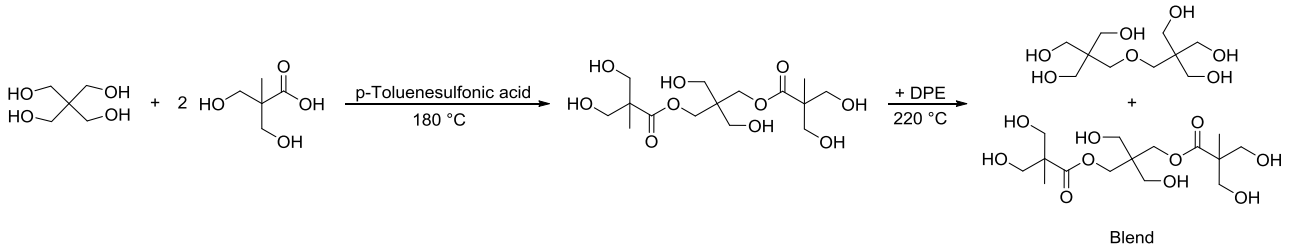

Figure 58: Example reaction after a patent of Ogemark *et al.*[169]

The synthesis procedure from Ogemark *et al.* was repeated to check if the reaction is suitable for the creation of P-containing polyols that possess a similar structure to **Charmor PP100**. **Charmor PP100** and the **reference blend** synthesized after the patent were compared by ^{1}H-NMR and hydroxyl value (OHV) for their structural similarity.

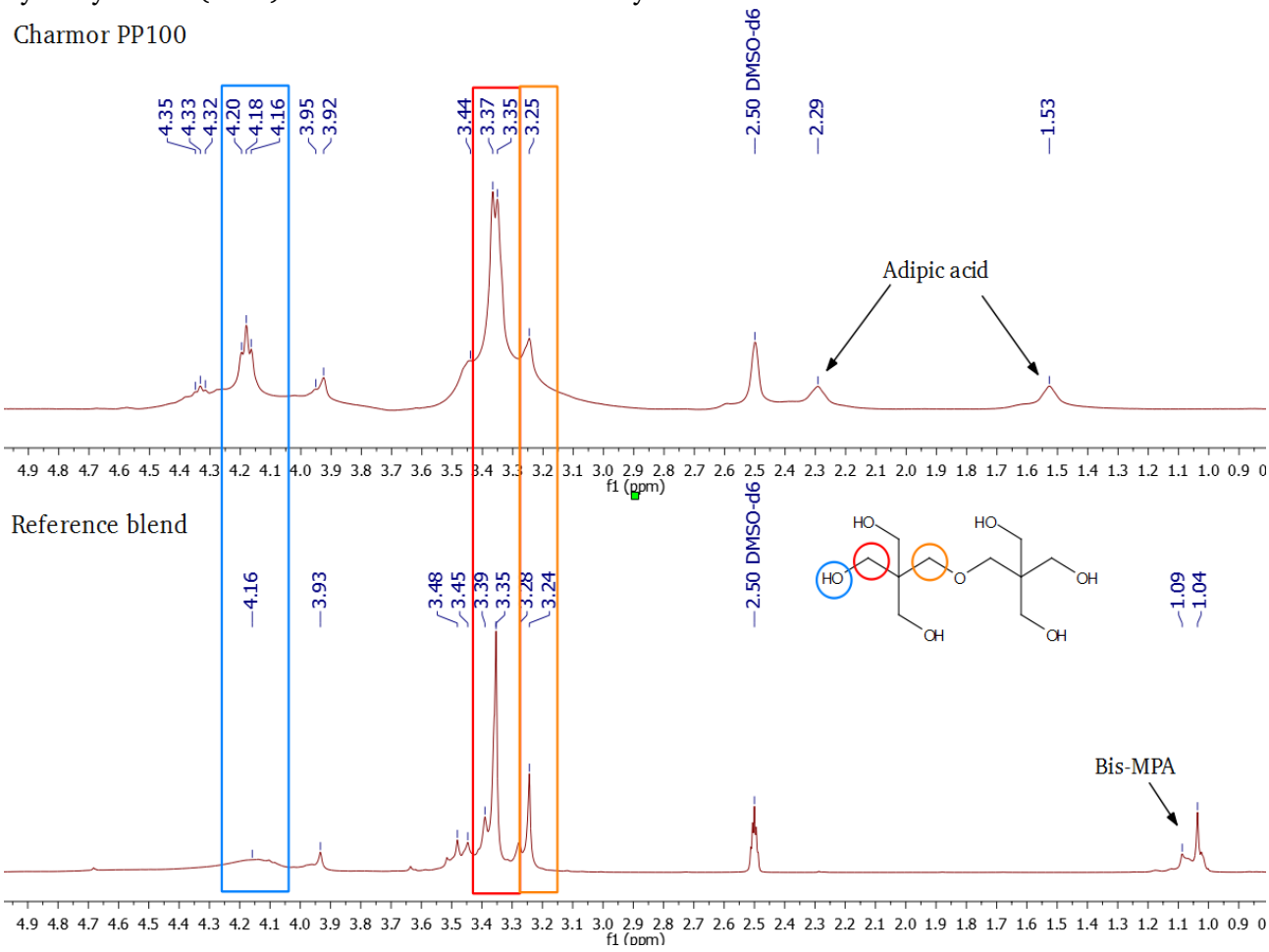

Figure 59: Comparison of the ^{1}H-NMR spectra of **Charmor PP100** (top) and the **reference blend** (bottom) in DMSO-d_6.

As can be seen in Figure 59, the structures are similar in the CH_2-ether and CH_2-OH region from around 3.25 to 3.50 ppm. In the **reference blend**, there seem to be fewer free hydroxyl functionalities than in **Charmor PP100**. Thus, an OHV determination via titration was performed of both **Charmor PP100** and the **reference blend**. The determined OHV for **Charmor PP100** is with 995 mg g^{-1} close to the given value from the data sheet of 1050 mg g^{-1}. The **reference blend** possesses an OHV of 862 mg g^{-1} what is in the same magnitude than **Charmor PP100.**

TGA of both substances were performed to compare their thermal behavior (Figure 60). They both possess a similar degradation process in one step with nearly no remaining char. The **reference**

blend though is close to 40 °C more stable. Interestingly, despite being utilized as additive in polyamides **Charmor PP100** only exhibits a $T_{2\%}$ of 224.57 °C which is usually below the extrusion temperature of, for example, PA 6 or 66. This indicates a possible reaction of **Charmor PP100** with the polyamide matrix during the extrusion process.

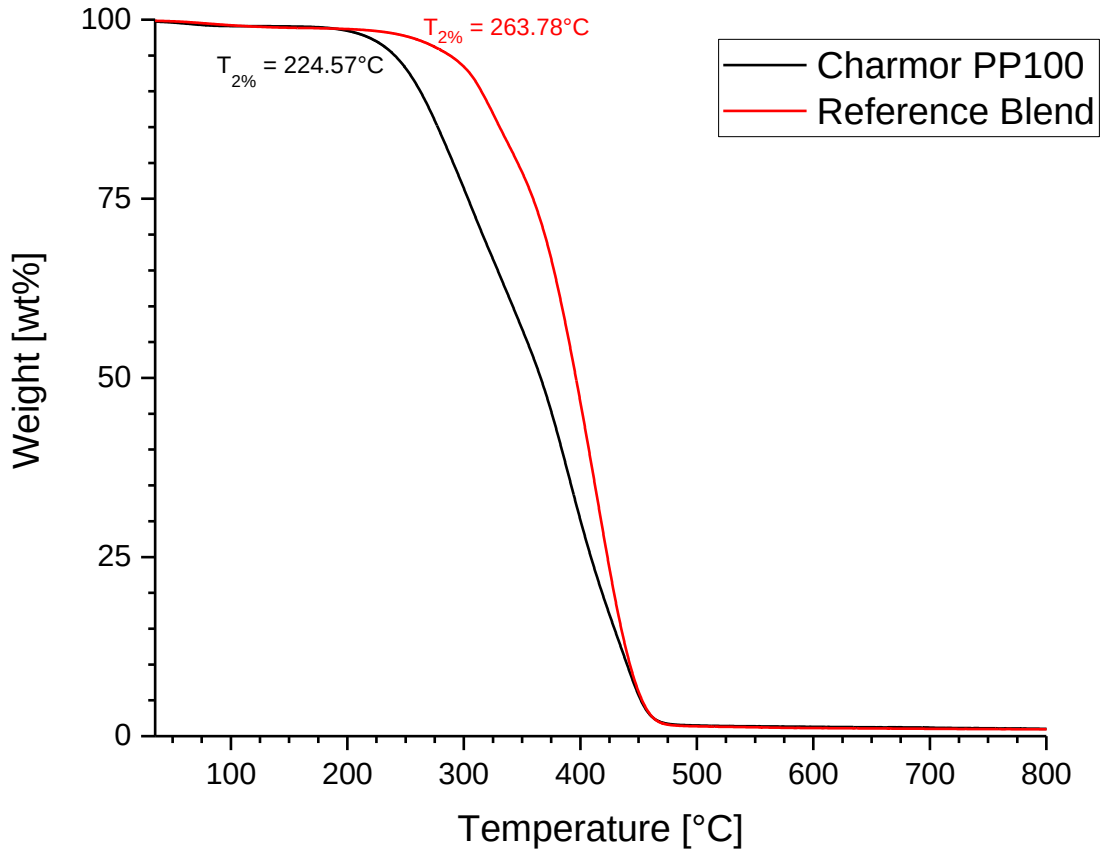

Figure 60: TGA comparison of **Charmor PP100** (black) and the **reference blend** (red).

Their melting and crystallization behavior was examined via DSC (Figure 61). Both **Charmor PP100** and the **reference blend** show broad melting and crystallization regions. For the **reference blend** DPE seems to be blended in well since on its own it has a melting point of around 220 °C[170] while the melting process of the blend stops around 170 °C. During the cooling process both substances behave in a similar fashion showing two crystallization peaks over a wide temperature range from around 30 °C to 140 °C.

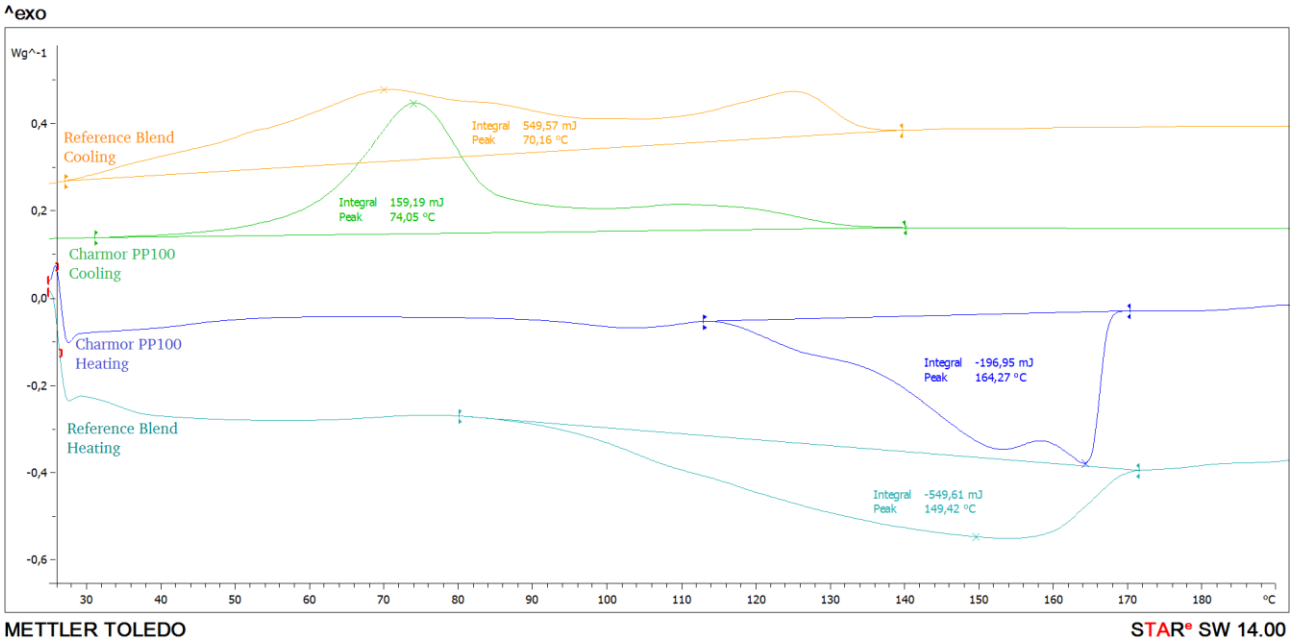

Figure 61: DSC of the second heating cycle of **Charmor PP100** (dark blue and green) and the **reference blend** (turquois and yellow). Heating rate: 10 K min^{-1}.

Due to the structural similarity of the two compounds and the enhanced thermal stability of the **reference blend** it was decided that the reaction for co-stabilizers of the patent of Ogemark *et al.*[169] is suitable for the synthesis of phosphorylated polyols (**P-Polyols**) (Figure 62; Table 9). One equivalent of the P-containing starting compounds synthesized in chapter 4.2.1 was added to a flask and mixed with x equivalents Bis-MPA and y equivalents of a polyol (DPE, PE or none) as showed in Table 9. The mixture was heated to 180 °C under reduced pressure until no gas formation could be observed from the melt. If not proceeding in a one-pot fashion, the hot melt was then filled into an aluminum pan and, after cooling down, pulverized with a mortar. The fine powder was then mixed with one weight equivalent of DPE and heated to 220 °C under reduced pressure until a homogeneous blend occurred. Again, the hot melt was allowed to cool down in an aluminum pan and the crude product was pulverized. The resulting powder had to be washed with sat. $NaHCO_3$ sol. and water since during both reaction steps a phosphorus based acid (depending on the P-starting compound) emerged that needed to be washed out. Due to that necessary purification step, the yield of the reactions was significantly lowered.

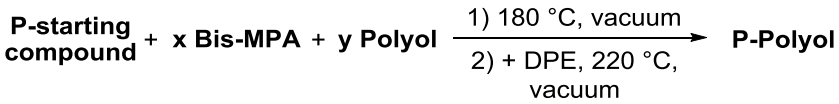

Figure 62: General synthesis procedure towards the different **P-Polyols**.

Table 9: Overview over the starting materials and reaction conditions for the various **P-Polyols**.

P-Polyol #	P-starting compound	x =	y =	Polyol =	One-Pot?
1	DiDOPO-PE	2	1	PE	No
2a	DOPO-TMP-d	2	1	PE	No
2b	DOPO-TMP	2	1	DPE	No
2c	DOPO-TMP	2	1	DPE	Yes
3	DOPO-TMP	1	0	-	No
4	Ph_2PO-TMP	1	0	-	Yes
5	$(PhO)_2PO$-TMP	1	0	-	Yes

To show the influence of a higher phosphorus amount in the generated P-Polyol, **P-Polyol 1** and **2a** with the defined **DiDOPO-PE** and **DOPO-TMP-d** as its P-starting compounds (Figure 63) were compared for their thermal properties with the non-phosphorus **Charmor PP100** and the **reference blend** (Figure 64). As can be seen, the doubled P-content of **P-Polyol 1** (P-content = 2.8 wt%) over **P-Polyol 2a** increases the thermal stability significantly from 240 to 267 °C. The residue is also slightly enhanced by 2 wt% from 8.6 to 10.6 wt%. The amount of residue indicates that DOPO acts partially in condensed phase but mostly in gas phase. However, the residue is not doubled despite a higher DOPO content, so there is no linear behavior between DOPO units and residue. Both P-containing Polyols are more stable than **Charmor PP100** and **P-Polyol 1** even reaches the stability of the reference blend. They both produce significantly more residue what might provide a good stabilizing effect. Despite showing the better thermal stabilities, **P-Polyol 1** cannot be produced in an atom-efficient scale due to the protective group chemistry and thus its application was not further pursued in this work.

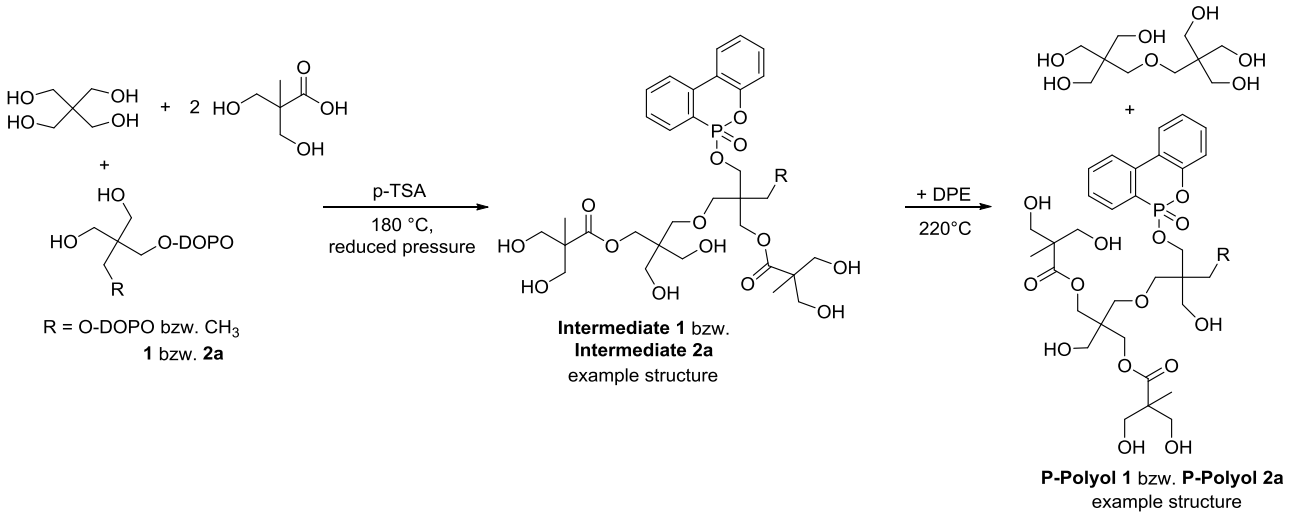

Figure 63: Proposed synthesis procedure of **P-Polyol 1** and **P-Polyol 2a**, respectively, using the defined starting materials **DiDOPO-PE** and **DOPO-TMP-d**.

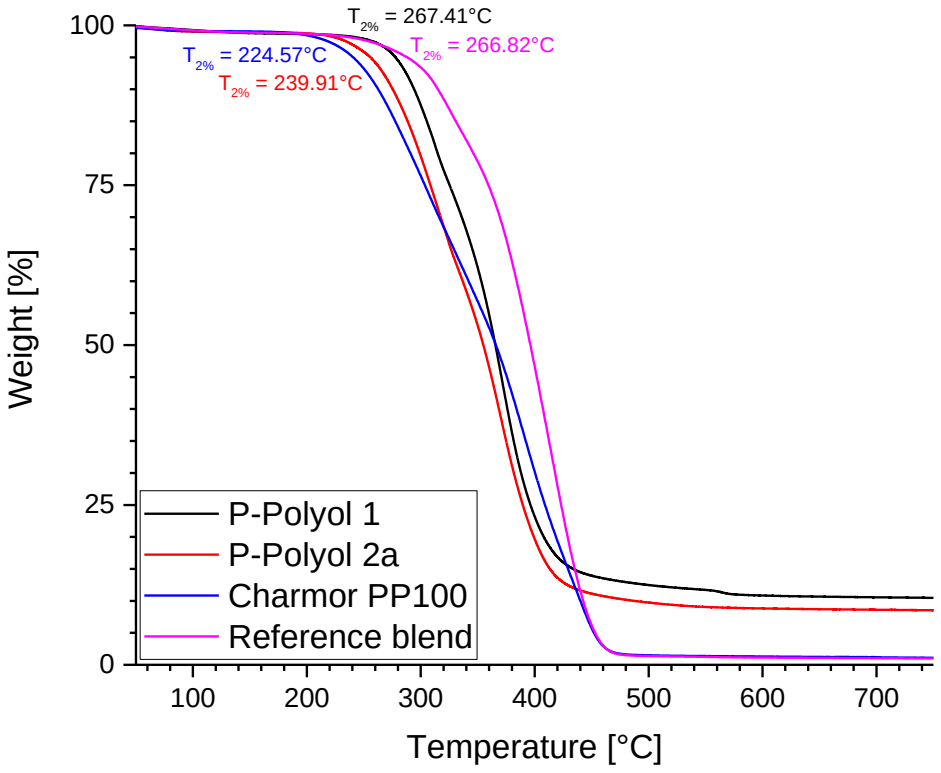

Figure 64: TGA comparison of **P-Polyol 1**, **2a**, **Charmor PP100** and the **reference blend**.

Because there was no possibility to filtrate the hot melt after the neutralization of p-TSA it was tested if the addition of p-TSA is necessary in the first step. Therefore, the first step towards **P-Polyol 1** (**Intermediate 1**) was performed with and without p-TSA and compared via ^{1}H-NMR (Figure 65).

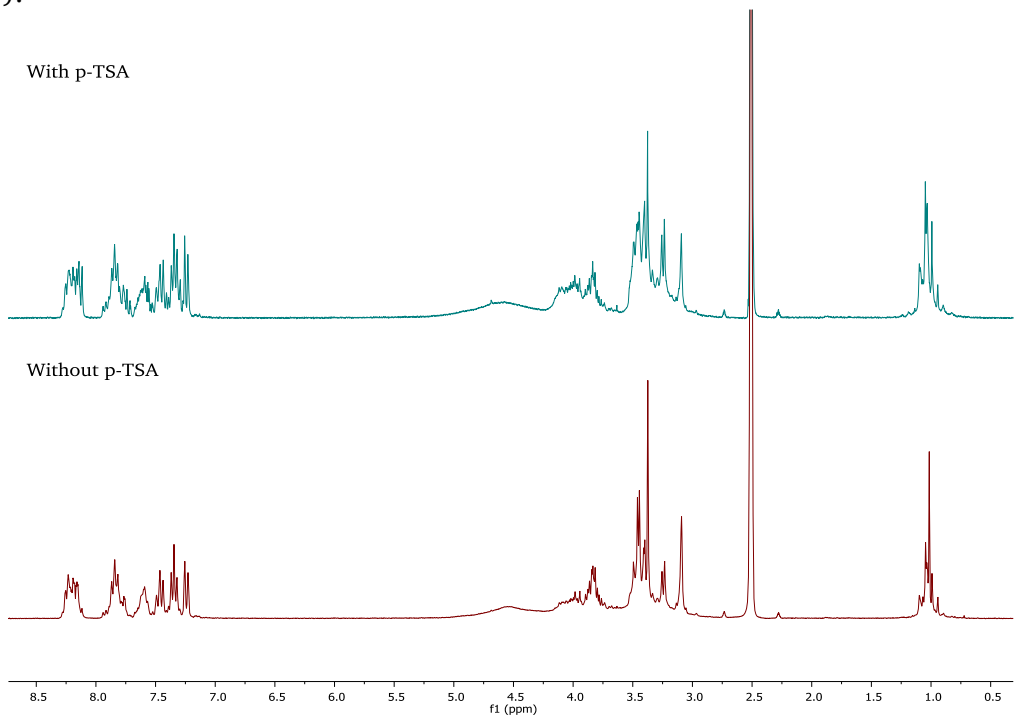

Figure 65: ^{1}H-NMR spectra of **intermediate 1** synthesized with p-TSA (top) and without p-TSA (bottom).

In both cases, Bis-MPA is condensed what can be seen from the methyl group signals around 1 ppm which should be a singlet if it did not react. Also, the signals in the ether and ester region are broadened, what indicates a successful reaction. This seems to be even more so with the use of p-TSA but nevertheless the reaction also proceeds without it. Thus, for all further synthesis of the P-Polyols no p-TSA was used.

To compare the influence of PE or DPE as additional polyol during the first reaction step, **P-Polyols 2a** and **2b** were compared. The addition of DPE instead of PE during the first step slightly increases the thermal stability by 11 °C but the higher amount of OH groups of **P-Polyol 2b** (OHV(P-Polyol 2a) = 786 mg g^{-1}; OHV(P-Polyol 2b) = 969 mg g^{-1}) does not enlarge the residue. This indicates that DPE does not act more efficient as a charring agent than PE in the interaction with DOPO.

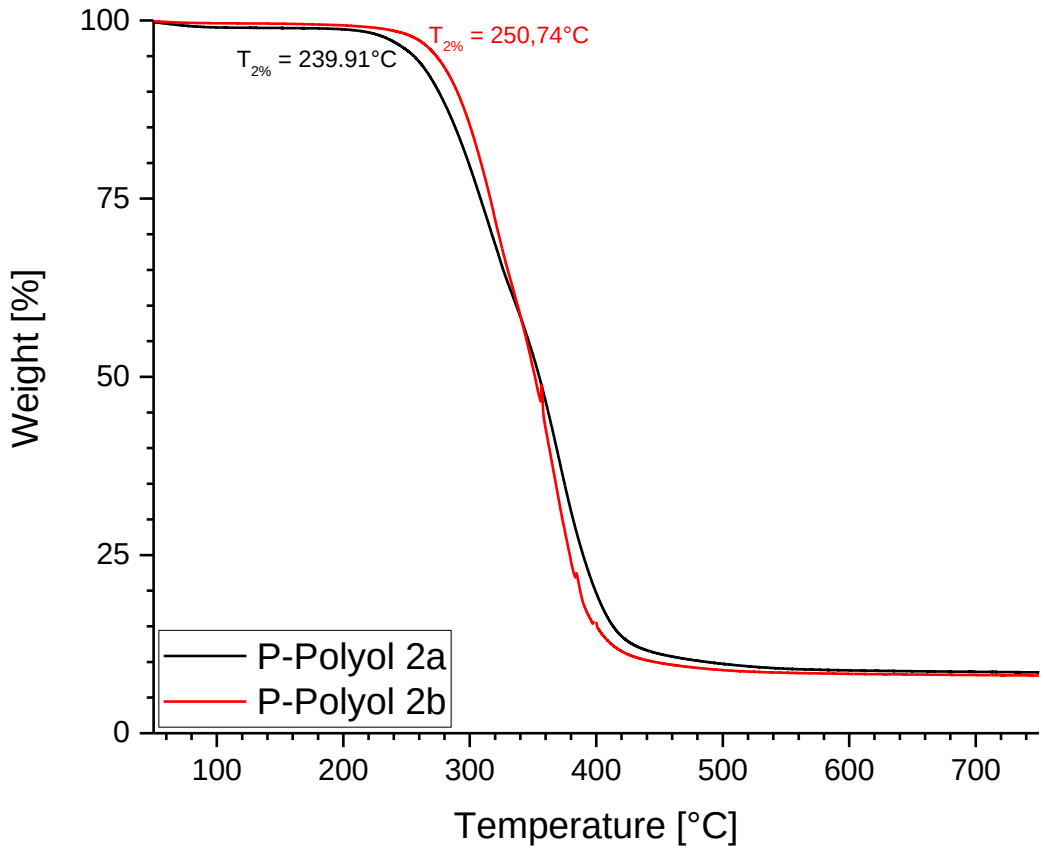

Figure 66: TGA comparison of the **P-Polyols 2a** (black) and **2b** (red).

It is assumed that the reaction is based on the condensation of the acid Bis-MPA with the OH-groups of the P-starting compound and the polyols but, due to the high temperature and the vacuum applied, also partially on the condensation of the OH-groups with each other to form a higher-molecular weight structure like in **Charmor PP100** (Figure 67).

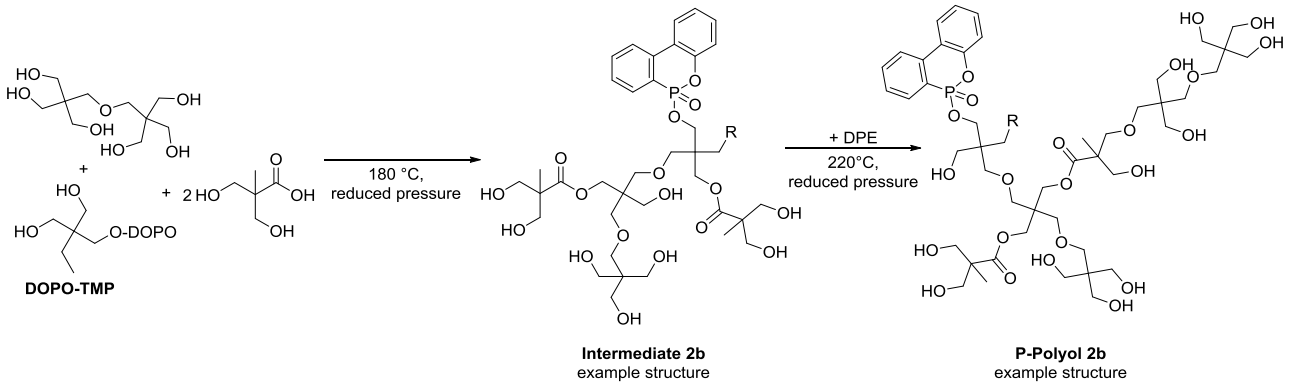

Figure 67: Proposed synthesis procedure of **P-Polyol 2b** using the starting material **DOPO-TMP**.

To gain a better insight on the reaction and the products, **P-Polyol 2b** was examined via matrix-assisted laser desorption/ionization time-of-flight mass spectrometry (MALDI-TOF) (Figure 68). No general repeating unit could be observed but fragments with molecular weights up to 1400 g mol^{-1}. A mixture of different low-molecular weight molecules of up to 800 g mol^{-1} can be proposed based on the results. Free **DOPO-TMP** and its by-products (di- and tri-substituted **DOPO-TMP**) can still be found. Esters of **DOPO-TMP** with Bis-MPA were also identified. Interestingly, DPE did not seem to react with Bis-MPA despite being present in the first reaction step. No condensation towards ether bonds was observed. Thus, it was concluded that at least in the first step no polyol (PE or DPE) is necessary, since it will not react with another component anyways and the P-content can be enlarged by cutting on the polyol content. If comparing the corresponding OHV from **P-Polyol 2b** and **P-Polyol 3** though, it is lowered from 969 to 808 mg g^{-1} (Table 10), which makes sense since more DPE is added in case of **P-Polyol 3**.

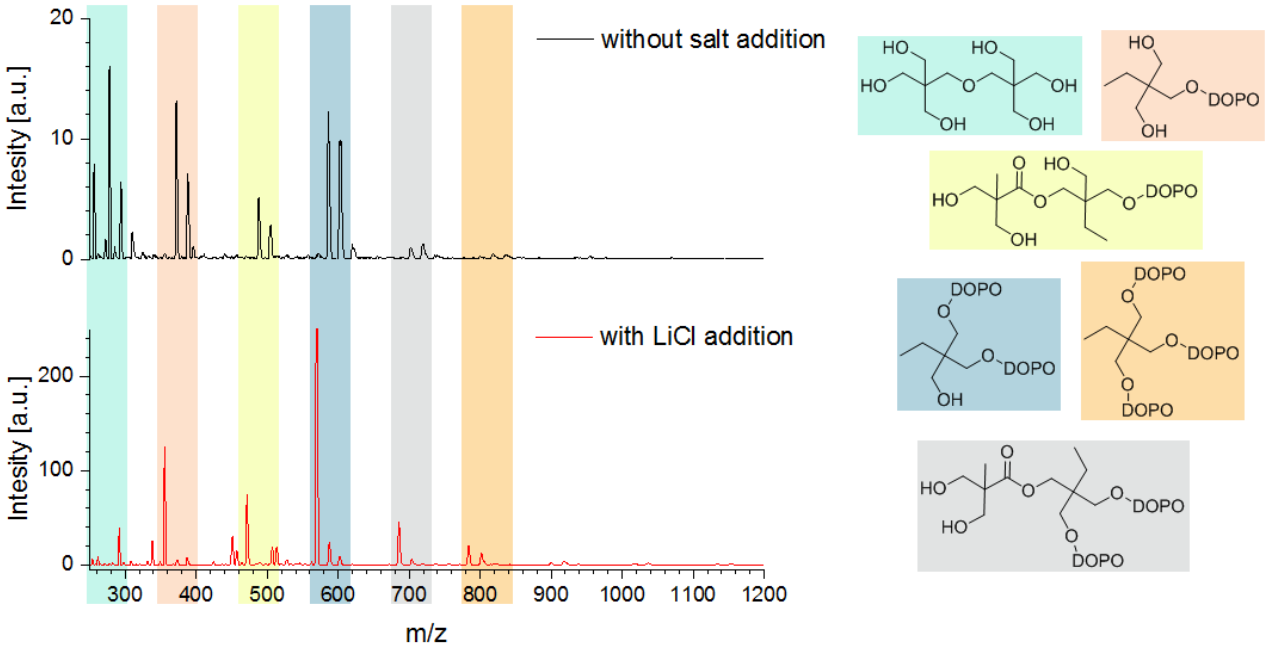

Figure 68: MALDI-TOF spectrum of **P-Polyol 2b** and thereon based structure suggestions.

Table 10: P-content calculated from ^{31}P-NMR spectra, OHV as well as TGA data for **P-Polyols 2b** and **3**.

P-Polyol	P-content / wt%	OHV / mg g^{-1}	$T_{2\%}$ / °C	Residue at 650°C / wt%
2b	1.8	969	250.06	8.2
3	2.3	808	229.54	9.0

When looking at the thermal stability of both **P-Polyols** (Table 10) they do behave very similar with an enhanced thermal stability for **P-Polyol 2b** but a slightly larger residue for **P-Polyol 3**. This is due to the higher P-content of **P-Polyol 3**.

To check the influence on the thermal properties of DPE addition in the blending step, a TGA of **DOPO-TMP**, **Intermediate 3** and **P-Polyol 3** (Figure 69) was performed (Figure 70, Table 11).

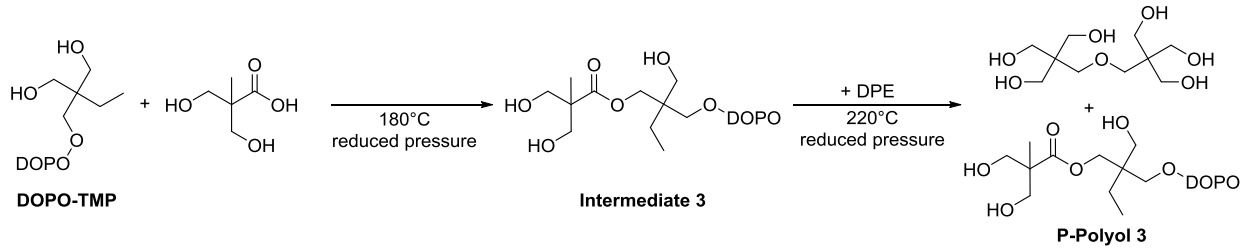

Figure 69: Reaction procedure towards **P-Polyol 3**.

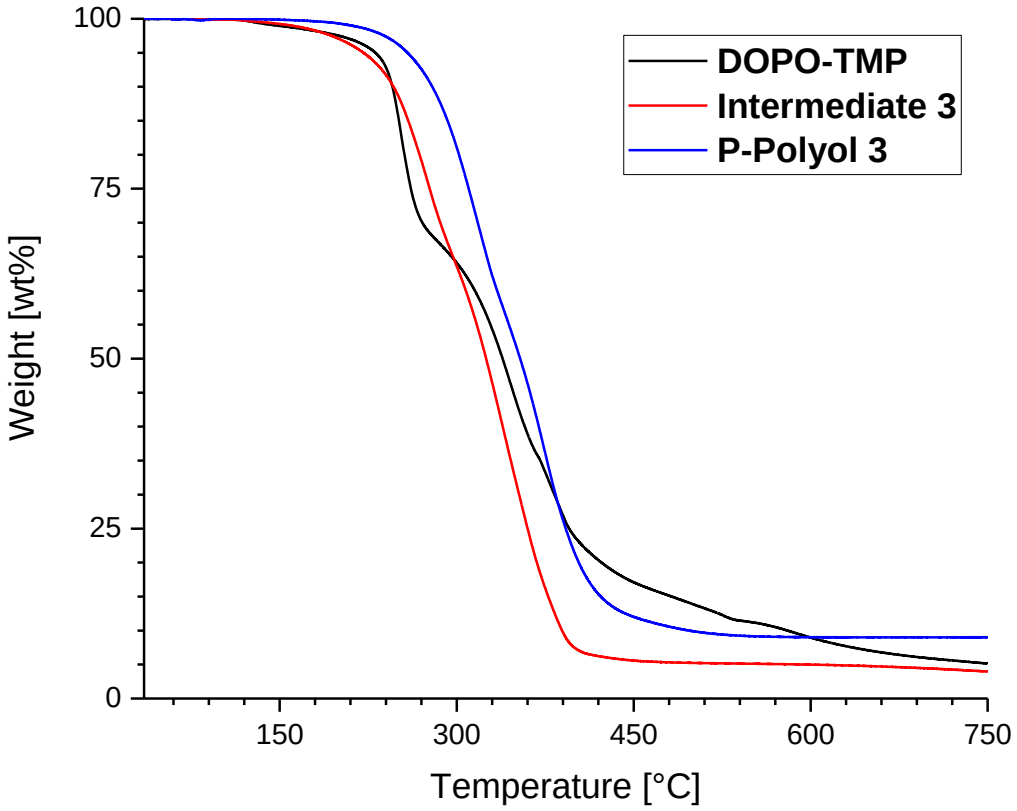

Figure 70: TGA comparison of the different reaction steps of **P-Polyol 3**.

Table 11: TGA data for the individual reaction steps for **P-Polyol 3** as well as the P-content for **DOPO-TMP**, **Intermediate 3** and **P-Polyol 3** calculated based on ^{31}P-NMR.

Sample	$T_{2\%}$ / °C	Residue at 650°C / wt%	P-content / wt%
DOPO-TMP	189.0	7.1	9.7
Intermediate 3	185.56	4.8	6.6
P-Polyol 3	229.54	9.0	2.3

Both **DOPO-TMP** and **Intermediate 3** start decomposing around 185-190 °C and due to the DPE addition the thermal stability is significantly enhanced by ~40 °C for **P-Polyol 3**. Despite a lower P-content (Table 11) for the P-Polyol compared to both the intermediate as well as **DOPO-TMP** it possesses an enhanced residue. This shows the role of DPE as a charring agent in in combination with phosphorus. It indicates that an acid is formed during heating that then can interact with DPE to form higher residue. Overall, blending of the intermediate product with DPE is beneficial for the desired thermal stability and enhanced residue and thus was executed for all following reactions.

Also, a one-pot approach for the generation of the P-Polyols was developed. For this process the intermediate product is not cooled down and pulverized and thus no prior, thorough mixing of the intermediate and DPE can be performed. It is necessary to mix the powder gradually into the hot melt. For **P-Polyol 2c** no mechanical stirrer, but only a stir bar was applied what lead to inhomogeneous mixing and significantly longer reaction times. Therefore increased degradation occurred and nearly 50 % (based on ^{31}P-NMR) of the phosphorus-based compound decomposed to the corresponding DOPO-based acid, 6-hydroxydibenzo[c,e][1,2]oxaphosphinine 6-oxide (DOPO-OH). However, when a mechanical stirrer was applied, these issues were eliminated and homogeneous melts with similar decomposition than the two-step procedure were produced.

P-Polyol 4 and **5** were synthesized based on the P-starting compounds **Ph_2PO-TMP** and **$(PhO)_2$PO-TMP**. Unfortunately though, **P-Polyol 5** could not be cleanly produced due to transesterification of the phenol groups when washing with $NaHCO_3$ sol. and water. Thus, only **P-Polyol 3** and **4** were compared for their thermal properties (Figure 71). As expected, the residue of **P-Polyol 4** with 3.2 wt% is significantly lower by 5.8 wt% compared to **P-Polyol 3** due to the mainly gas-phase activity of the phosphinate group compared to the phosphonate DOPO. It does, however, still possess a higher residue than the non-phosphorus-containing **Charmor PP100** or the **reference blend**. The thermal stability of **P-Polyol 4** though is slightly higher than for **P-Polyol 3**. As expected, the OHV for both Polyols are very similar around 800 mg g^{-1} due to the same synthesis procedure.

The thermal properties and OHV values for all synthesized **P-Polyols** are summarized in Table 12. There is a clear trend for the DOPO-containing **P-Polyols 1**, **2a**, **2b**, and **3** to generate more residue than the phosphinate-containing **P-Polyol 4** and the non-phosphorous polyols. Also, the OHV is the higher the more DPE or PE is in a sample, which is rather logical. **P-Polyol 2b** nearly possesses the same OHV as **Charmor PP100** and thus is a good candidate for heat stabilization.

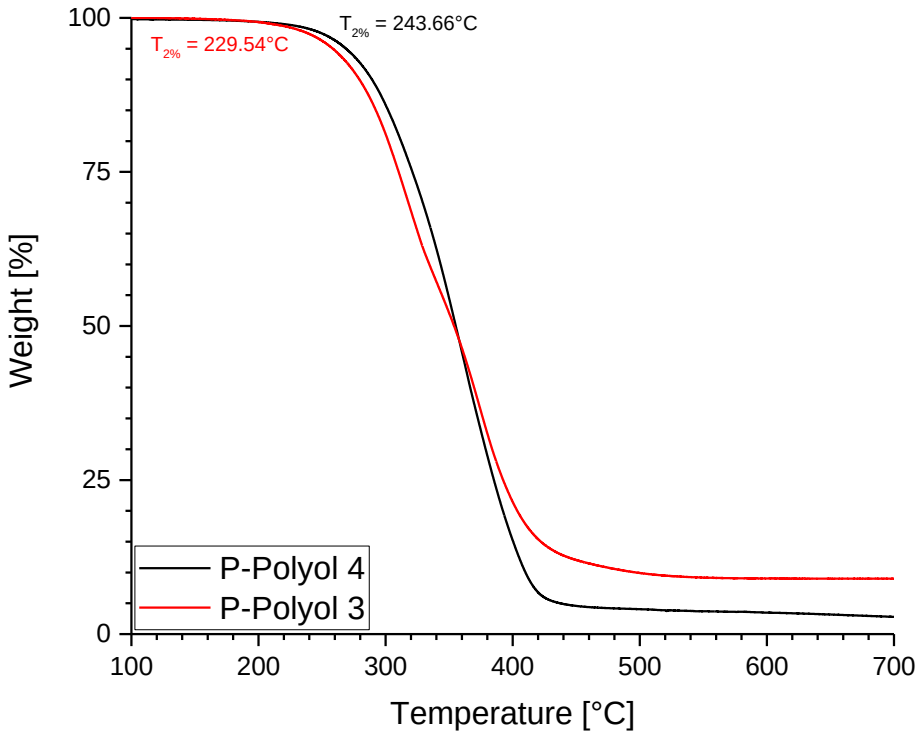

Figure 71: TGA comparison of **P-Polyol 3** and **4**.

Table 12: $T_{2\%}$ and char yields at 650 °C for the **P-Polyols** and the references **Charmor PP100** and the **reference blend**.

Sample	$T_{2\%}$ / °C	Residue at 650°C / wt%	OHV / mg g^{-1}	P-content* / wt%
P-Polyol 1	267.41	10.6	751	2.8
P-Polyol 2a	240.31	8.6	786	1.6
P-Polyol 2b	250.06	8.2	969	1.8
P-Polyol 3	229.54	9.0	808	2.3
P-Polyol 4	243.66	3.2	781	3.5
Charmor PP100	210.64	1.0	995	–
Reference Blend	266.82	1.0	862	–

*Calculated from ^{31}P-NMR.

Py-GC/MS at 600 °C of **P-Polyol 3** and **4** were performed to check if the expected FR mode of action in the gas phase can be confirmed. Since no **P-Polyol 5** could be obtained **$(PhO)_2$PO-TMP** was also measured under the same conditions as a phosphate for comparison. For all three components various low-molecular-weight aldehydes, alkenes and alcohols as well as CO_2 were found as gaseous decomposition products of the polyol part. The found fragments that emerged from the phosphorus species are shown in Figure 72. For the phosphinate-containing **P-Polyol 4** the phosphinic acid, a methanol ester and the diphenyl phosphinate radical were detected. Also, benzene radicals were vaporized occurring as possible decomposition products from the phosphinate that would lead to PO· radicals. The DOPO-containing **P-Polyol 3** released the expected molecules biphenyl, o-hydroxybiphenyl and DBF, which are typical DOPO decomposition products. The oxidized version of DOPO could also be detected as well as the DOPO radical. The main decomposition product of **$(PhO)_2$PO-TMP** is phenol. Since it is expected to act via a condensed-phase mechanism towards phosphoric acid this is within the expectations as well as undecomposed TMP that also emerged. However, phosphorus species' also were released as a phosphoric acid diphenyl ester and a bicyclic transesterification product with TMP, 4-ethyl-2,6,7-

trioxa-1-phosphabicyclo[2.2.2]octane 1-oxide. This is in agreement with the experiments regarding the synthesis of **P-Polyol 5** where transesterification occurred. Overall, the found fragments are in good agreement with the expected theory regarding the FR action mechanisms of phosphinates, phosphonates and phosphates.

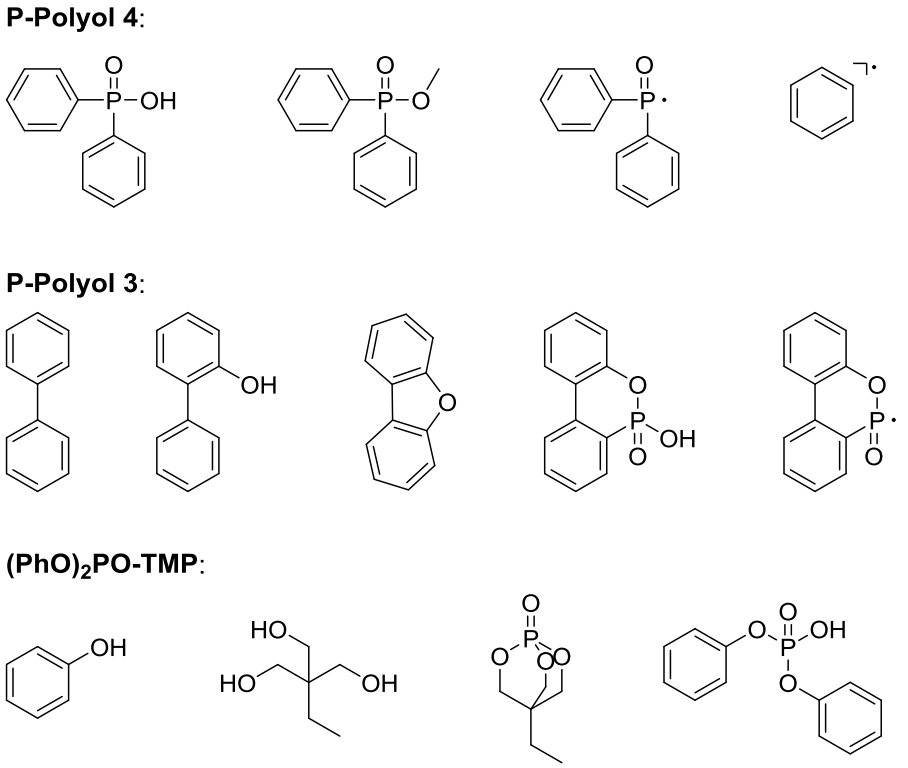

Figure 72: Gaseous decomposition fragments of **P-Polyol 3**, **4** and **$(PhO)_2PO$-TMP** detected via py-GC/MS at 600 °C.

4.2.3. Flame Retardancy Tests and Heat Stabilization of the Synthesized P-Polyols

For the heat stabilization of polyamides preferably only small amounts of polyols (0.25 to 6 wt%), like DPE or **Charmor PP100**, are applied.[136, 137, 139, 140] Due to the low P-content of the P-Polyols described in chapter 4.2.2 they would not be able to reach a classification during the UL94 test if used on their own as flame retardant in such concentrations. Thus, they were not incorporated in non-reinforced PA 6 and 66 on their own, but in mixture with DEPAL to check, whether they could reduce the necessary amount of DEPAL for a V-0 rating. To find a concentration at which DEPAL as a stand-alone flame retardant only reaches a V-1 rating, a concentration screening in PA 6 and 66 was performed (Compounds **X1**-**3**, Table 13 and Compounds **Y1**-**3**, Table 14). In PA 6, DEPAL reaches a V-1 rating when applied with 12 wt%, while in PA 66 a V-1 rating is reached with 8 wt%. A higher concentration will give a V-0 rating. Thus, **P-Polyol 3** (containing DOPO as phosphorus species), **P-Polyol 4** (containing Ph_2PO as phosphorus species) and, as a non-phosphorous reference, **Charmor PP100** were applied in PA 6 and 66 each with 1, 3 and 6 wt% in mixture with 12 wt% DEPAL for PA 6 and 8 wt% DEPAL for PA 66, respectively. The corresponding mixtures and UL94 ratings with the cumulated burning times over all measured samples are shown in Table 13 and Table 14.

Table 13: Extruded mixtures and UL 94 results of polyols and DEPAL in non-reinforced PA 6. UL 94 ratings are based on four specimens.

Sample	A1	A2	A3	B1	B2	B3	C1	C2	C3	X1	X2	X3
PA 6	82	85	87	82	85	87	82	85	87	85	87	88
DEPAL	12	12	12	12	12	12	12	12	12	15	13	12
P-Polyol 3 (DOPO)	6	3	1									
P-Polyol 4 (Ph_2PO)				6	3	1						
Charmor PP 100							6	3	1			
UL 94 1.6 mm	V2	V0	V0	V0	V0	V0	V0	V0	V2	V0	V0	V1
Cumulated burning time / s	63	8	12	8	8	11	10	8	10	13	9	36

Table 14: Extruded mixtures and UL 94 results of polyols and DEPAL in non-reinforced PA 66. UL 94 ratings are based on four specimens.

Sample	D1	D2	D3	E1	E2	E3	F1	F2	F3	Y1	Y2	Y3
PA 66	86	89	91	86	89	91	86	89	91	89	91	92
DEPAL	8	8	8	8	8	8	8	8	8	11	9	8
P-Polyol 3 (DOPO)	6	3	1									
P-Polyol 4 (Ph_2PO)				6	3	1						
Charmor PP 100							6	3	1			
UL 94 1.6 mm	V1	V0	V2	V0	V0	V0	V2	V0	V2	V0	V0	V1
Cumulated burning time / s	45	22	23	10	18	32	23	15	25	16	17	29

In PA 6, both P-Polyols give a V-0 rating with 1 wt% while with 1 wt% **Charmor PP100** the UL94 rating is V-2 and therefore worse than with 12 wt% DEPAL on its own. Interestingly, if more than 1 wt% **Charmor PP100** is applied a V-0 rating is achieved even without phosphorus. A higher amount of **P-Polyol 3** is not beneficial to the flame retardancy since sample **A1** gives a V-2 rating compared to the V-0 of **A2** and **A3**. This is contrary to samples **B1** and **C1** and indicates that DOPO is not a good synergist with DEPAL in PA 6 for an enhanced flame retardancy.

In PA 66, samples **E1**-**E3**, containing **P-Polyol 4**, give a V-0 rating. The cumulated burning time decreases with the increase of the P-Polyol concentration. In contrast to PA 6, the DOPO-containing sample **D3** gives a V-2 rating if applied with 1 wt% as does sample **F3**. Also, 6 wt% does only give a V-1 rating for sample **D1** and a V-2 rating for **F1**, respectively. This is inconsistent with both **D2** and **F2** which achieve a V-0 rating with 3 wt% of the respective polyol. This indicates an enhanced decomposition of PA 66 with a higher amount of either **Charmor PP100** or **P-Polyol 3**. This is in contrast to the **P-Polyol 4**-containing sample **E1**, for which the cumulated burning time of 10 s and a V-0 rating was achieved and thus no accelerated decomposition can be observed.

Overall, **P-Polyol 4** yields V-0 for both matrix polymers ratings in any concentration and thus can replace 1 wt% of DEPAL in PA 6 and PA 66, while **P-Polyol 3** can do the same but only in PA 6.

For testing the heat stabilization of the P-polyols, a concentration screening 0.5, 1 and 1.5 wt% in non-reinforced PA 6 was performed. Therefore, **Charmor PP100** and **P-Polyol 2b** were incorporated into PA 6 and those compounds as well as a reference sample of pure PA 6 without any stabilizer were aged at 200 °C (Table 15). Mechanical tests were conducted after 0, 258 and 500 h.

Table 15: Extruded mixture of different polyols in PA 6 for aging experiments.

Compound	1	2	3	4	5	6	PA 6
PA6	98.5	99.0	99.5	98.5	99.0	99.5	100
Charmor PP100	1.5	1.0	0.5	0	0	0	0
P-Polyol 2b	0	0	0	1.5	1.0	0.5	0

To check on the influence of the additives before aging, the maximum stress at 0 h was compared for all compounds (Figure 73). As expected, samples **3** and **6** had the least influence on the maximum stress due to only 0.5 wt% additive. Sample **4** with 1.5 wt% **P-Polyol 2b** also possesses a similar influence on the maximum stress of the material, however, sample **4** also has the highest error value.

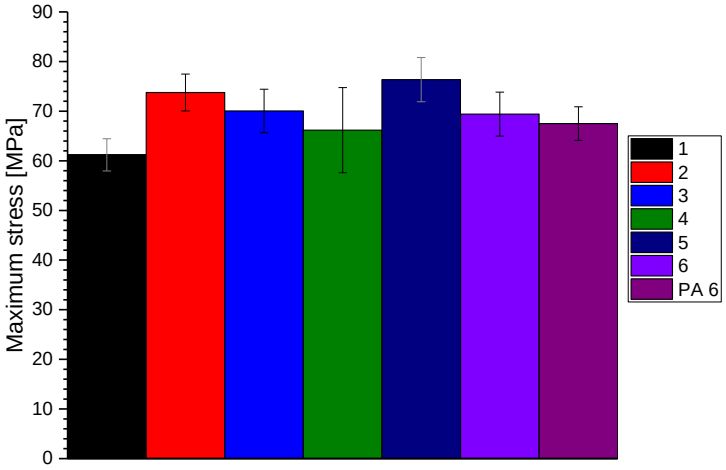

Figure 73: Maximum stress time for the stabilized and unstabilized, non-reinforced PA 6 samples before treatment at 0 h.

However, when comparing the maximum stress for the aged samples no clear result for the mechanical behavior was obtained since the samples after 258 and 500 h did break comparatively fast resulting in very large error values. The high inaccuracy of the measurement can be understood when looking at the elongation at break versus aging time (Figure 74). The samples do not retain their elongation at all and thus the mechanical behavior is changed completely making it not meaningful to compare the maximum stress. An example of the changed mechanical behavior of the mechanical test of a specimen of compound **3** with 0.5 wt% **Charmor PP100** is given in Figure 75. At 0 h, prior aging, the material shows necking and a high toughness and formability. After aging the material becomes brittle. These results show that even the reference **Charmor PP100** does not stabilize non-reinforced PA 6.

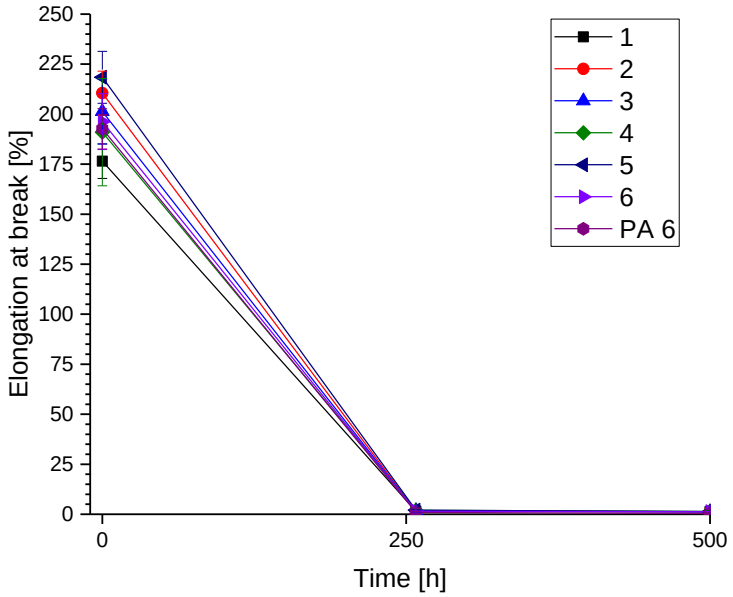

Figure 74: Elongation at break versus aging time for the stabilized and unstabilized, non-reinforced PA 6 samples.

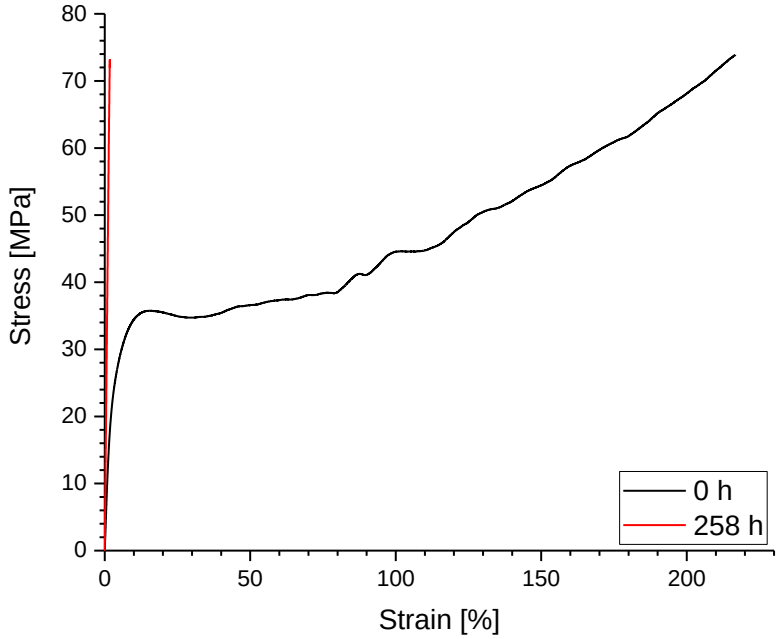

Figure 75: Stress versus strain for one test specimen of compound **3** before aging and after 258 h at 200 °C.

When looking in the literature, in which polyols are utilized as thermal stabilizers, all specified examples containing polyols were performed with GF-reinforced polyamides as matrix systems.[137, 139-141] Thus, **Charmor PP100** and **P-Polyol 2b** were also incorporated with 0.5 wt% in 30% GF-reinforced PA 6 which already contains a halogen-free FR (Ultramid® B3U50G6[2]). The specimens were also aged at 200 °C for up to 500 h and tensile tests were performed after 0, 48, 150, 300 and

[2] Material data sheet: Ultramid® B3U50G6, BASF SE. Ludwigshafen, 2018.

500 h. Figure 76 shows the maximum stress versus the aging time for both compounds as well as the target value of the unstabilized polymer without thermal aging. **P-Polyol 2b** does not influence the maximum stress after the incorporation whereas **Charmor PP100** does enlarge it from 170 to 186 MPa (Table 16). This indicates partial cross-linking during the extrusion process what is possibly due to starting decomposition of **Charmor PP100**. Even with the addition of only 0.5 wt% **Charmor PP100** the material does retain 82 % of its maximum stress after 500 h of aging. **P-Polyol 2b** does also maintain 75 % of the materials maximum stress and is thus slightly less efficient. Nevertheless, the synthesized **P-Polyol** shows a promising trend as a combination of FR and heat stabilization since they can save currently used flame-retardants while still retain mechanical properties of GF-reinforced polyamides.

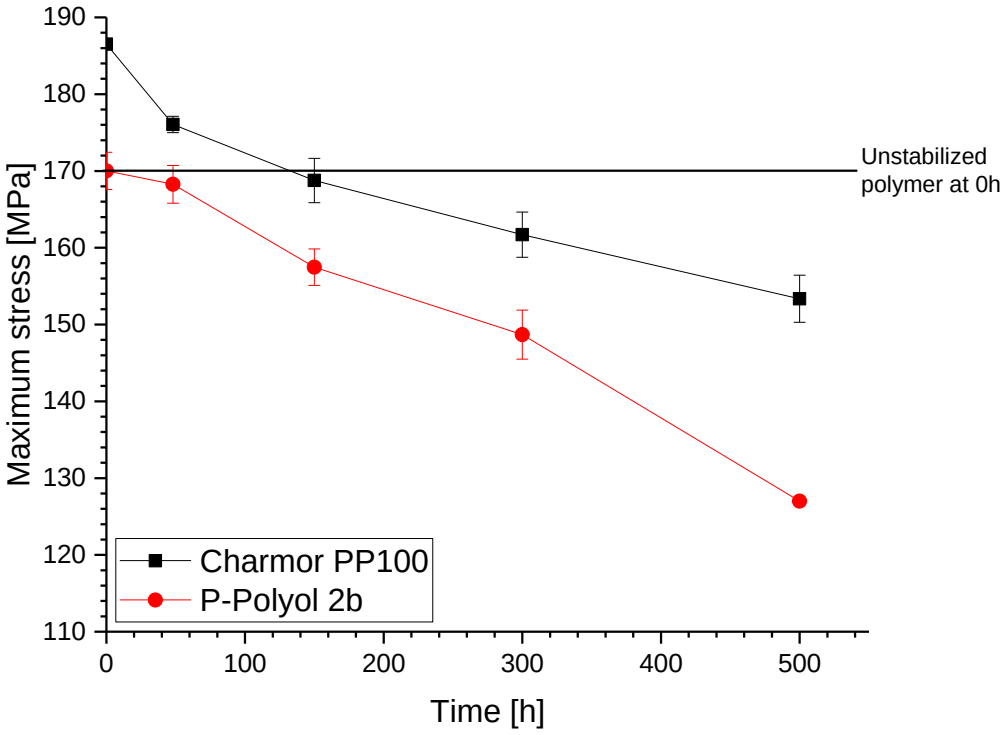

Figure 76: Maximum stress versus aging time at 200 °C of GF-reinforced compounds with 0.5 wt% **Charmor PP100** (black) and **P-Polyol 2b** (red), respectively. The black line corresponds to the unstabilized polymer at 0 h. The value is taken from the material data sheet.[2]

Table 16: Retention of the maximum stress of the aged compounds after 500 h with 0.5 wt% addition of the respective additive.

Compound	Maximum Stress at 0 h aging time / MPa	Maximum Stress at 500 h aging time / MPa	Retention of maximum stress at 500 h / %
Charmor PP100	186	153	82
P-Polyol 2b	170	127	75

4.2.5. P- and OH-containing Polyacrylamides, Polyacrylates and Copolymers

Another approach towards the combination of heat stabilization and flame retardancy in one molecule was the copolymerization of phosphorus-containing acrylates and acrylamides with OH-containing ones. OH-containing acrylates and acrylamides are usually applied due to their hydrophilic nature. They also can easily be copolymerized with other acrylates or acrylamides for the combination of different functionalities.[171-173] They may be used as biocompatible films[174, 175], as anti-fouling material[176-178], as component in adhesive resins in the dental sector[179, 180] or as hydrogels for various applications[181-184] like, for example, contact lenses[185] but there is a wide scope of potential applications. In the case of heat stabilization, the influence of the amount and chemical environment of the hydroxyl groups should be investigated in comparison to the P-Polyols.

The molecules shown in Figure 77 were chosen as monomers for homo- and copolymerizations in multiple combinations in order to vary in the number of OH groups, the phosphorus content, the polymer structure (thermoset or thermoplastic) and the chemical properties (acrylamide or acrylate). The P-containing molecules needed to be synthesized prior polymerization. Compound **1-A** was synthesized *in situ* prior copolymerization as described in chapter 4.1.1. **DOPO-*N*-HEAA** was prepared according to literature in an Atherton-Todd reaction (Figure 78).[186] The synthesis of **DOPO-HEA** was conducted with the same reaction conditions.

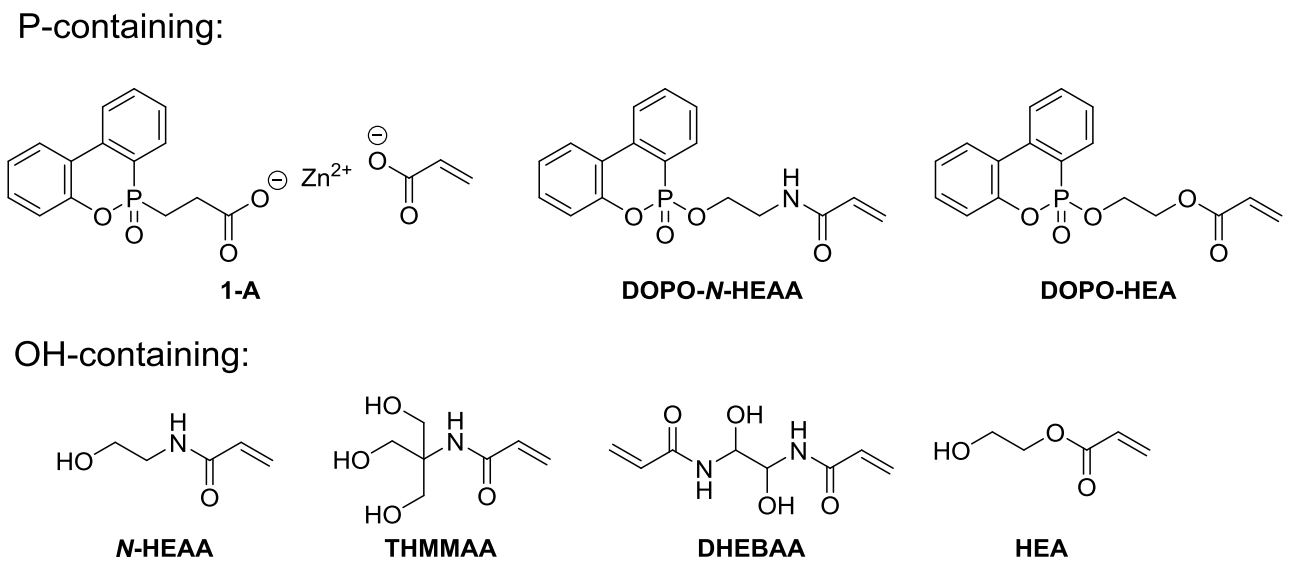

Figure 77: Monomers for the polymerization and copolymerization of P- and OH-containing polymers.

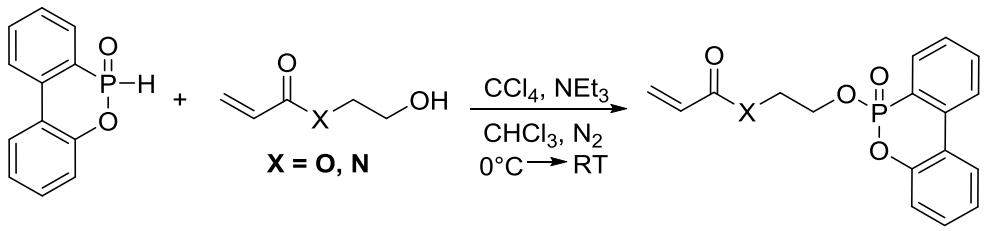

Figure 78: Atherton-Todd reaction of DOPO with HEA (X=O) or *N*-HEAA (X = N).

For polymerizations, the conditions shown in Table 17 were applied. They were all initiated with the radical starter AIBN. The linear polymer **Poly(DOPO-*N*-HEAA)** as well as its monomer were prepared earlier in our research group.[186]

Table 17: Polymerization conditions for the different polyacrylates and –acrylamides.

Polymer	Monomer A	Monomer B	Monomer ratio	Solvent
Poly(*N*-HEAA)	N-HEAA	–	–	THF/toluene
Poly(HEA)[187]	HEA	–	–	ethanol
Poly(DOPO-*N*-HEAA)	DOPO-N-HEAA	–	–	toluene
Poly(DOPO-HEA)	DOPO-HEA	–	–	ethanol
DHEBAA:*N*-HEAA-Copolymer	N-HEAA	DHEBAA	9:1	DMAc
DOPO-*N*-HEAA/*N*-HEAA-Copolymer	N-HEAA	DOPO-N-HEAA	1:1	acetonitrile
DOPO-HEA/HEA-Copolymer	HEA	DOPO-HEA	1:1	ethanol
1-A/N-HEAA-Copolymer	N-HEAA	1-A	1:1	DMAc
THMMAA/*N*-HEAA-Copolymer	N-HEAA	THMMAA	9:1	acetonitrile/toluene

To test the difference between a linear and a cross-linked polyacrylamide, *N*-HEAA was copolymerized with DHEBAA in a ratio of 9:1 in DMAc. A swollen hydrogel emerged that showed strong decomposition upon drying in a vacuum oven at elevated temperature. Thus, it can be concluded that the cross-linked structure is not suitable for the incorporation into polyamides and no further experiments on this copolymer were performed.

To examine the influence of an enlarged amount of OH-groups a 9:1 copolymer of *N*-HEAA and THMMAA was produced. The corresponding TGA curve in comparison with pure **Poly(*N*-HEAA)** can be seen in Figure 79. As expected, the thermal stability does not differ significantly. Since no char forming agent like a phosphorus species is involved, the higher amount of OH-groups of the copolymer does not result in a remarkably higher amount of char.

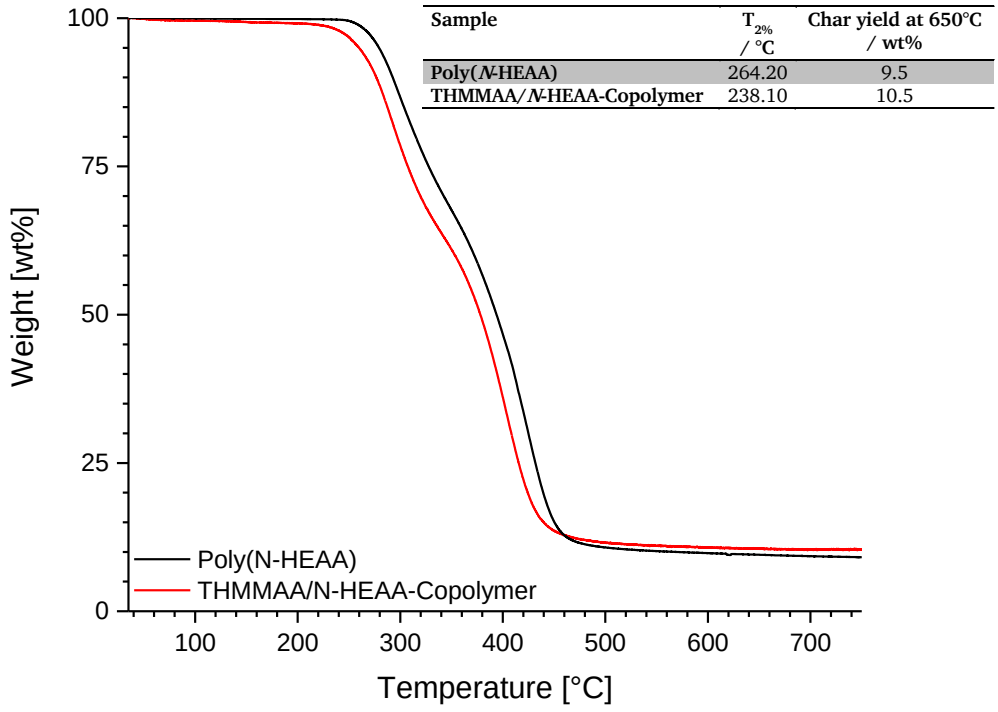

Figure 79: TGA comparison of **Poly(*N*-HEAA)** (black) and the **THMMAA/*N*-HEAA-Copolymer** (red).

When comparing the hydroxyl-containing polyacrylate to the -acrylamide, it is notably that the thermal stability is significantly enhanced by more than 35 °C for the polyacrylate (Figure 80). This shows that the dissociation energy for the C–N-bond is lower than for the C–O-bond in case of the hydroxyethyl-substituted polyacrylate and -acrylamide. The curve progression for **Poly(HEA)** undergoes a sudden weight loss at 325 °C which is corresponding to ethylene glycol.[188] The abrupt drop occurred on multiple measurements under nitrogen or air and a possible explanation could be the physical appearance of the polymer. It is a highly viscous gel with a T_g of 14.15 °C. Due to this liquid-like structure, during the degradation a bubble with trapped gaseous degradation products can be formed by the polymer that then erupts at 325 °C releasing the gases all at once what results in this steep step.[189] However, this does not seem to influence the amount of residue when compared to literature.[189, 190] The formed residue at 650 °C is higher for **Poly(*N*-HEAA)** by nearly 5 wt%. This as well as the viscous aggregate state make pure **Poly(HEA)** not as desirable for the incorporation into polyamides as heat stabilizer.

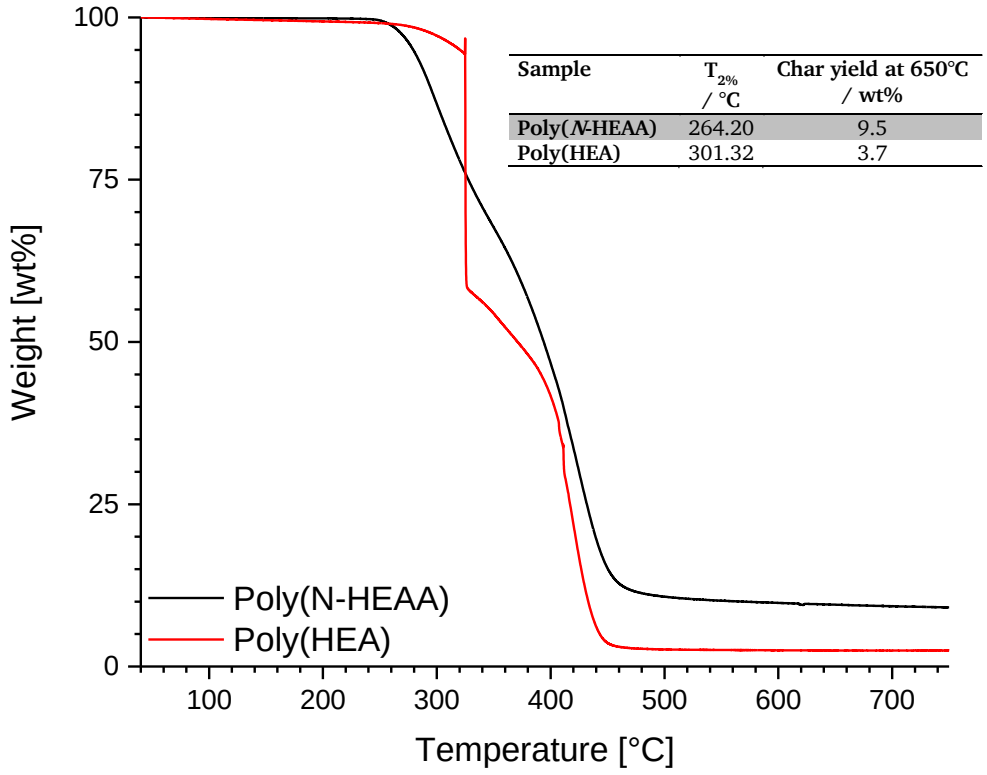

Sample	$T_{2\%}$ / °C	Char yield at 650°C / wt%
Poly(*N*-HEAA)	264.20	9.5
Poly(HEA)	301.32	3.7

Figure 80: TGA comparison of **Poly(*N*-HEAA)** (black) and **Poly(HEA)** (red).

To combine phosphorus and hydroxyl groups in one polymer **DOPO-*N*-HEAA** was copolymerized with one equivalent ***N*-HEAA** in an acetonitrile solution using AIBN as initiator. For comparison also the homopolymer **Poly(DOPO-*N*-HEAA)** was synthesized. The thermal degradation of both polymers and **Poly(*N*-HEAA)** is shown in Figure 81. What is remarkable is that both homopolymers are far more stable than the copolymer by over 70 °C. **Poly(DOPO-*N*-HEAA)** starts decomposing at 266.7 °C, which is nearly the same temperature as for **Poly(*N*-HEAA)** though the yield of residue is larger by roughly 4.5 wt%. This effect of an enlarged residue was observed before for several substances where DOPO was combined with nitrogen in one molecule.[191-194] As can be seen, for the **DOPO-*N*-HEAA/*N*-HEAA**-copolymer the residue is again significantly higher although it has a lower phosphorus content than **Poly(DOPO-*N*-HEAA)** (Table 18). This is due to the combination of phosphorus and primary hydroxyl functionalities that can be dehydrated.

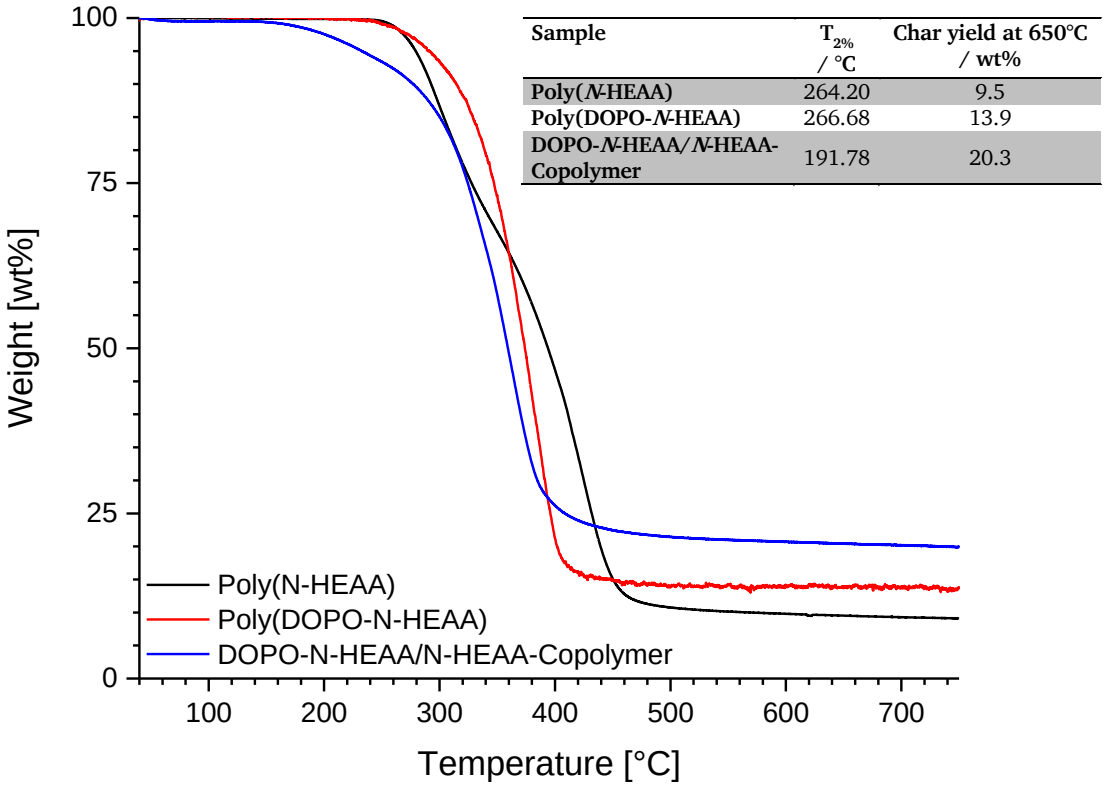

Sample	$T_{2\%}$ / °C	Char yield at 650°C / wt%
Poly(*N*-HEAA)	264.20	9.5
Poly(DOPO-*N*-HEAA)	266.68	13.9
DOPO-*N*-HEAA/*N*-HEAA-Copolymer	191.78	20.3

Figure 81: TGA comparison of **Poly(*N*-HEAA)** (black), **Poly(DOPO-*N*-HEAA)** (red) and the **DOPO-*N*-HEAA/*N*-HEAA-copolymer** (blue).

Similar trends are followed for the corresponding polyacrylates **Poly(HEA)**, **Poly(DOPO-HEA)** and the **DOPO-HEA/HEA**-copolymer (Figure 82). Again, the thermal stability for the copolymer is lower although with 25 °C this effect is not as distinct as for the **DOPO-*N*-HEAA/*N*-HEAA**-copolymer. Also, its char yield at 650 °C is the highest of the three polyacrylates. Compared to the respective polyacrylamides, the residue for the DOPO-containing polyacrylates is slightly higher despite pure **Poly(HEA)** possessing a lower char yield than **Poly(*N*-HEAA)**. As explained in chapter 2.3.2, phosphorus-containing FRs act via dehydration in the condensed phase and thus are more efficient in oxygen-containing moieties. Since acrylates contain more oxygen atoms than acrylamides they form a larger amount of residue. The drawback of **Poly(HEA)** being a viscous gel was overcome by the addition of DOPO to the monomer structure with a T_g of 76.17 °C for **Poly(DOPO-HEA)** and 61.22 °C for the 1:1 copolymer.

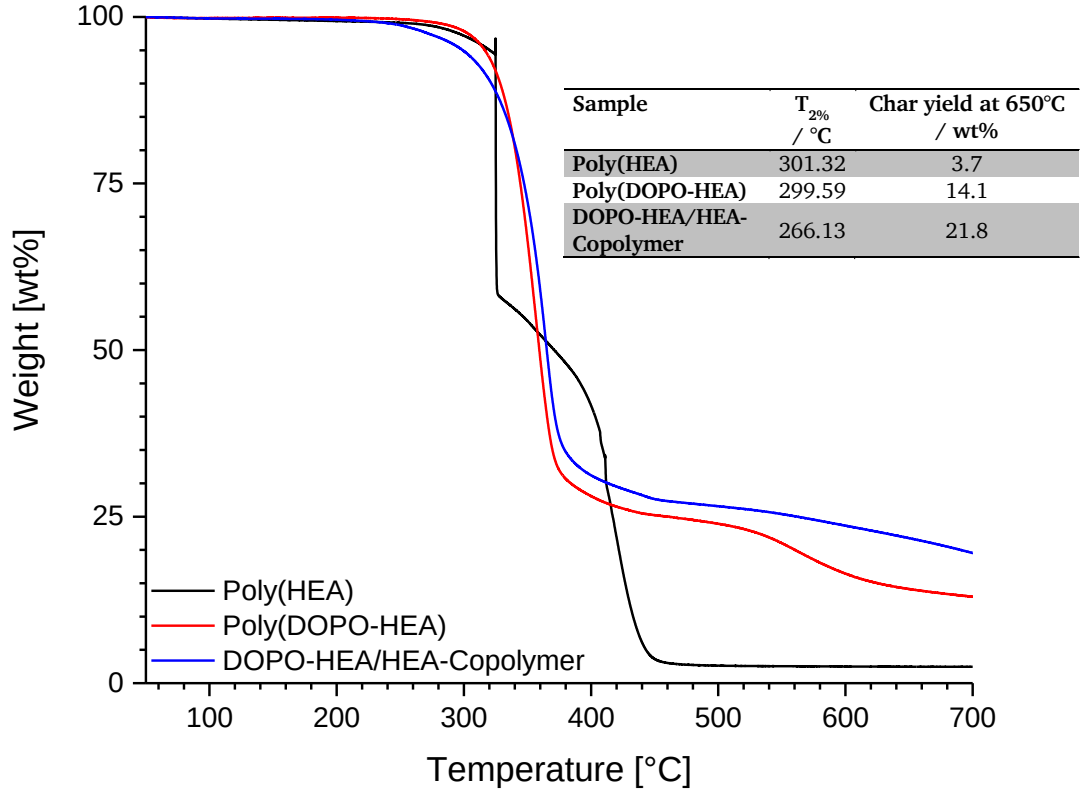

Sample	$T_{2\%}$ / °C	Char yield at 650°C / wt%
Poly(HEA)	301.32	3.7
Poly(DOPO-HEA)	299.59	14.1
DOPO-HEA/HEA-Copolymer	266.13	21.8

Figure 82: TGA comparison of **Poly(HEA)** (black), **Poly(DOPO-HEA)** (red) and the **DOPO-HEA/HEA-copolymer** (blue).

Because of the assumption that an enlarged char yield supports the shielding mechanism of heat stabilization, compound **1-A** (described in chapter 4.1.1) was copolymerized with ***N*-HEAA** in DMAc. Therefore, **1-A** was synthesized *in situ* as described earlier and one equivalent ***N*-HEAA** followed by an AIBN solution was added to the reaction solution. As can be seen in Figure 83, the copolymer possesses a similar thermal stability as **Poly(*N*-HEAA)**. This differs from the previous copolymers which were always less stable than the respective homopolymers. However, the homopolymers' stabilities are around 40 °C apart from each other which was not the case previously. Again, the residue at 650 °C is the largest for the copolymer despite possessing a lesser content of zinc and phosphorus than **Poly(1-A)** (Table 18).

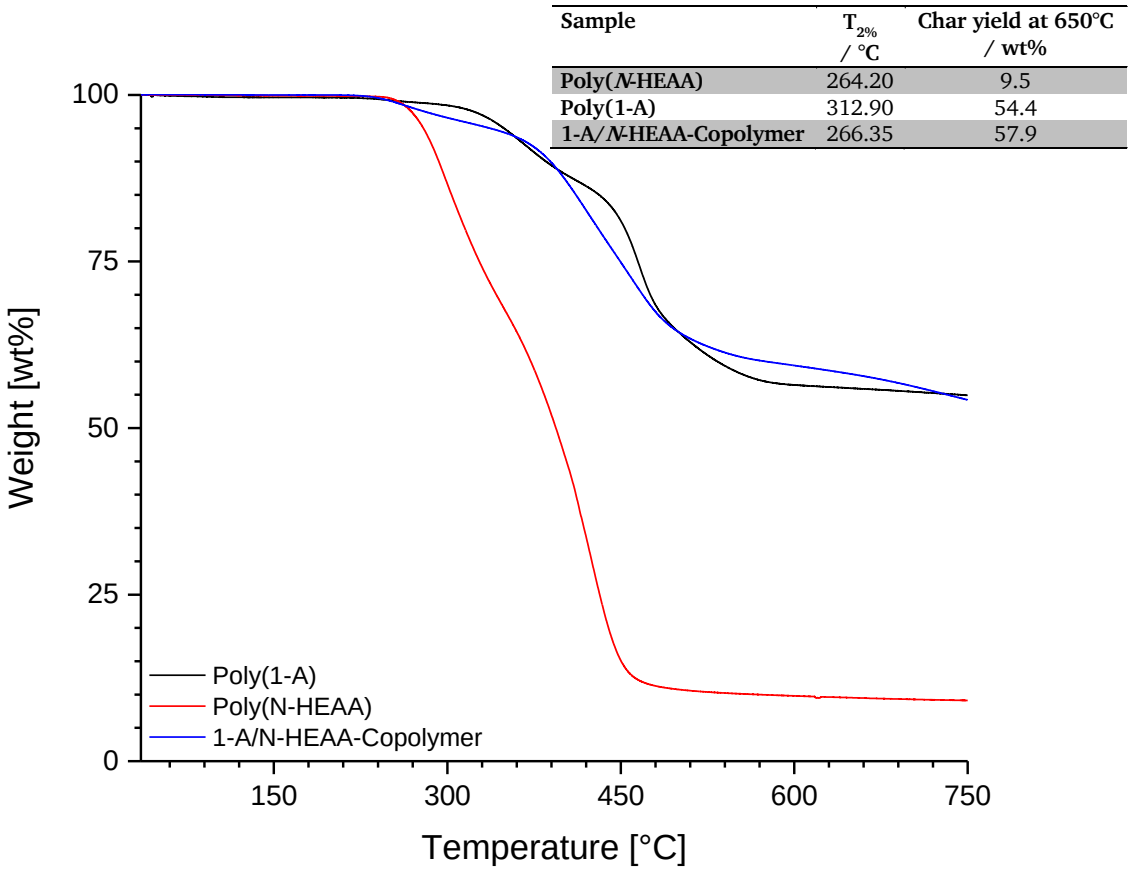

Figure 83: TGA comparison of **Poly(1-A)** (black), **Poly(*N*-HEAA)** (red) and the **1-A/*N*-HEAA-copolymer** (blue).

Table 18 shows the char yields and decomposition temperatures as well as the phosphorus content of all synthesized polyacrylates, –acrylamides and copolymers. In summary, it can be stated that the combination of phosphorus and hydroxyl groups in one polymer, as expected, does yield in higher amounts of residue what might be beneficial for both flame retardancy and heat stabilization. The acrylate-containing polymers tend to have higher thermal stabilities what is beneficial to the incorporation into polyamides. Though, the reference stabilizer **Charmor PP100** is only thermally stable up to 210 °C and is being used in polyamides nonetheless.

Table 18: Summarized decomposition temperatures, char yields at 650 °C and calculated P-content of the different Polyacrylates and –acrylamides measured via TGA under nitrogen.

Sample	$T_{2\%}$ / °C	Char yield at 650°C / wt%	P-content* / wt%
Poly(N-HEAA)	264.20	9.5	–
Poly(HEA)	301.32	3.7	–
Poly(DOPO-*N*-HEAA)	266.68	13.9	9.4
Poly(DOPO-HEA)	299.59	14.1	9.4
Poly(1-A)	312.90	54.4	7.3
DOPO-*N*-HEAA/*N*-HEAA-Copolymer	191.78	20.3	7.0
DOPO-HEA/HEA-Copolymer	266.13	21.8	6.9
1-A/N-HEAA-Copolymer	266.35	57.9	3.8
THMMAA/*N*-HEAA-Copolymer (1:9)	238.10	10.5	–

*P-content calculated based on stoichiometric conversion.

4.2.6. Heat Stabilization of OH-containing Acrylamides

To check if the concept of OH-containing acrylamides or acrylates is feasible for the heat stabilization of polyamides, **Poly(*N*-HEAA)** was incorporated into the same GF-reinforced PA 6 as **P-Polyol 2b** (Ultramid® B3U50G6) with 0.5 wt%, since non-reinforced PA 6 was not stabilized even by **Charmor PP100**. The influence of the amount of OH-groups was tested with the incorporation of 0.5 wt% of the **THMMAA/*N*-HEAA**-Copolymer. Both compounds were aged in a circulating air oven at 200 °C and tensile tests were performed after 0, 48, 150, 300 and 500 h. Figure 84 shows the maximum stress versus the aging time of the specimen as well as of the reference polyol **Charmor PP100** and Table 19 summarizes their retention of the maximum stress.

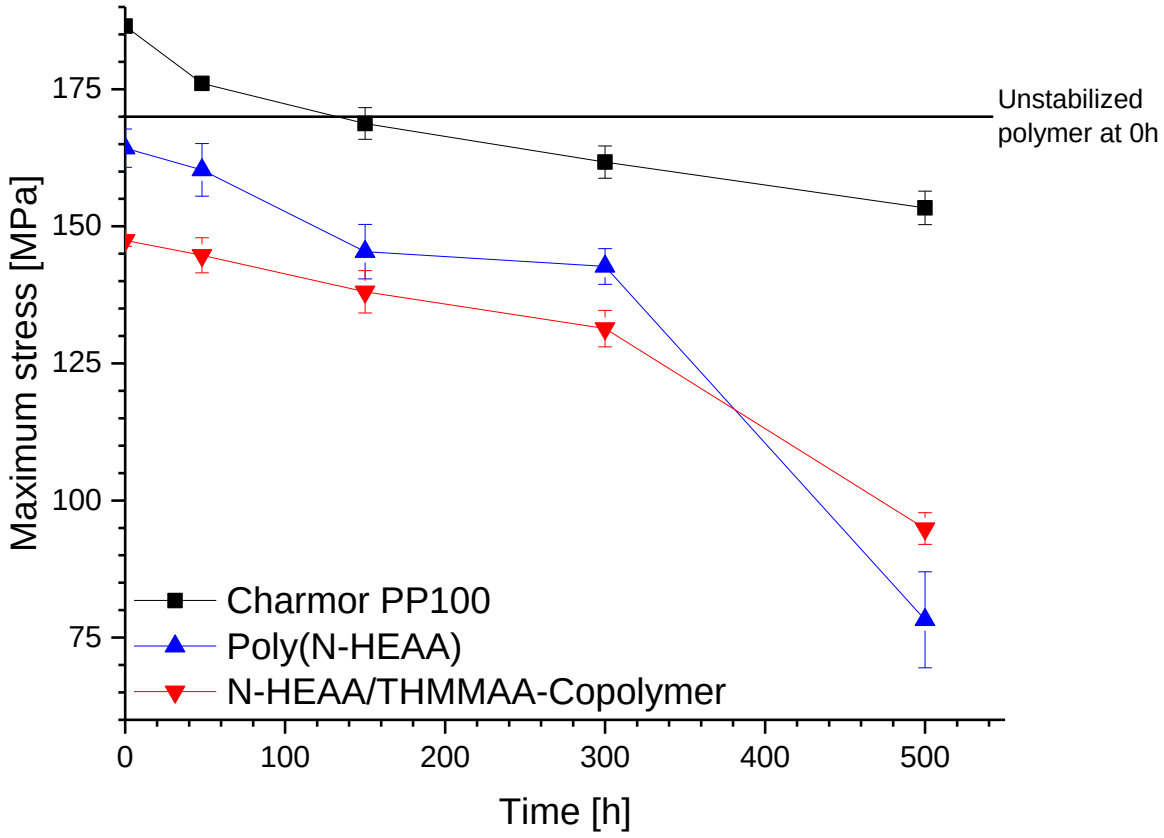

Figure 84: Maximum stress versus aging time at 200 °C of GF-reinforced PA 6 compounds with 0.5 wt% **Charmor PP100** (black), **Poly(*N*-HEAA)** (blue) and the **THMMAA/*N*-HEAA-copolymer** (red), respectively. The black line corresponds to the unstabilized polymer at 0 h. The value is taken from the material data sheet.

Table 19: Retention of the maximum stress of the aged compounds after 500 h.

Compound	Maximum Stress at 0 h aging time / MPa	Maximum Stress at 500 h aging time / MPa	Retention of maximum stress at 500 h / %
Charmor PP100	186	153	82
Poly(*N*-HEAA)	164	78	48
THMMAA/*N*-HEAA-copolymer	147	95	65

As can be seen, the enlarged amount of OH-groups for the copolymer does have a significant enhanced stabilizing effect over the homopolymer since the retention of the maximum stress is only 17 % higher. Both polyacrylamide-containing compounds start at lower maximum stress prior aging than the unstabilized PA 6, what alludes to decomposition of the polyamide during the extrusion process. This effect is stronger for the copolymer-containing compound than for the **Poly(N-HEAA)**-stabilized one. This is most likely due to decomposition products since the **THMMAA/N-HEAA**-copolymer does possess a lower decomposition temperature than **Poly(N-HEAA)**. Overall it can be stated, that OH-containing polyacrylamides do not stabilize PA sufficient compared to **Charmor PP100** or even the former synthesized **P-Polyol 2b**. Thus, no further incorporation and aging of other polyacrylates or -acrylamides was performed.

4.2.7. Pudovik Reaction Adducts and their Polymerization

Another approach towards the synthesis of OH- and P-containing molecules was the Pudovik addition of P–H to carbonyl compounds. As educts the bio-based compounds 5-hydroxymethyl furfural (HMF) and acrolein were chosen. Acrolein can be obtained from glycerol which is for example the by-product of the biodiesel synthesis[195], while HMF itself is a bio-based material that is generated, for example, during the caramelization of saccharides and can be catalytically obtained from sugars and cellulose[196-198]. Also, acrolein does possess a low amount of carbon, which automatically results in a high P-content of the Pudovik-product depending on the utilized P–H compound what leads to lower loading amounts for a good FR result. After the Pudovik reaction both substances possess further functional groups than the resulting hydroxyl group what makes them good candidates for polymerization or further functionalization.

For the reaction of acrolein with a P–H compound, a similar approach to Pamies and Bäckvall for the synthesis of β-hydroxyalkanephosphonates was chosen.[199] At first, their reaction was reproduced with diethyl phosphite as P–H compound. A ^{31}P-NMR of the reaction mixture was taken as reaction control showing a 62 % conversion with multiple side products. Though, when trying to isolate the product, as described, with aqueous hydrochloric acid (HCl) total decomposition of the product occurred. Therefore, further products were not purified under acidic conditions. For the generation of novel substances, DOPO was chosen as reactant. The reaction was carried out in THF at 0 °C utilizing 1,8-diazabicyclo[5,4,0]undec-7-ene (DBU) as catalytic base. However, the use of DBU did not yield in the desired product but multiple side reactions aroused. Acrolein as an unsaturated aldehyde has two competing functional groups, a C=O- and an activated C=C-bond, and thus can perform both a Pudovik and a Phospha-Michael reaction. To minimize the possibility of a Phospha-Michael addition, the base was varied to lithium diisopropylamine (LDA) because, as described in chapter 2.4.2, lithium-based catalysts like LDA should cause the reaction to perform exclusively in 1,2-position for unsaturated aldehydes.[92] As expected, the Pudovik addition of DOPO to acrolein proceeded in a regioselective fashion onto the C=O-bond with the use of LDA (Figure 85).

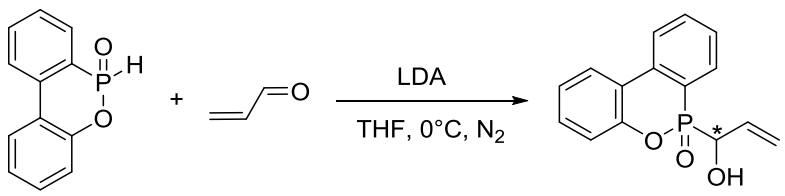

Figure 85: Base-catalyzed Pudovik reaction of DOPO and acrolein.

The resulting product **DOPO-acrolein** is a stereoisomer and can be obtained as single crystals via recrystallization from water. An X-ray crystal structure of the molecule was recorded that is shown in Figure 86.

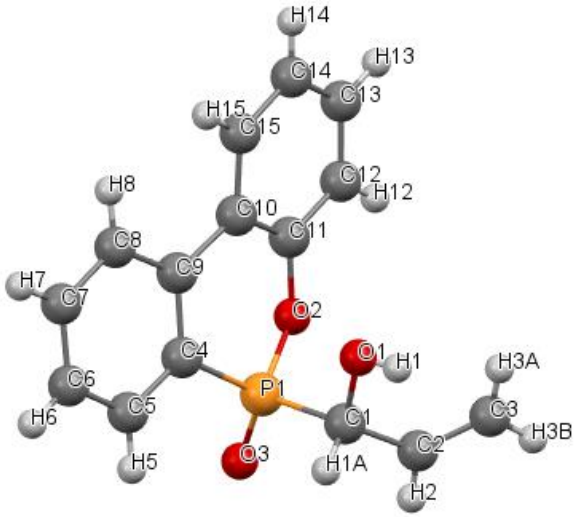

Figure 86: X-ray crystal structure of **DOPO-Acrolein**.

Due to the two asymmetric centers at the tertiary carbon (C1) and the phosphorus atom (P1) it consists of two stereoisomers S_1 and S_2 as can be seen in the ^{31}P- and ^{1}H-NMR spectra (Figure 87).

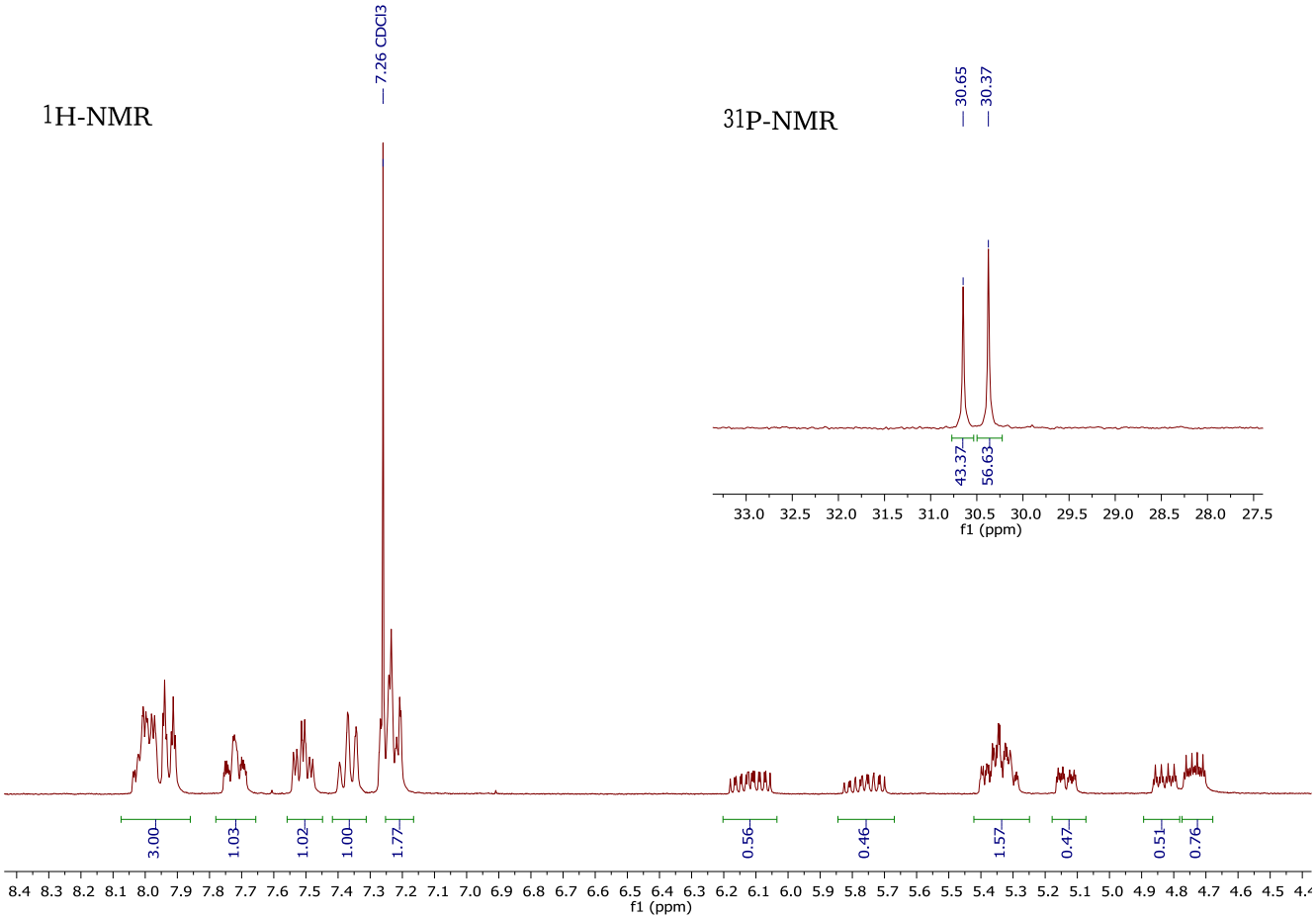

Figure 87: ^{1}H-NMR and ^{31}P-NMR spectra of the **DOPO-acrolein** crystals in $CDCl_3$.

To check on the stereoselectivity of the reaction for different starting materials, instead of an aldehyde methylvinylketone was applied under same reaction conditions (Figure 88). The reaction

proceeded very slowly. After one week reaction time still 43 % DOPO (determined via ^{31}P-NMR) remained in the solution.

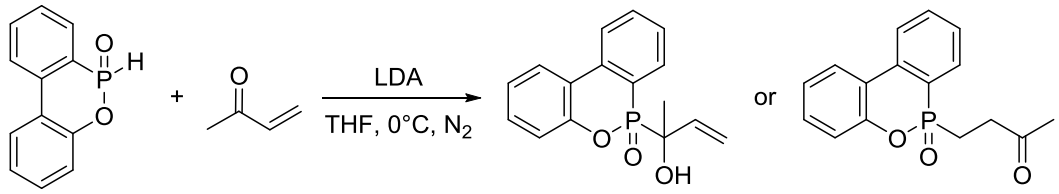

Figure 88: Pudovik reaction of DOPO and methylvinylketone.

After work-up, a ^{31}P-NMR spectrum of the product mixture was recorded (Figure 89). It revealed that a product mixture of both the Pudovik (25.9 %) and the Phospha-Michael (44.4 %) adduct occurred as well as a di-substituted species (8.5 %). Also, despite the work-up there was still a significant amount of DOPO in the product mixture (12.6%).

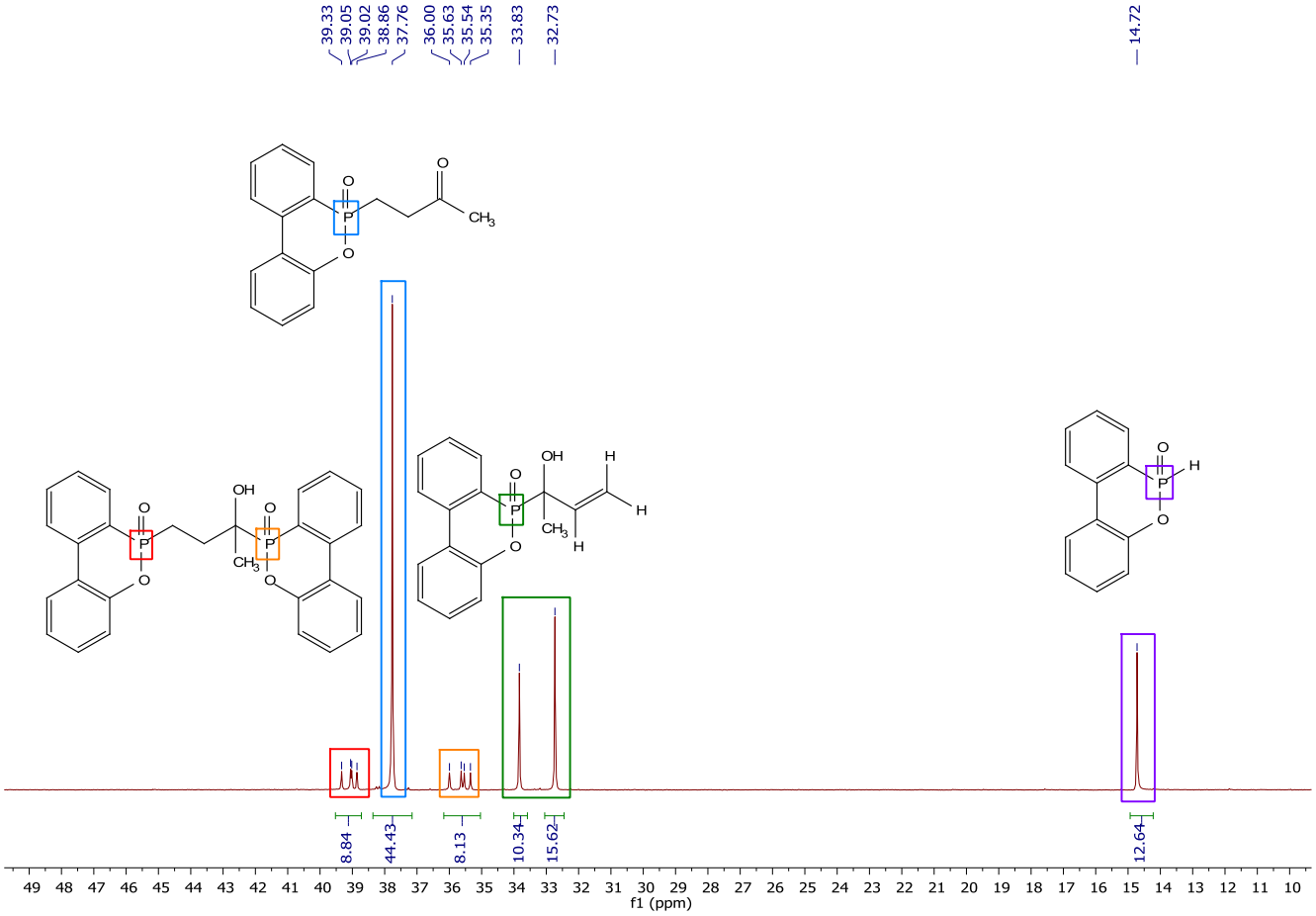

Figure 89: ^{31}P-NMR spectrum of the worked-up product mixture of the reaction of DOPO and methylvinylketone in $CDCl_3$.

These percentages are in good agreement with the corresponding signals in the ^{1}H-NMR (Figure 90). These results show that the Pudovik reaction is only stereospecific in the case of aldehydes as carbonyl compound but not for ketones.

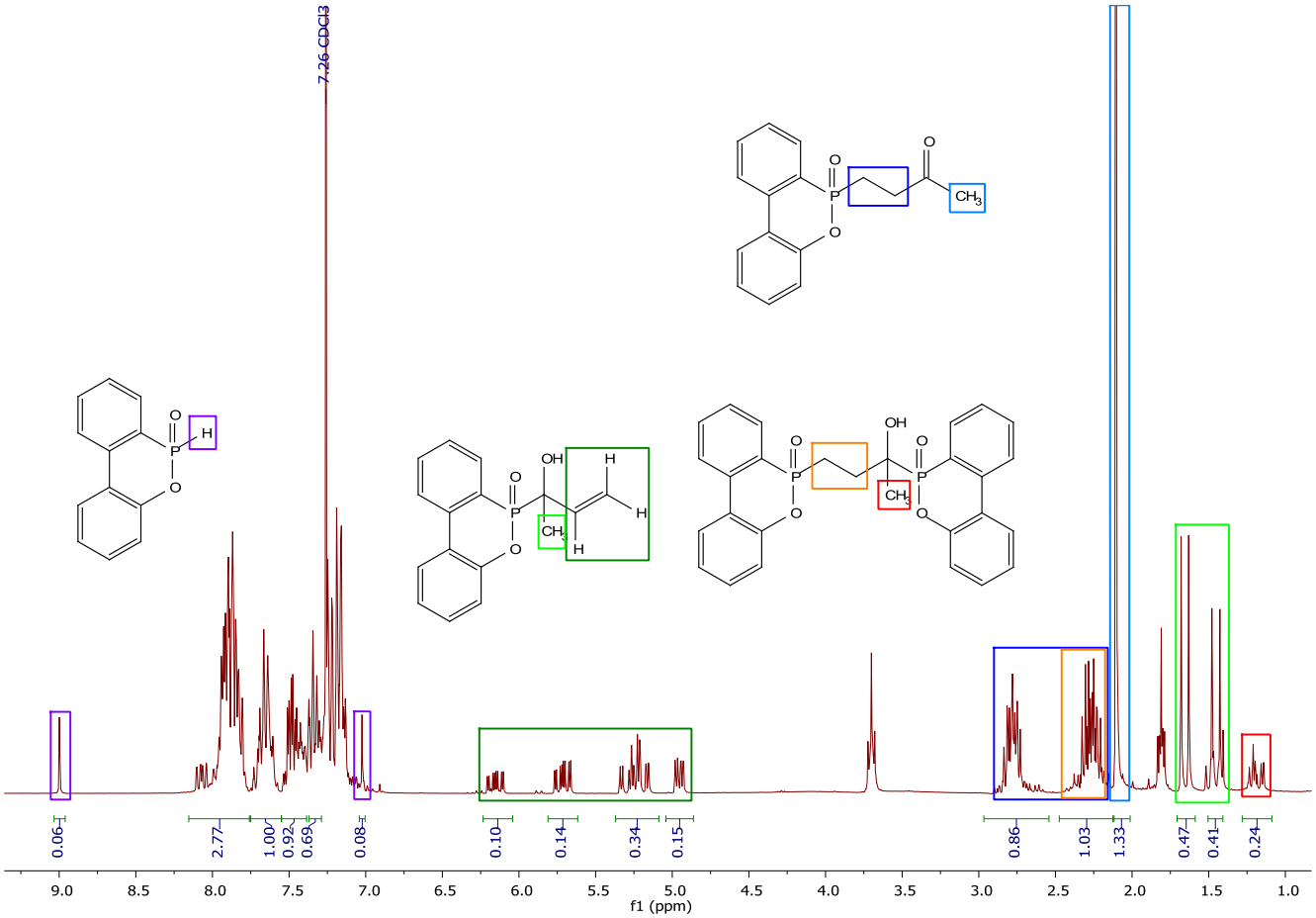

Figure 90: ^{1}H-NMR spectrum of the worked-up product mixture of the reaction of DOPO and methylvinylketone in $CDCl_3$.

To further analyze the Pudovik reaction of DOPO and acrolein, also two equivalents of DOPO were applied to check whether the di-substituted adduct would occur. In fact, even after a reaction time of 5 d only a negligible amount of 2 % (determined by ^{31}P-NMR) appeared as di-substituted while, besides the Pudovik product, the excess DOPO remained unreacted in solution. This shows the high selectivity of this reaction and also indicates a low reactivity for the remaining double bond.

When trying to polymerize **DOPO-acrolein** in solution via radical polymerization no reaction occurred. This can be explained when looking at the structure of the molecule. After the Pudovik reaction the molecule possesses an allyl alcohol like structure. Allylic compounds are known for their inhibition of radical processes.[200, 201] The formed radical is stabilized due to delocalization of the electron between two resonance structures (Figure 91).[201]

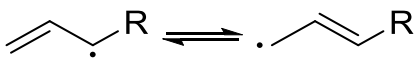

Figure 91: Radical stabilization of allylic compounds due to isomerization.

When a DSC of pure **DOPO-acrolein** was recorded though, an endothermic process occurred that peaked at ~160 °C. During the cooling cycle and the second heating cycle only a T_g could be observed. This led to the conclusion that a thermal polymerization just below the decomposition temperature ($T_{2\%}$ = 186 °C under nitrogen) might be possible.

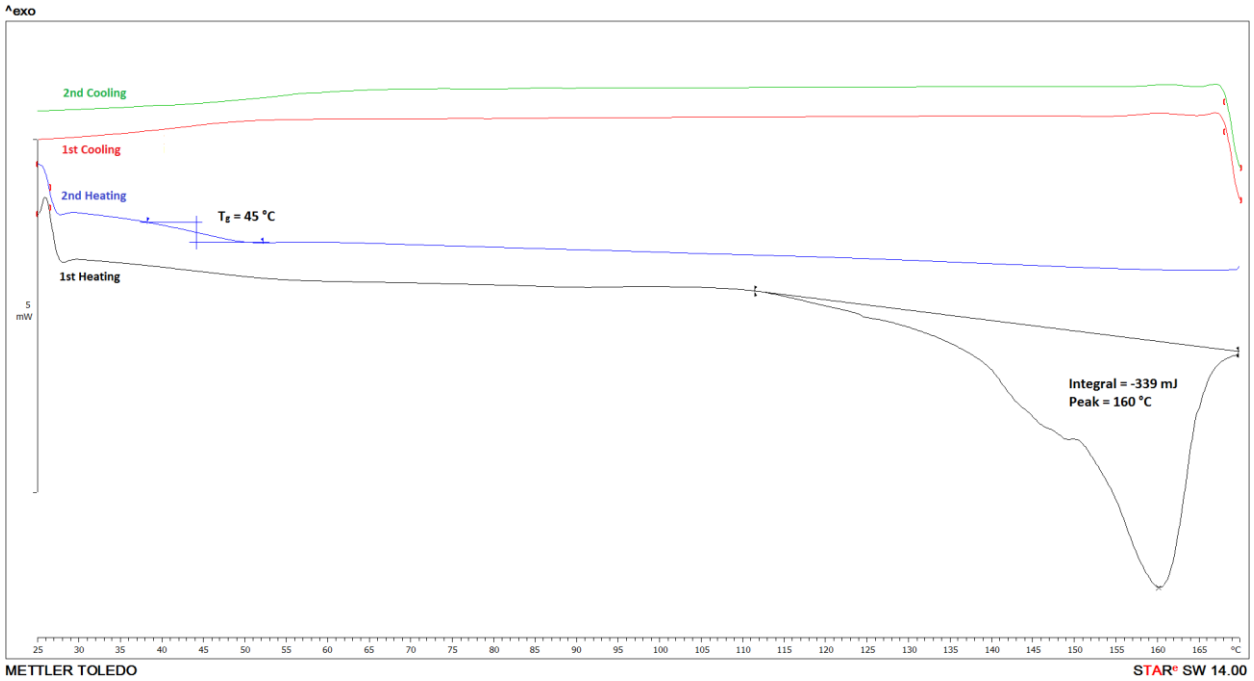

Figure 92: DSC of **DOPO-acrolein**. Two heating cycles with a heating rate of 10 K min^{-1}.

Therefore, **DOPO-acrolein** was filled into an aluminum pan and allowed to react at 160 °C in a vacuum oven and a ^{1}H-NMR was recorded. If the NMR spectra of both the starting compound and the product of the thermal reaction were compared (Figure 93), it can be seen that no allylic double bond remains in the molecule and a broad signal between 2 and 2.5 ppm appeared indicating a polymerization reaction.

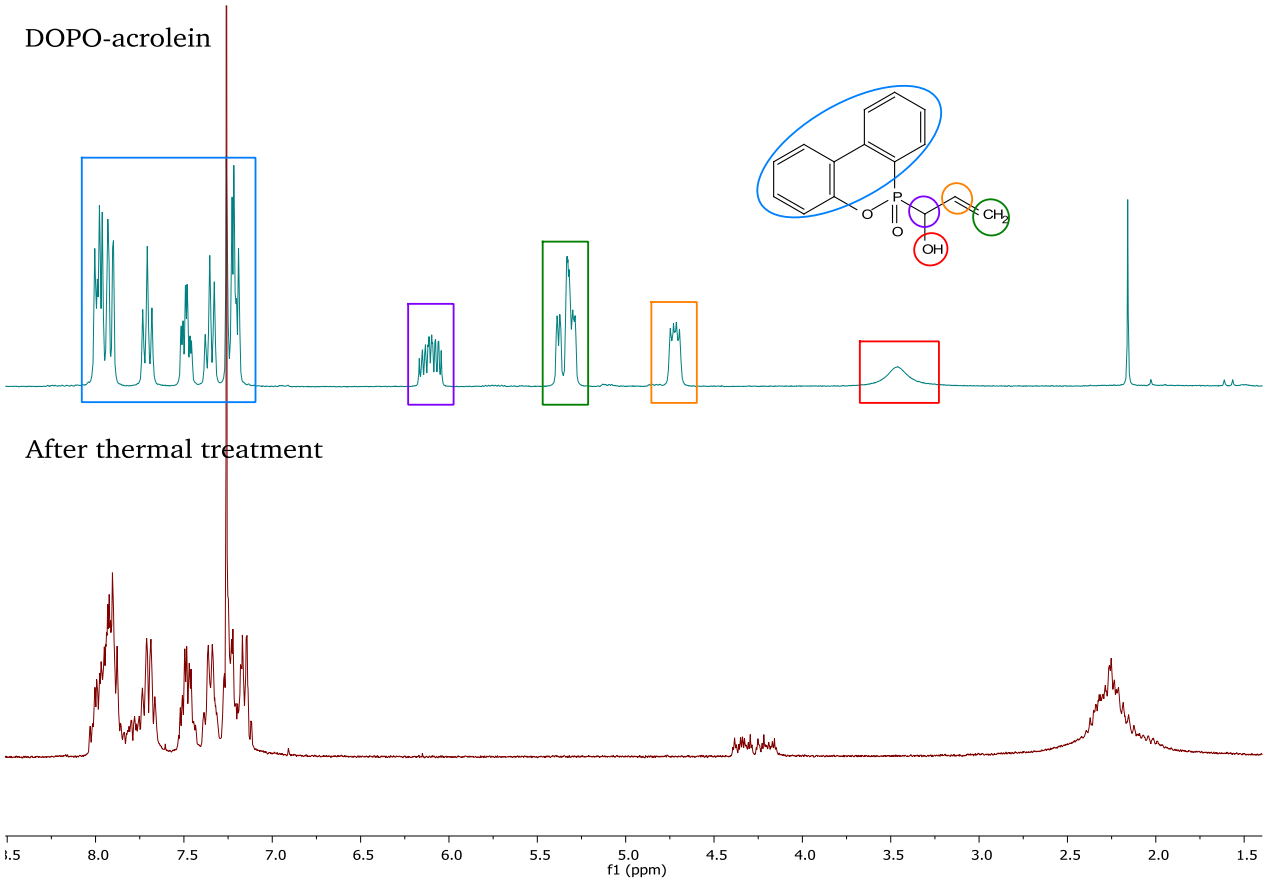

Figure 93: ^{1}H-NMR comparison of **DOPO-acrolein** and the product after thermal treatment at 160 °C in $CDCl_3$.

To further analyze the structure of the potential **poly(DOPO-acrolein)** a MALDI-TOF spectrum was recorded. It revealed that a maximum molecular weight of 959 g mol^{-1} was reached. Also, the following intervals where observed, where n = 0–2:

A = H-(272)$_1$-(254)$_n$-(18)$_1$-H
B = H-(272)$_1$-(254)$_n$-H
C = H-(272)$_1$-(254)$_n$-(216)$_1$-H
D = H-(272)$_1$-(254)$_1$-(216)$_2$-H

This shows that the repeating unit of the oligomers is not only the desired **DOPO-acrolein**, which has a molecular weight of 272 g mol^{-1}, but also a mass fragment of 216 g mol^{-1}, which correspond to DOPO, and 254 g mol^{-1} appeared. Due to the weight difference of 18 g mol^{-1} (between the 272 and the 254 g mol^{-1}) it was assumed that water might be released and some kind of condensation occurs during the reaction. To prove that assumption, the reaction was carried out in a reaction flask with an attached gas trap to entrap released gaseous side products. In case of a condensation reaction between the OH-groups water should be gathered. After the reaction was finished, the colorless liquid that settled in the gas trap was taken up in deuterated chloroform and a ^{1}H-NMR was taken. The NMR spectrum identified the only gaseous by-product to be acrolein. Thus, it can be concluded that no radical polymerization of **DOPO-acrolein** occurred but the back reaction of the Phospha-Michael addition and other side reactions proceeded. Therefore, this approach was not further pursued.

To enhance the polymerizability, one idea was to selectively oxidize the hydroxyl group to form back a carbonyl group and hence activate the double bond. Two different oxidation approaches were carried out (Figure 94). The first method was the Corey-Kim oxidation with *N*-chlorosuccinimide (NCS) and dimethylsulfide, since Montchamp *et al.* did oxidize α-hydroxyalkylphosphinates applying these conditions before in quantitative yields.[202] The second pathway was the Parikh-Doering oxidation, that was shown to selectively oxidize the hydroxyl group in the presence of a double bond for α-hydroxyalkylphosphonates. However, both oxidation procedures did not result in the desired oxidized form of **DOPO-acrolein**.

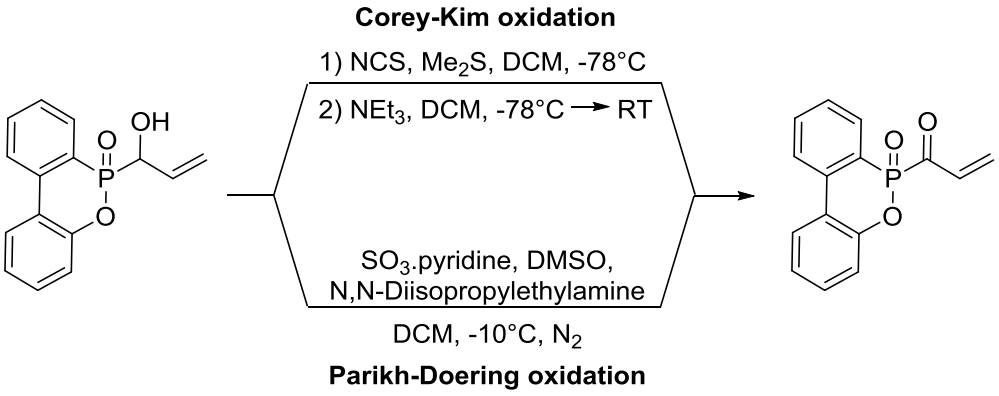

Figure 94: Corey-Kim and Parikh-Doering oxidation of **DOPO-acrolein**.

For utilization of **DOPO-acrolein** aside polymerization as low-molecular weight additive for polyamides the hydroxyl group was functionalized with DOPO via an Atherton-Todd reaction (Figure 95).

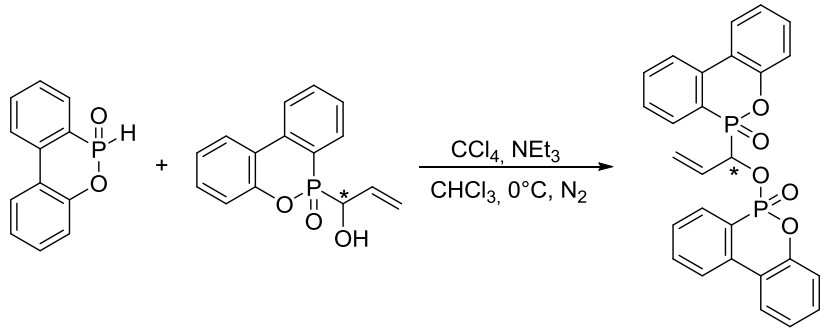

Figure 95: Atherton-Todd reaction of **DOPO-acrolein** and DOPO.

The reaction proceeded with an 88 % yield and single crystals for X-ray analysis were obtained from recrystallization in methanol (Figure 96). Again, different stereoisomers were produced due to the asymmetry of both P atoms (P1 and P2) and the tertiary C atom (C13) as can be seen from the ^{31}P-NMR spectrum (Figure 97).

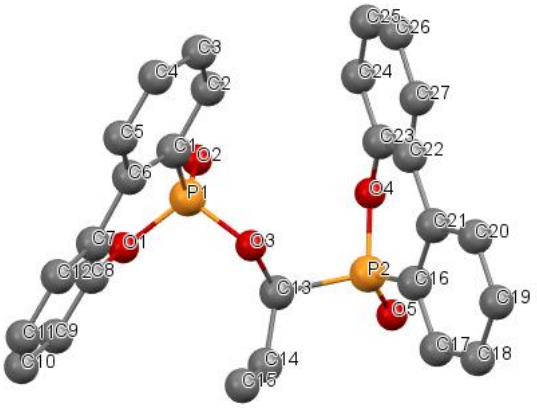

Figure 96: X-ray crystal structure of **DOPO-acrolein-O-DOPO**. For better visualization, H atoms are omitted.

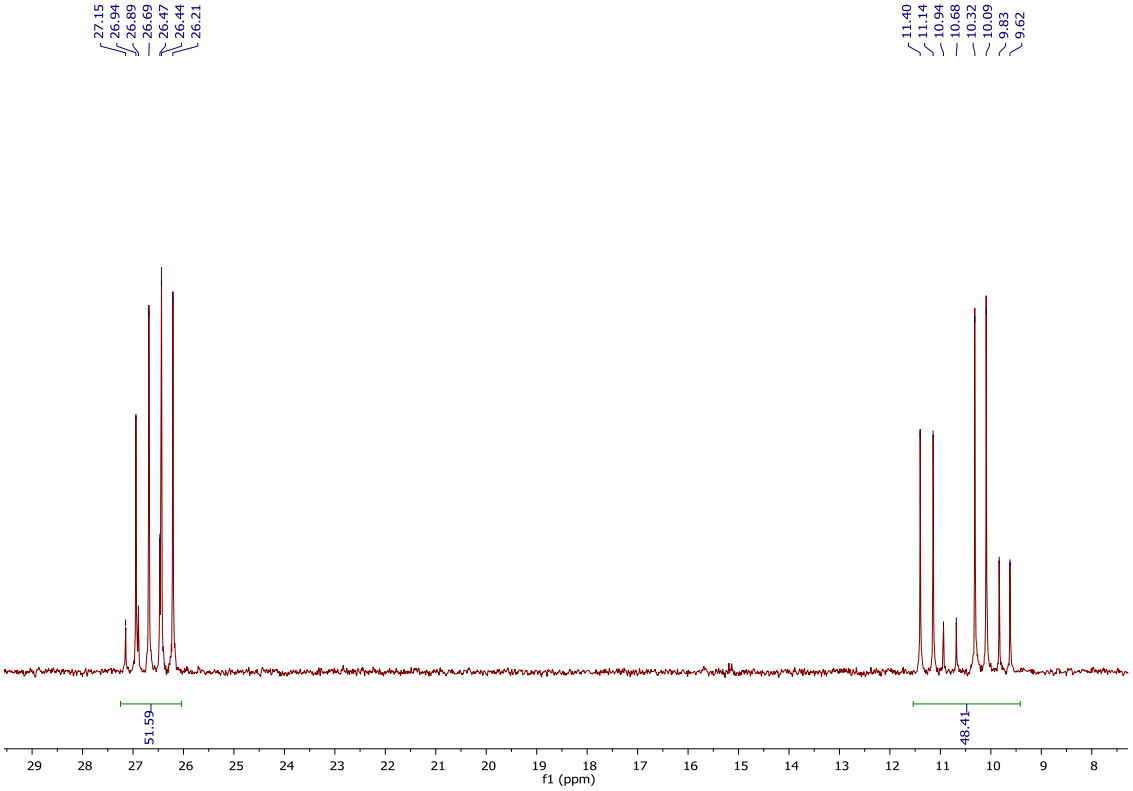

Figure 97: ^{31}P-NMR spectrum of **DOPO-acrolein-O-DOPO**.

DOPO-acrolein-O-DOPO is thermally stable up to 231 °C which is not high enough for a low-molecular weight flame retardant for engineering plastics.

As mentioned in the beginning of this chapter, the second Pudovik product that was synthesized was **DOPO-HMF**. Since HMF only contains aromatic double bonds, there is no selectivity problem like for **DOPO-acrolein** and thus triethylamine as a weaker base was chosen. The reaction proceeded smoothly at 70 °C with a small excess of DOPO (Figure 98). Like for **DOPO-acrolein**, again different stereoisomers were observed via NMR spectroscopy (Figure 99).

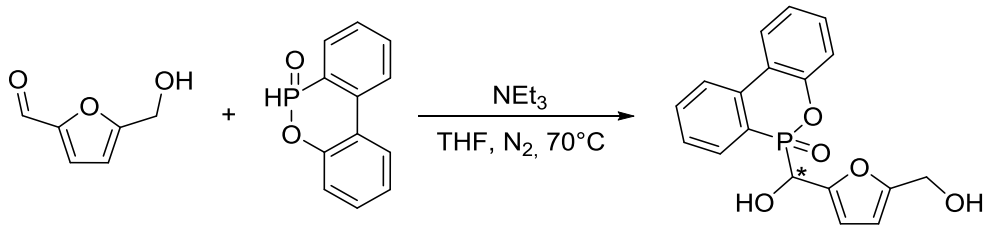

Figure 98: Pudovik reaction of DOPO and HMF.

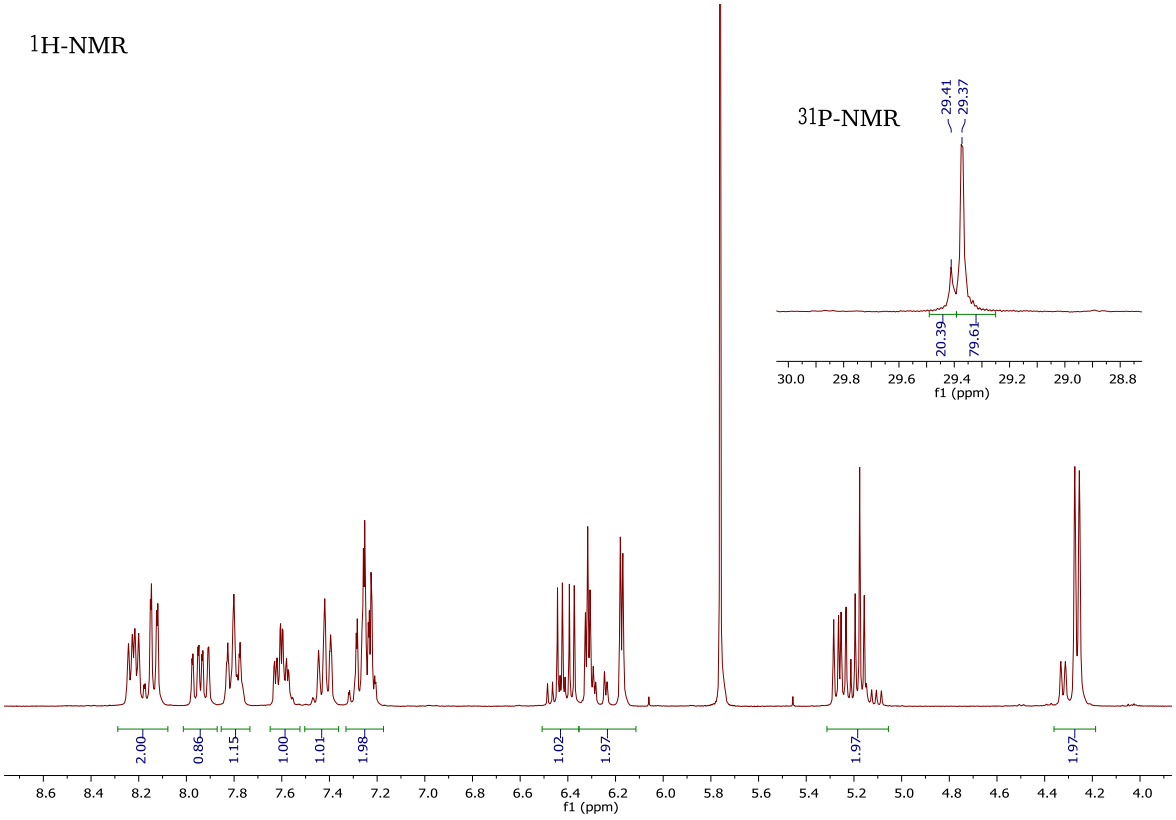

Figure 99: ^{1}H-NMR and ^{31}P-NMR spectra of DOPO-HMF in DMSO-*d6*.

DOPO-HMF is thermally stable up to 175 °C after which it decomposes in two steps to leave a relatively high residue of 25 wt% at 650 °C. To enlarge its thermal stability and to embed it into a polymer structure, it was combined with 3,9-dichloro-2,4,8,10-tetraoxa-3,9-diphosphaspiro[*5,5*]undecane 3,9-dioxide (SPDCP) in a step-growth polymerization in accordance with Hu *et al.*[203] who preceded the same reaction with a $(DOPO)_2$-terephthaldicarboxaldehyde adduct. This would also combine the gas-phase active phosphorus species DOPO with the condensed-phase mechanism of a phosphate in one polymer. The reaction was carried out in acetonitrile at 70 °C (Figure 100). However, during the reaction **DOPO-HMF** decomposed probably due to emerging HCl that catalyzes side reactions on the furan ring[204] since all signals according to furan disappear in the ^{1}H-NMR spectrum. Thus, this approach was not further pursued.

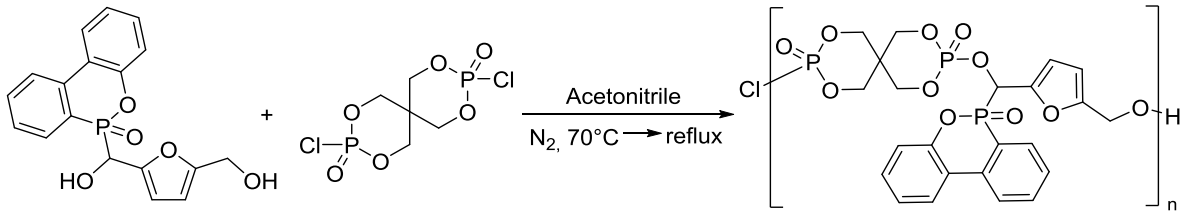

Figure 100: Attempted polymerization of DOPO-HMF and SPDCP.

Overall, the novel OH-containing monomers **DOPO-acrolein** and **DOPO-HMF** were successfully synthesized in a regioselective fashion. However, their thermal stability is not sufficient for the application as combined heat stabilizer and FR in PA 6 or 66. Therefore, their polymerizability was investigated. Neither the radical, thermally-induced polymerization of **DOPO-acrolein**, nor the dehydrochlorination of **DOPO-HMF** did lead to the desired polymers due to decomposition of the respective monomer. To still utilize **DOPO-acrolein** as FR, its thermal stability was enhanced by the Atherton-Todd reaction with one equivalent DOPO to form the component **DOPO-acrolein-O-DOPO**. Anyways, the thermal stability of this new compound was still not high enough for its application as FR for engineering plastics.

Since **DOPO-acrolein** could be applied as reactive FR for different polymer systems due to its free hydroxyl group, e.g. in polyurethanes, or double bond as co-monomer, its FR activity was investigated anyways via py-GC/MS at 600 °C. Figure 101 shows the measured chromatogram with the assigned structures. As expected, acrolein is one of the decomposition products occurring from the back reaction of the Phospha-Michael addition. The main decomposition product is DOPO, which passes into the gas phase mostly as an intact molecule. However, the typical DOPO decomposition side products dibenzofuran and o-hydroxylbiphenyl were found as well. Also, the DOPO radical can be observed as well as a DOPO-allylic compound resulting from dehydration of the OH group. This measurement in combination with the relatively low amount of residue determined by TGA (3.8 wt% at 650 °C) indicates a typical gas-phase mechanism for the FR activity of **DOPO-acrolein**.

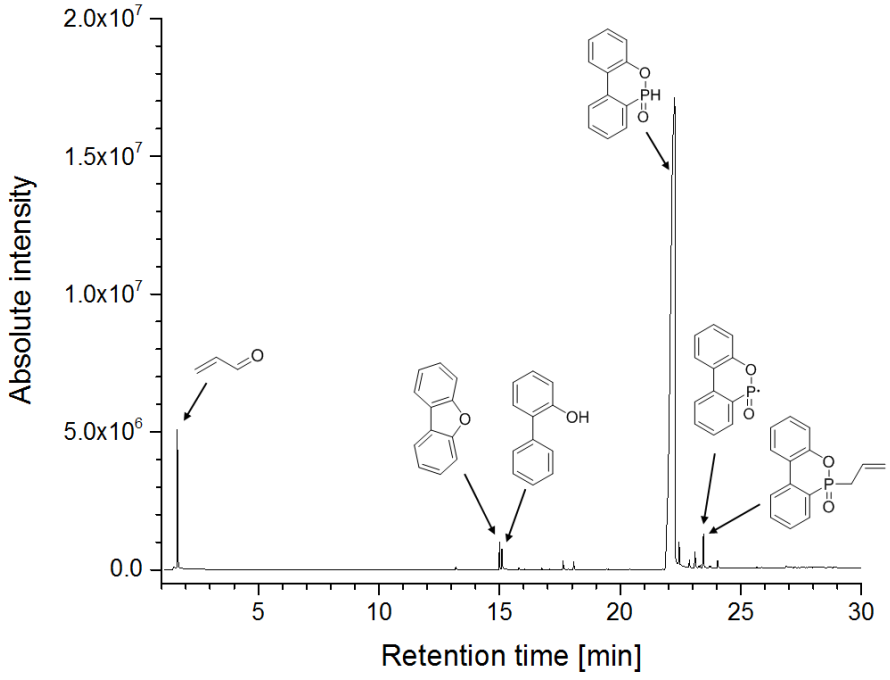

Figure 101: Chromatogram of **DOPO-acrolein** at 600 °C with corresponding structures.

5. Conclusion and Perspective

In the first part of this work, a phosphorus-containing zinc polyacrylate, **Poly(1-A)**, and its corresponding molecular zinc complex compound, **3**, were synthesized for the incorporation into PA 6 and 66 as FR in different compositions. The synthesis of the polyacrylate was performed selectively with one equivalent of DOPO in a one-pot procedure yielding in an insoluble polymer that is thermally stable up to 300 °C and leaves high amounts of residue. A similar thermal stability was found for complex **3**. However, during the incorporation into the different PAs a drop in the viscosity number was examined that aroused from the phosphorus-containing additives and could be due to early, DOPO-typical decomposition products that were observed via py-GC/MS. Despite low afterburn times in pure PA, the FR samples showed severe dripping thus resulting in a V-2 rating. To impede dripping, the new FR additives were incorporated into GF-reinforced PA and also tested in different compositions with MPP. These measures, however, did mostly not yield in improved results. Only one sample with a mixture of 30 wt% GF-reinforced PA 66 with 6 wt% **Poly(1-A)** and 12 wt% MPP resulted in a V-1 rating. For following work on these additives it could be interesting to examine the decomposition products that remain in the condensed phase since, despite DOPO usually mainly reacts in gas phase, the residue of the novel components showed a high phosphorus content indicating that a condensed-phase mechanism occurs as well. Also, the application range could be broadened up to polymers possessing a lower extrusion temperature.

During the second part of this work the focus lay on the combination of phosphorus and hydroxyl groups in one oligo- or polymer for the combined application as FR synergist and as long-term heat stabilizer. In a first approach phosphorylated TMP diols were synthesized that were then merged with Bis-MPA and DPE to yield **P-Polyols** with high hydroxyl numbers and different FR mechanisms. These **P-Polyols** were incorporated into PA 6 and 66 in different concentrations in combination with DEPAL in order to check whether they could work as a synergist to save the addition of DEPAL while also being able to stabilize the PA. Only a mixture containing **Ph_2PO** could replace 1 wt% of DEPAL in both PA 6 and 66 and thus being the most promising species regarding flame retardancy. In a next step a Polyol containing DOPO units was incorporated into non-reinforced PA 6 in different concentrations and compared with the reference polyol **Charmor PP100**. However, it was shown that neither of them could stabilize non-reinforced PA 6. Due to similar experiments in the literature, the same compounds were incorporated into GF-reinforced PA 6 with 0.5 wt%. The DOPO-containing **P-Polyol 2b** did not influence the starting mechanical properties of the polyamide and retained 75 % of maximum stress after 500 h, while **Charmor PP100** retained 82 % but enlarged the starting maximum stress. Thus, the phosphorylated Polyols are a promising approach for the combination of heat stabilizer with FR and further aging experiments with the **Ph_2PO**-containing **P-Polyol 4** should be conducted.

In a second approach hydroxyl-containing acrylamides and acrylates were combined with phosphorus-containing ones in copolymerizations. All copolymers were compared for their thermal stabilities with their individual homopolymers showing that the copolymers are overall less stable. As a first test for this approach on heat stabilization, the non-phosphorus-containing **Poly(*N*-HEAA)** and **THMMAA/*N*-HEAA-copolymer** were tested in GF-reinforced PA 6 to check on the influence of the amount of hydroxyl groups. However, both polyacrylamides did not result in a sufficient stabilization and thus this approach was not further pursued. In further work it could be interesting to test the phosphorus-containing copolymers both as FRs and as heat stabilizers. Also, the concentration could be varied to check whether with a higher concentration the stabilization effect is enhanced.

The last approach was the Pudovik reaction of DOPO with the bio-based molecules acrolein and HMF. In both cases a structure with a newly generated hydroxyl group and further functionalities was obtained. Experiments of the polymerization, either radically for **DOPO-acrolein** or via dehydrochlorination for **DOPO-HMF**, of both compounds did not yield in the desired results.

DOPO-acrolein was auto-inhibited by the allylic group while **DOPO-HMF** was decomposed by resulting hydrochloric acid. Selective oxidation of the hydroxyl group of **DOPO-acrolein** also did not work, but an Atherton-Todd reaction of DOPO onto the hydroxyl group was successfully conducted. However, the allylic group still inhibited a polymerization. These synthesized molecules were not thermally stable enough for the incorporation into polyamides. Though, in further studies it would be possible to incorporate them as reactive FRs, for example in polyurethanes, where their OH-functionalities can be used to react into the molecular network.

6. Experimental

6.1. Materials and Instruments

All chemicals and solvents were purchased from commercial sources and used without further treatment, if not stated otherwise.

The recorded nuclear magnetic resonance (NMR) spectra were measured on a Bruker Ultrashield 300. Spectra were exploited with the software MestReNova from Mestrelab Research. The signal multiplicities are abbreviated as follows: s: singlet, d: duplet, t: triplet, q: quartet, m: multiplet.

Elemental analyses of carbon and hydrogen were recorded on a CHNOS device elemental analyzer Vario EL. The zinc content was determined by a Perkin Elmer AAS Model Analyst 200. Phosphorus percentage was identified photometrical on a Specord 50Plus of AnalytikJena.

Attenuated total reflection Fourier-transform infrared spectroscopy (ATR/FT-IR) was conducted with a Nicolet 8700 FT-IR spectrometer of Thermo Scientific with an MCT-A detector and a Golden Gate ATR by Specac. ATR/FT-IR spectra were analyzed with the software OMNIC of Thermo scientific. The signal intensities are abbreviated as follows: w: weak, m: medium, st: strong, br: broad.

Thermogravimetric analyses (TGA) were conducted on a TGA Q500 (TA Instruments) from 35 to 800 °C at a heating rate of 10 °C min^{-1} under nitrogen or synthetic air with a flow rate of 60 mL min^{-1}. Platinum pans were used for the non-phosphorus-containing samples while for the phosphorus-containing ones ceramic pans were applied. The gathered data were evaluated with the software TA Instruments Universal Analysis 2000.

For pyrolysis – gas chromatography/mass spectroscopy (py-GC/MS) two different systems were used. One was equipped with pyrolyser PY-2020iD, autosampler AS-1020E and Cryotrap MJT-1030Ex from Frontier Lab. The applied GC/MS was GCMS-QP2010 Plus from Shimadzu with an Ultra-Alloy 5 column from Frontier Lab. Recorded spectra were identified with the software GCMSsolution 2.70. The other system was an AS 1020 pyrolyser from Frontier Lab with an Agilent 7890B gas chromatograph and an Agilent 5977 MassHunter workstation. The used columns were an Agilent 19091S-433 and a Frontier Ultra.

PA 6 (Ultramid B27), 30 % GF-reinforced PA 6 (Ultramid B3EG6), PA 66 (Ultramid A24), 30 % GF-reinforced PA 66 (Ultramid A3EG6) and melamine polyphosphate (Melapur 200) for the extrusion of specimens were obtained from BASF SE. Charmor PP100 was obtained from Perstorp. After weighing in 20 g total weight of each of the different mixtures they were dried under reduced pressure overnight at 80 °C. Compounding was conducted on an Xplore Micro compounder MC 15 (15 mL) with a dwell time of 3 min at 260 and 280 °C for PA 6 and PA 66, respectively. The hot melt was transferred to a melt vessel that was also heated to 260 or 280 °C, respectively, and then immediately used for injection molding of two 1.6 mm thick UL94 V test specimens with an Xplore injection molder IM 12 (12 mL). The temperature of the mold was 80 °C and the applied pressure was 16 bar / 2 s or 14 bar / 4 s.

The UL 94 V tests were performed after standard DIN EN 60695-11-10 with a LAT Scientific Instruments UL 94 burning chamber. Unless otherwise noted, the sample size is 125 mm x 13 mm x 1.6 mm (length x width x height). A maximum of two specimens per compound was used for the classification and it was averaged over those two specimens for the burning times. Also, the samples were not aged as specified in the norm.

Viscosity numbers (VN) of the different compounds were determined after standard DIN EN ISO 307:2013-08. All compounds were dried for 16 h at 80 °C under reduced pressure. Sulfuric acid (96%) was used as the solvent and the generated solutions possessed a polymer concentration of 0.005 g mL^{-1}. The viscosity measurement system was an AVSPro of SI Analytics with an Ubbelohde viscometer II (SI Analytics). The VN was measured twice for each sample and it was averaged over those two values.

Glass transition temperatures (T_g) and melting points (T_m) were determined via differential scanning calorimetry (DSC) on a METTLER TOLEDO DSC 822^e. Usual measurements were performed with two heating and cooling cycles with a heating rate of 10 °C min^{-1}. Between the steps the temperature was held isothermal for 10 min each. The measured data was evaluated with the METTLER TOLEDO STARe evaluation software.

Mass spectrometry (MS) measurements were carried out on an Impact II of Bruker in case of electrospray ionization (ESI) and atmospheric pressure chemical ionization (APCI) or on a Finnigan MAT 95 or Fisons MD 800 for electron ionization (EI).

6.2. Synthesis procedures

6.2.1. Zinc- and P-containing acrylates

6.2.1.1. 3-(6-Oxidodibenzo[*c,e*][1,2]oxaphosphinin-6-yl)propionate acrylate zinc, (1-A)

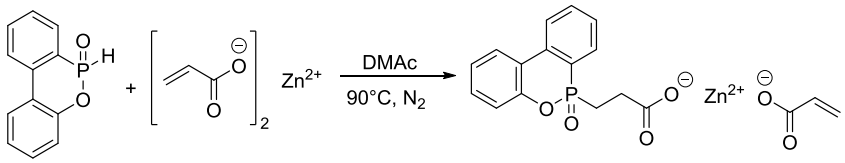

A three-necked round-bottomed flask was equipped with a mechanical stirrer, a condenser, a nitrogen inlet and a bubble counter and the whole apparatus was evacuated, heated and set under nitrogen atmosphere three times. 21.62 g (0.1 mol) DOPO and 20.75 g (0.1 mol) zinc acrylate were added to the flask and dissolved in 150 mL of dry *N*,*N*-dimethylacetamide (DMAc). It was heated to 90 °C and it was stirred for 30 min. The clear solution was used without purification in the next step.

^{1}H-NMR (300 MHz, DMSO-d_6) δ = 8.19 (ddd, J = 9.9, 7.9, 3.1 Hz, 2H), 7.94 (ddd, J = 12.8, 7.5, 1.3 Hz, 1H), 7.78 (t, J = 7.9 Hz, 1H), 7.59 (td, J = 7.5, 3.0 Hz, 1H), 7.45 (t, J = 7.9 Hz, 1H), 7.36 – 7.23 (m, 2H), 6.06 (d, J = 3.0 Hz, 1H), 6.04 (s, 1H), 5.59 (dd, J = 7.6, 5.0 Hz, 1H), 2.43 – 2.19 (m, 4H).

^{31}P-NMR (122 MHz, DMSO-d_6) δ = 37.15 (s, 1P).

^{13}C-NMR (76 MHz, DMSO-d_6) δ = 176.00 (d, J = 16.7 Hz), 171.30 (s), 134.67 (d, J = 5.3 Hz), 133.32 (d, J = 2.3 Hz), 133.26 (s), 130.78 (s), 129.82 (d, J = 12.2 Hz), 128.72 (d, J = 12.9 Hz), 126.71 (s), 125.73 (s), 125.49 (s), 124.72 (s), 124.34 (d, J = 9.1 Hz), 123.92 (s), 121.98 (d, J = 11.4 Hz), 120.17 (d, J = 6.1 Hz), 27.63 (d, J = 3.8 Hz), 24.58 (d, J = 98.8 Hz).

6.2.1.2. Polymerization of (DOPO-propionate)Zn(acrylate), Poly(1-A)

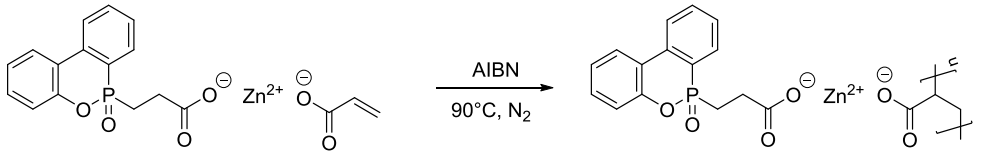

The reaction solution of **1-A** in dry DMAc was heated to 90 °C under nitrogen and 5 mL of an 0.2 M azobisisobutyronitrile (AIBN) solution in toluene were added dropwise. A colorless precipitate emerged and it was allowed to react for 1 h. The precipitate was filtrated under inert conditions and washed with dry DMAc and dry tetrahydrofuran (THF). The colorless solid was gathered in a Schlenk flask with a stir bar and it was dried at 180 °C under vacuum while stirring.

Overall yield: 22.82 g ≡ 0.054 mol ≡ 54 %

IR (ATR) ν (cm^{-1}): 2932 (w, br), 2290 (w), 2164 (w), 2110 (w), 1973 (w), 1554 (st, br), 1477 (m), 1429 (st, br), 1318 (m), 1277 (m), 1190 (st, br), 1141 (st), 1118 (st), 1042 (m), 1006 (m), 919 (m, br), 830 (m), 753 (st), 716 (m), 678 (m), 616 (m), 596 (st), 516 (st), 426 (st), 416 (st), 407 (st).

Repeating unit ($C_{18}H_{15}O_6Zn$) (423.67): Calcd. C 51.03, H 3.57, P 7.31, Zn 15.43; Found C 49.10, H 3.80, P 6.48, Zn 16.58.

T_g = 185.2 °C

6.2.1.3. Zinc-(II)-bis(3-(6-oxidodibenzo[*c,e*][1,2]oxaphosphinin-6-yl)propionate), (3)

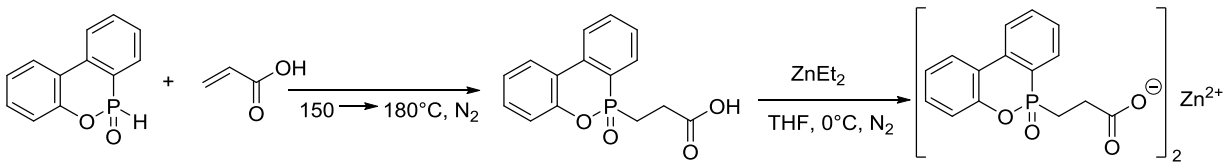

DOPO-propionic acid was prepared according to literature except for the recrystallization.[154] 20 g (0.093 mol) DOPO were molten under nitrogen at 130 °C and the temperature was raised to 150 °C. 7.33 g (0.102 mol) acrylic acid were added dropwise and the temperature was raised to 180 °C. It was stirred at 180 °C until all DOPO reacted (verified by ^{31}P-NMR). Residual acrylic acid was evaporated in a nitrogen flow. The DOPO-propionic acid was allowed to cool down to 70 °C and dry THF was added to dissolve the glassy product. The clear solution was cooled down to 0 °C with an ice bath and 46 mL of a 1 M solution of diethylzinc in hexanes was added dropwise so that the temperature would not exceed 10 °C. A colorless solid precipitated that was filtrated under inert conditions and washed with dry THF. The product was gathered in a Schlenk flask and dried at 150 °C under vacuum while stirring.

Yield: 24.95 g ≡ 0.039 mol ≡ 85 %

^{1}H-NMR (300 MHz, DMSO-d_6) δ = 8.27 – 8.12 (m, 2H), 7.94 (ddd, J = 12.8, 7.6, 1.4 Hz, 1H), 7.84 – 7.75 (m, 1H), 7.66 – 7.55 (m, 1H), 7.51 – 7.40 (m, 1H), 7.38 – 7.25 (m, 2H), 2.44 – 2.13 (m, 4H).

^{31}P-NMR (122 MHz, DMSO-d_6) δ = 37.27 (s, 2P).

^{13}C-NMR (76 MHz, DMSO-d_6) δ = 176.29 (d, J = 16.7 Hz, 2C), 149.08 (d, J = 8.4 Hz, 2C), 135.06 (d, J = 5.3 Hz, 2C), 133.82 (s, 2C), 131.25 (s, 2C), 130.25 (d, J = 12.2 Hz, 2C), 129.18 (d, J = 12.9 Hz, 2C), 126.19 (s, 2C), 125.83 (s, 1C), 125.19 (s, 2C), 124.80 (d, J = 8.4 Hz, 2C), 124.26 (s, 1C), 122.36 (d, J = 10.6 Hz, 2C), 120.62 (d, J = 5.3 Hz, 2C), 27.99 (d, J = 3.0 Hz, 2C), 24.90 (d, J = 98.0 Hz, 2C).

T_g = 131.6 °C

IR (ATR) ν (cm^{-1}): 3063 (w, br), 2919 (w, br), 2324 (w), 2162 (w), 2051 (w), 1981 (w), 1727 (w, br), 1594 (st), 1581 (st), 1560 (st), 1477 (m), 1446 (m), 1430 (st), 1411 (st), 1316 (w), 1277 (m), 1193 (st, br), 1145 (st), 1118 (st), 1084 (m), 1043 (m), 1008 (w), 911 (st, br), 823 (m).

Elemental analysis for ($C_{30}H_{24}O_8Zn$) (639.84): Calcd. C 56.32, H 3.78, P 9.68, Zn 10.22; Found C 54.74, H 3.94, P 8.68, Zn 11.10.

6.2.1.4. Poly(zinc diacrylate), (4)

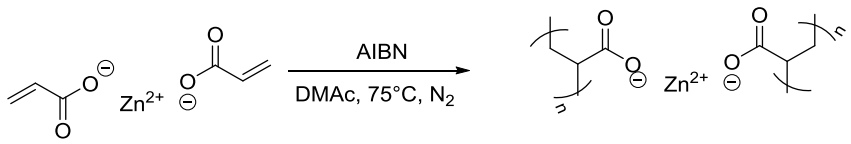

A two-necked round-bottomed flask was equipped with a stir bar, a condenser, a nitrogen inlet and a bubble counter and the whole apparatus was evacuated, heated and set under nitrogen atmosphere three times. 8.30 g (0.04 mol) zinc acrylate were filled into the flask and dissolved in 40 mL of dry DMAc. The reaction solution was heated to 80 °C and 6 mL of an AIBN solution (0.2 M in toluene) were added dropwise. A white solid precipitated and 20 mL more of DMAc were added to keep the solution agitable. It was stirred at 80 °C for 2.5 h. The solid was filtered off under nitrogen atmosphere and washed with dry THF. The white solid was gathered in a Schlenk flask with a stir bar and it was dried at 180 °C under vacuum while stirring.

IR (ATR) ν (cm^{-1}): 3225 (w, br), 2945 (w), 1545 (st), 1411 (st), 1329 (m), 1123 (w), 1036 (w), 858 (w), 831 (w), 767 (m), 599 (m).

6.2.2. Synthesis of P-containing Alcohols

6.2.2.1. 6-(1-Hydroxyallyl)dibenzo[*c,e*][1,2]oxaphosphinine 6-oxide, (DOPO-acrolein)

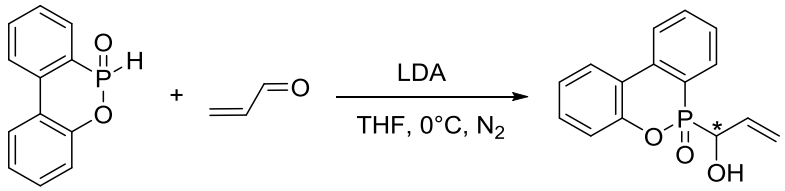

A three-necked round-bottomed flask was equipped with a stir bar, a condenser, a thermometer, a nitrogen inlet and a bubble counter and the whole apparatus was evacuated, heated and set under nitrogen atmosphere 3 times. 50 g (0.231 mol) DOPO were added to the flask and dissolved in 250 mL dry THF at 60 °C. The solution was cooled down with an ice bath and 12.70 g (0.231 mol) distilled acrolein was added. 3.47 mL lithium diisopropylamide solution (2 M in THF/ethylbenzene/heptane) were added dropwise at 0 °C. It was stirred for 1.5 h while the mixture was allowed to reach room temperature. The yellow solution was concentrated and a colorless solid precipitated. The precipitate was filtered off and washed with THF. The product may be recrystallized from water, THF or acetone and contains 2 stereoisomers S_1 and S_2.

Yield: 37.10 g ≡ 0.136 mol ≡ 59 %

^{1}H-NMR (300 MHz, $CDCl_3$) δ = 8.06 – 7.85 (m, 3H), 7.76 – 7.66 (m, 1H), 7.51 (tdt, *J* = 7.5, 3.1, 0.9 Hz, 1H), 7.37 (m, 1H), 7.25 – 7.15 (m, 2H), 6.12 (dddd, *J* = 17.2, 10.6, 5.4, 4.0 Hz, 1H (S_1)), 5.76 (dddd, *J* = 17.2, 10.6, 5.7, 4.3 Hz, 1H (S_2)), 5.42 – 5.25 (m, 1H + 1H (S_1)), 5.13 (ddt, *J* = 10.6, 4.3, 1.5 Hz, 1H (S_2)), 4.83 (ddt, *J* = 11.9, 5.6, 1.7 Hz, 1H (S_2)), 4.74 (ddt, *J* = 10.3, 5.4, 1.9 Hz, 1H (S_1)).

^{31}P-NMR (122 MHz, $CDCl_3$) δ = 30.65 (s, 1P (S_2)), 30.37 (s, 1P (S_1)).

^{13}C-NMR (76 MHz, $CDCl_3$) δ = 149.92 (d, *J* = 9.1 Hz, 1C), 136.67 (d, *J* = 6.1 Hz, 1C), 133.90 (d, *J* = 2.3 Hz, 1C), 131.99 (d, *J* = 10.0 Hz, 1C), 131.61 (s, 1C), 130.74 (s, 1C), 128.39 (d, *J* = 12.9 Hz, 1C), 125.14 (s, 1C), 124.67(s, 1C), 123.63 (d, *J* = 9.7 Hz, 1C), 122.42 (s, 1C (S_1)), 121.83 (d, *J* = 10.0 Hz, 1C), 120.90 (s, 1C (S_2)), 120.26 (d, *J* = 6.4 Hz), 118.43 (d, *J* = 11.3 Hz, 1C), 73.14 (s, 1C (S_2)), 71.64 (s, 1C (S_1)).

IR (ATR) ν (cm^{-1}): 3208 (m, br), 2847 (w), 1638 (w), 1609 (w), 1594 (w), 1585 (w), 1479 (m), 1448 (w), 1430 (m), 1278 (w), 1223 (st, br), 1174 (m), 1116 (m), 1082 (m), 1047 (w), 990 (m), 937 (m), 921 (st), 876 (w), 809 (w), 784 (m), 774 (w), 755 (st), 713 (st), 683 (m, br), 616 (w), 597 (m), 571 (m), 517 (m), 498 (m), 490 (m), 429 (m).

MS (APCI+): m/z calculated for $C_{15}H_{13}O_3P$: $[M+H]^+$ 273.07; found: $[M+H]^+$ 273.06.

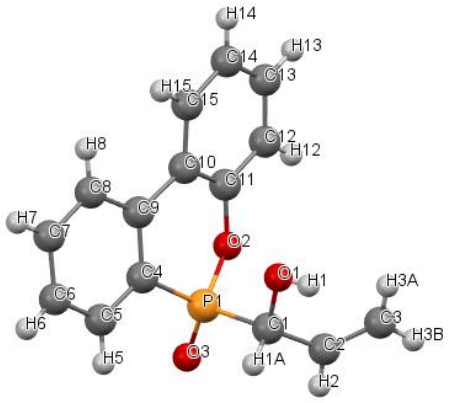

Empirical formula	$C_{15}H_{13}O_3P$
Formula weight	272.22
Temperature/K	180.15
Crystal system	triclinic
Space group	P-1
a / Å	9.8854(17)
b / Å	10.4649(17)
c / Å	12.8235(18)
α / °	85.487(12)
β / °	75.941(13)
γ / °	84.551(14)
Volume/Å^3	1278.9(4)
Z	4
ρ_{calc} / g/cm^3	1.414
μ / mm^{-1}	0.215
F(000)	568.0
Crystal size / mm^3	0.45 × 0.29 × 0.13
Radiation	MoKα (λ = 0.71073)
2Θ range for data collection / °	3.28 to 51.446
Index ranges	$-12 \leq h \leq 12$, $-12 \leq k \leq 12$, $-15 \leq l \leq 15$
Reflections collected	10888
Independent reflections	4783 [R_{int} = 0.0888, R_{sigma} = 0.1372]
Data/restraints/parameters	4783/0/346
Goodness-of-fit on F^2	0.796
Final R indexes [I ≥ 2σ (I)]	R_1 = 0.0499, wR_2 = 0.0986
Final R indexes [all data]	R_1 = 0.1462, wR_2 = 0.1238
Largest diff. peak/hole / e Å^{-3}	0.40/-0.24

6.2.2.2. 6-((1-(6-Oxidodibenzo[*c,e*][1,2]oxaphosphinin-6-yl)allyl)oxy)dibenzo[*c,e*][1,2]oxaphosphinine 6-oxide, (DOPO-Acrolein-O-DOPO)

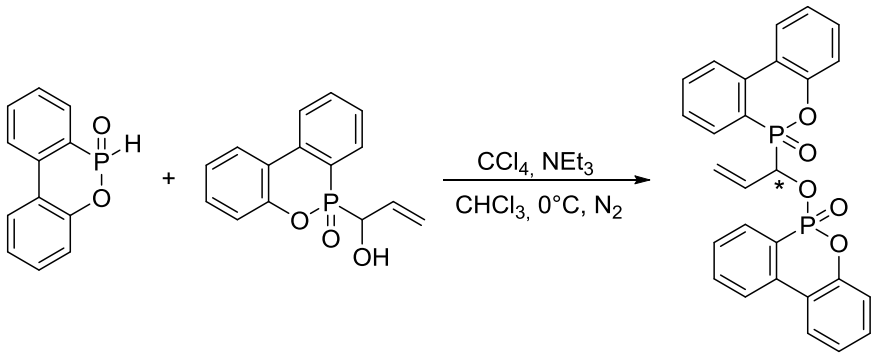

A three-necked round-bottomed flask was equipped with a stir bar, a condenser, a thermometer, a nitrogen inlet and a bubble counter and the whole apparatus was evacuated, heated and set under nitrogen atmosphere three times. 1.98 (9.2 mmol) DOPO were filled into the flask and dissolved in 10 mL chloroform at 60 °C. 2.50 g (9.2 mmol) DOPO-acrolein were added and dissolved at 70 °C. The solution was cooled down with an ice bath to 0 °C and 1.02 g (10.1 mmol) dry triethylamine were added to the solution. Then 1.55 g (10.1 mmol) tetrachloromethane were added dropwise to the solution at 0 °C. The reaction solution was stirred overnight while it was allowed to reach room temperature. For purification, the solution was washed with 0.1 M HCl solution and water. The organic phase was separated, dried over $MgSO_4$ and the solvent was removed with a rotary evaporator. The crude product contains multiple stereoisomers. It may be recrystallized from methanol.

^{1}H-NMR (300 MHz, $CDCl_3$) δ = 7.92 – 7.58 (m, 8H), 7.38 – 7.27 (m, 4H), 7.24 – 7.09 (m, 2H), 7.07 – 6.94 (m, 2H), 6.14 – 5.96 (m, 1H), 5.66 – 5.51 (m, 1H), 5.42 (dd, *J* = 10.2, 3.5 Hz, 1H), 5.29 (dd, *J* = 17.2, 4.6 Hz, 1H).

^{31}P-NMR (122 MHz, $CDCl_3$) δ = 26.76 (d, *J* = 31.2 Hz), 11.25 (d, *J* = 31.2 Hz).

^{13}C-NMR (76 MHz, $CDCl_3$) δ = 150.14 – 149.25 (m, 2C), 136.90 (dd, *J* = 14.4, 7.3 Hz, 1C), 134.05 (s, 1C), 133.68 (d, *J* = 2.5 Hz, 1C), 132.62 – 132.17 (m, 1C), 130.76 (d, *J* = 4.9 Hz, 1C), 130.53 – 130.26 (m, 2C), 129.00 (d, *J* = 17.8 Hz, 1C), 128.54 – 127.82 (m, 2C), 125.30 – 124.90 (m, 3C), 124.75 (d, *J* = 4.3 Hz, 2C), 123.99 – 123.39 (m, 2C), 122.23 (d, *J* = 7.7 Hz, 1C), 121.58 (dd, *J* = 21.0, 11.4 Hz, 1C), 121.18 – 120.82 (m, 2C), 120.49 – 120.00 (m, 3C), 77.36 (s, 2C).

IR (ATR) ν (cm^{-1}): 3065 (w), 1607 (w), 1595 (w), 1583 (w), 1561 (w), 1476 (m), 1448 (w), 1430 (m), 1258 (m), 1239 (m), 1199 (m), 1151 (m), 1118 (m) 1084 (w), 1004 (m), 919 (st), 847 (m), 782 (m), 750 (st), 713 (st), 685 (m), 616 (m), 601 (m), 559 (w), 498 (m), 429 (m).

MS (EI+): m/z calculated for $C_{27}H_{20}O_5P_2$: [M] 486; found: $[M+H]^+$ 486.

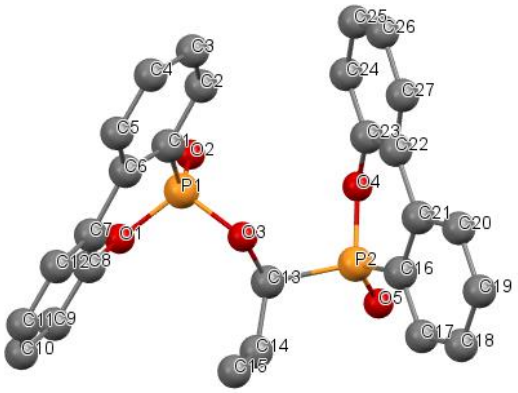

Empirical formula	$C_{27.5}H_{22}O_{5.5}P_2$
Formula weight	502.39
Temperature/K	180.15
Crystal system	monoclinic
Space group	$P2_1/n$
a / Å	9.1178(5)
b / Å	13.9703(10)
c / Å	19.0318(12)
α / °	90
β / °	100.362(5)
γ / °	90
Volume / $Å^3$	2384.7(3)
Z	4
ρ_{calc} / g/cm^3	1.399
μ / mm^{-1}	0.223
F(000)	1044.0
Crystal size / mm^3	0.38 × 0.06 × 0.05
Radiation	MoKα (λ = 0.71073)
2Θ range for data collection / °	3.638 to 51.52
Index ranges	$-11 \leq h \leq 10$, $-16 \leq k \leq 16$, $-23 \leq l \leq 23$
Reflections collected	16065
Independent reflections	4483 [R_{int} = 0.0409, R_{sigma} = 0.0394]
Data/restraints/parameters	4483/1/326
Goodness-of-fit on F^2	0.999
Final R indexes [$I \geq 2\sigma(I)$]	R_1 = 0.0369, wR_2 = 0.0855
Final R indexes [all data]	R_1 = 0.0642, wR_2 = 0.0937
Largest diff. peak/hole / e $Å^{-3}$	0.49/-0.36

6.2.2.3. Attempted Polymerization of DOPO-Acrolein

170 g (0.624 mol) DOPO-acrolein were filled into an aluminum pan and placed in a vacuum oven. The temperature was set to 150 °C at reduced pressure until a homogeneous melt occurred. Then the temperature was raised to 160 °C for 6 h yielding 154 g of crude product. For purification, the product was dissolved in chloroform and washed with distilled water. It was precipitated from hexane to yield a colorless solid that was dried in a vacuum oven at 80 °C under reduced pressure.

Yield: 146 g ≡ 0.536 mol ≡ 86%.

^{31}P-NMR (122 MHz, $CDCl_3$) δ = 39.47 – 38.98 (m, 1P), 38.74 (dd, *J* = 9.7, 2.0 Hz, 1P), 33.08 (dd, *J* = 6.6, 2.2 Hz, 1P), 32.56 – 31.73 (m, 1P).

6.2.2.4. 6-(Hydroxy(5-(hydroxymethyl)furan-2-yl)methyl)dibenzo[*c,e*][1,2]oxaphosphinine 6-oxide, (DOPO-HMF)

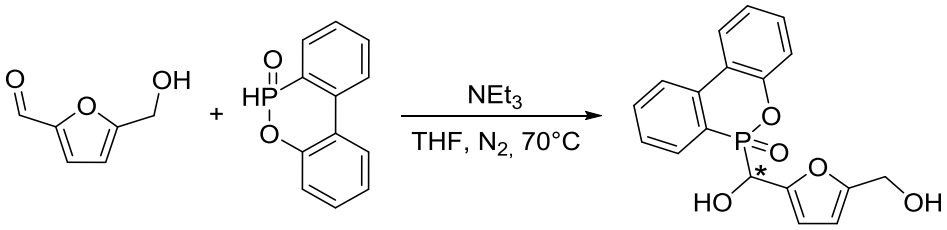

A two-necked round-bottomed flask was equipped with a stir bar, a condenser, a nitrogen inlet and a bubble counter and the whole apparatus was evacuated, heated and set under nitrogen atmosphere 3 times. 5.00 g (0.040 mol) HMF and 8.57 g (0.040 mol) DOPO were added to the flask and dissolved in 50 mL of dry THF at 70°C. 4.05 g (0.040 mol) dry triethylamine were added and it was stirred at 70 °C for 3 h. The solution was allowed to react overnight at room temperature. A highly viscous gel emerged. The solvent was evaporated under vacuum in a rotary evaporator and the remaining gel was taken up in dichloromethane (DCM). When the DCM solution was washed with dist. water a slightly orange solid precipitated that was filtered off and washed with further DCM. The DCM phase was separated, combined with the washing phase and dried over $MgSO_4$. It was filtered and the solvent was evaporated with a rotary evaporator. The residue was combined with the precipitated solid and dried in a vacuum oven at 60 °C. The product exists as two stereoisomers S_1 and S_2.

Yield: 7.84 g ≡ 0.023 mol ≡ 57 %.

^{1}H-NMR (300 MHz, DMSO-d_6) δ = 8.22 (dd, J = 8.2, 4.9 Hz, 1H), 8.14 (dd, J = 7.9, 1.6 Hz, 1H), 7.94 (ddd, J = 12.5, 7.6, 1.4 Hz, 1H), 7.80 (tt, J = 8.2, 1.4 Hz, 1H), 7.60 (tdd, J = 7.4, 3.0, 0.9 Hz, 1H), 7.46 – 7.38 (m, 1H), 7.33 – 7.17 (m, 2H), 6.45 (dd, J = 15.8, 6.4 Hz, 1H (S_2)), 6.41 (dd, J = 15.0, 6.2 Hz, 1H (S_1)), 6.32 (t, J = 3.0 Hz, 1H (S_1)), 6.26 (dd, J = 14.3, 3.2 Hz, 2H (S_2)), 6.17 (d, J = 3.2 Hz, 1H (S_1)), 5.26 (dd, J = 9.3, 6.2 Hz, 1H (S_1)), 5.21 (s, 1H (S_2)), 5.18 (t, J = 5.7 Hz, 1H (S_1)), 5.12 (dd, J = 12.4, 6.4 Hz, 1H (S_2)), 4.32 (d, J = 5.7 Hz, 1H (S_2)), 4.26 (d, J = 5.7 Hz, 2H (S_1)).

^{31}P-NMR (122 MHz, DMSO-d_6) δ = 29.41 (s, 1P (S_2)), 29.37 (s, 1P (S_1)).

^{13}C-NMR (76 MHz, $CDCl_3$) δ = 155.64 (d, J = 12.3 Hz, 1C), 149.76 (dd, J = 12.1, 9.1 Hz, 1C), 149.21 (s, 1C), 136.20 – 135.73 (m, 1C), 133.73 (d, J = 10.5 Hz, 1C), 131.50 (dd, J = 51.3, 10.3 Hz, 1C), 130.62 (d, J = 11.6 Hz, 1C), 128.38 (t, J = 13.0 Hz, 1C), 125.41 (d, J = 10.6 Hz, 1C), 124.33 (d, J = 10.7 Hz, 1C), 123.71 (dd, J = 15.1, 9.3 Hz, 1C), 123.05 (d, J = 26.2 Hz, 1C), 121.83 – 121.03 (m, 1C), 119.91 – 119.51 (m, 1C), 110.04 (dd, J = 19.0, 6.4 Hz, 1C), 107.77 (s, 1C), 66.07 (dd, J = 122.2, 58.6 Hz, 1C), 55.63 (d, J = 4.2 Hz, 1C).

IR (ATR) ν (cm^{-1}): 3254 (m, br), 2927 (w), 1607 (w), 1593 (w), 1585 (w), 1555 (w), 1480 (m), 1446 (w), 1430 (m), 1278 (w), 1237 (m), 1204 (st), 1176 (m), 1120 (m), 1082 (w), 1068 (m), 1021 (w), 999 (m), 978 (m), 935 (st), 861 (w), 817 (m), 779 (m), 744 (st), 712 (m), 681 (m), 650 (m), 635 (m), 615 (w), 591 (w), 531 (st), 507 (m), 492 (w), 474 (m), 430 (m).

MS (ESI+): m/z calculated for $C_{18}H_{15}O_5P$: $[M+Na]^+$ 365.05; found: $[M+Na]^+$ 365.06.

6.2.2.5. 6,6'-((2,2-Bis(hydroxymethyl)propane-1,3-diyl)bis(oxy))bis(dibenzo[*c,e*][1,2]oxaphosphinine 6-oxide), (DiDOPO-PE)[165]

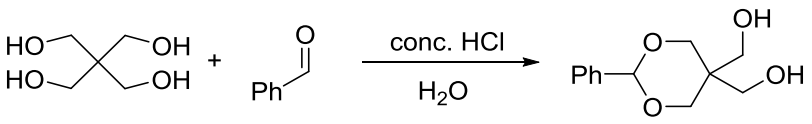

The protection of PE with benzaldehyde was conducted after Issidorides *et al.*[205] The crude product was recrystallized two times giving a yield of 60 % pure product.

^{1}H-NMR (300 MHz, DMSO-d_6) δ = 7.51 – 7.24 (m, 5H), 5.40 (s, 1H), 4.57 (dt, J = 24.2, 5.2 Hz, 2H), 3.91 (d, J = 11.6 Hz, 2H), 3.79 (d, J = 11.7 Hz, 2H), 3.67 (d, J = 5.2 Hz, 2H), 3.24 (d, J = 5.0 Hz, 2H).

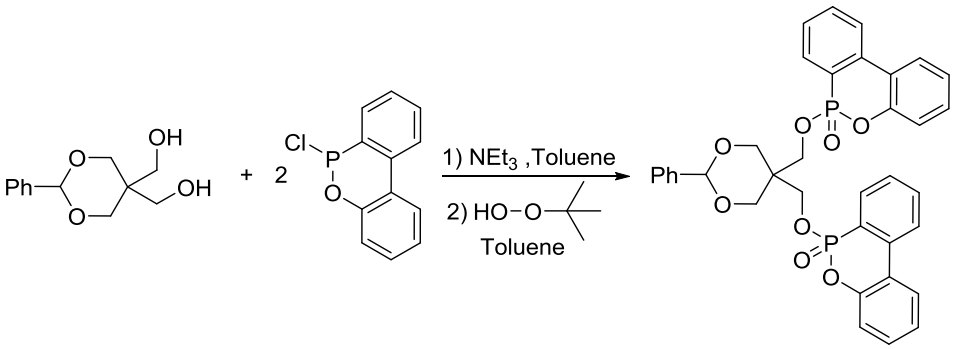

A three-necked round-bottomed flask was equipped with a stir bar, a condenser, a dropping funnel, a thermometer, a nitrogen inlet and a bubble counter and the whole apparatus was evacuated, heated and set under nitrogen atmosphere three times. 4.00 g (0.018 mol) of the protected PE and 3.64 g (0.036 mol) dry triethylamine were added to the flask and dissolved in 30 mL of dry toluene. The reaction mixture was cooled with an ice bath. A solution of DOP-Cl in 20 mL of dry toluene was filled into the addition funnel and added dropwise so that the temperature did not exceed 5 °C. It was allowed to react at room temperature overnight. The reaction mixture was filtrated under inert condition and the flask containing the gathered filtrate was connected to a condenser. A solution of *tert*-butyl hydroperoxide in toluene (with a concentration 41.4 wt%) was prepared and 8.83 g were filled into an addition funnel. The funnel was connected to the reaction flask and the reaction vessel was cooled with an ice bath. The peroxide solution was added dropwise to the flask and it was allowed to react at room temperature for 3 h. The reaction solution was washed twice with brine and the phases were separated. The organic phase was dried over $MgSO_4$, it was filtrated and the solvent was evaporated with a rotary evaporator.

Yield: 10.90 g ≡ 0.017 mol ≡ 93 %.

^{1}H-NMR (300 MHz, DMSO-d_6) δ = 8.31 – 8.05 (m, 4H), 7.98 – 7.75 (m, 4H), 7.67 – 7.53 (m, 2H), 7.51 – 7.06 (m, 6H), 4.30 – 4.05 (m, 2H), 3.83 – 3.69 (m, 2H), 3.69 – 3.47 (m, 4H).

^{31}P-NMR (122 MHz, DMSO-d_6) δ = 9.93 (s, 1P), 9.76 (s, 1P).

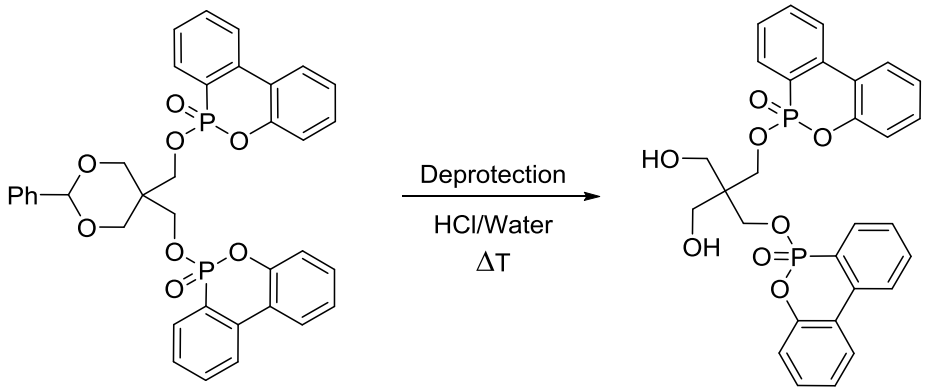

The protected DiDOPO-PE was dissolved in 300 mL of a toluene/water mixture (1:1) and it was filled in a distillation flask. 7 mL of conc. HCl were added and it was distilled at 70 °C and 200 mbar. During the distillation process more toluene, water and conc. HCl were added, if necessary. It was distilled for 6 d during which a white precipitate emerged in the distillation flask. The resulting solid product was filtered off and dried in vacuum.

Yield: 5.12 g ≡ 0.009 mol ≡ 53 %.

^{1}H-NMR (300 MHz, DMSO-d_6) δ = 8.30 – 8.04 (m, 4H), 7.90 – 7.69 (m, 4H), 7.59 (tddd, *J* = 7.4, 3.6, 1.7, 0.9 Hz, 2H), 7.45 (dddd, *J* = 8.4, 7.4, 2.7, 1.3 Hz, 2H), 7.34 (tdd, *J* = 7.3, 1.5, 0.7 Hz, 2H), 7.23 (dt, *J* = 8.1, 1.7 Hz, 2H), 4.52 (s, 2H), 3.90 – 3.69 (m, 4H), 3.08 (s, 4H).

^{31}P-NMR (122 MHz, DMSO-d_6) δ = 9.73 (s, 2P).

6.2.2.6. 6-(2,2-Bis(hydroxymethyl)butoxy)dibenzo[*c,e*][1,2]oxaphosphinine 6-oxide, (DOPO-TMP)[168]

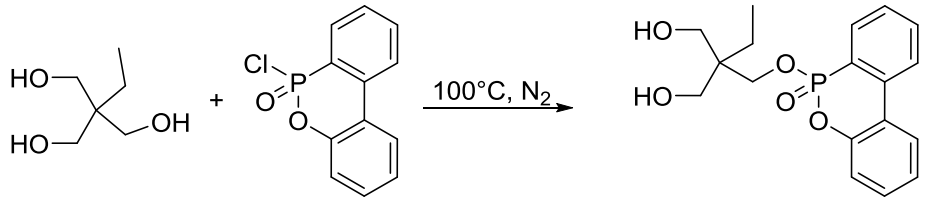

A two-necked round-bottomed flask was equipped with a stir bar, a condenser, a nitrogen inlet and gas washing bottles filled with sodium hydroxide sol. and the apparatus was evacuated, heated and set under nitrogen atmosphere. 64.24 g (0.479 mol) TMP were filled into the flask and dried prior use at 100 °C under vacuum for 2 h. 40.41 g (0.161 mol) DOPO-Cl were added in small portions over 4 h at 100 °C and it was allowed to react overnight. The crude product was dissolved in chloroform and washed with water, sat. $NaHCO_3$ sol. and again with water. Phases were separated, the organic phase was dried over $MgSO_4$, it was filtrated and the solvent was evaporated. It may be further purified by column chromatography with an eluent of MeOH:$CHCl_3$/1:9 but for further reactions, this purification was not applied. The product is a colorless solid.

Yield: 50.90 g ≡ 0.146 mol ≡ 91 %.

^{1}H-NMR (300 MHz, $CDCl_3$) δ = 8.06 – 7.89 (m, 3H), 7.82 – 7.68 (m, 1H), 7.55 (tdd, *J* = 7.5, 3.7, 1.1 Hz, 1H), 7.46 – 7.35 (m, 1H), 7.36 – 7.22 (m, 2H), 4.45 (t, *J* = 11.1 Hz, 1H), 4.12 (dd, *J* = 10.9, 9.4 Hz, 1H), 3.62 (td, *J* = 6.5, 4.9 Hz, 4H), 3.48 (dt, *J* = 32.3, 6.3 Hz, 2H), 1.17 (q, *J* = 7.7, 6.7 Hz, 2H), 0.74 (t, *J* = 7.6 Hz, 3H).

^{31}P-NMR (122 MHz, $CDCl_3$) δ = 13.18 (s, 1P).

^{13}C-NMR (76 MHz, $CDCl_3$) δ = 149.79 (d, *J* = 7.8 Hz, 1C), 137.21 (d, *J* = 7.1 Hz, 1C), 133.94 (d, *J* = 2.5 Hz, 1C), 130.79 (s, 1C) , 130.28 (d, *J* = 9.1 Hz, 1C), 128.53 (d, *J* = 15.6 Hz, 1C), 125.42 (s, 1C), 125.08 (s, 1C), 124.31 (d, *J* = 12.3 Hz, 1C), 122.93 – 122.34 (m, 1C), 120.33 (d, *J* = 6.7 Hz, 2C), 66.70 (d, *J* = 6.8 Hz, 1C), 65.50 (d, *J* = 1.2 Hz, 2C), 43.56 (d, *J* = 3.6 Hz, 1C), 22.22 (s, 1C), 7.34 (s, 1C).

IR (ATR) ν (cm^{-1}): 3470 (m, br), 3426 (m, br), 2970 (w), 2932 (w), 2888 (w, br), 1608 (w), 1597 (w), 1581 (w), 1561 (w), 1477 (w), 1466 (w), 1449 (w), 1429 (w), 1392 (w), 1330 (w), 1282 (w), 1229 (m), 1190 (m), 1153 (m), 1118 (w), 1067 (m), 1033 (st), 1020 (w), 991 (m), 936 (st), 893 (w), 826 (m), 790 (m), 756 (st), 717 (m), 686 (w), 602 (m), 543 (m), 526 (m), 514 (m), 494 (m), 448 (m), 428 (m), 407 (m).

MS (APCI+): m/z calculated for $C_{18}H_{21}O_5P$: $[M+H]^+$ 349.12; found: $[M+H]^+$ 349.12.

6.2.2.7. 2,2-Bis(hydroxymethyl)butyl diphenylphosphinate, (Ph_2PO-TMP)

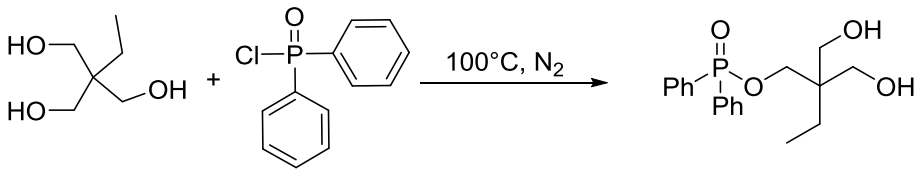

Ph_2PO-TMP was synthesized after the same procedure as DOPO-TMP with 5.10 g (0.038 mol) TMP and 3.00 g (0.013 mol) Ph_2PO-Cl instead of DOPO-Cl. It was not purified by column chromatography and yielded a highly viscous, colorless liquid.

Yield: 3.92 g ≡ 0.012 mol ≡ 90 %.

^{1}H-NMR (300 MHz, $CDCl_3$) δ = 7.86 – 7.66 (m, 4H), 7.57 – 7.33 (m, 6H), 4.27 (s, 2H), 4.07 (d, *J* = 9.6 Hz, 2H), 3.60 (s, 4H), 1.32 (q, *J* = 7.6 Hz, 2H), 0.86 (t, *J* = 7.6 Hz, 3H).

^{31}P-NMR (122 MHz, $CDCl_3$) δ = 35.48 (s, 87%), 33.74 (s, 13%, di-substituted TMP).

^{13}C-NMR (76 MHz, $CDCl_3$) δ = 132.56 (d, *J* = 2.8 Hz, 2C), 131.57 (d, *J* = 10.3 Hz, 4C), 129.80 (d, *J* = 8.0 Hz, 2C), 128.76 (d, *J* = 13.3 Hz, 4C), 65.14 (d, *J* = 6.1 Hz, 1C), 64.69 (s, 2C), 43.85 (d, *J* = 3.7 Hz, 1C), 22.22 (s, 1C), 7.46 (s, 1C).

IR (ATR) ν (cm^{-1}): 3371 (w, br), 3058 (w), 2963 (w, br), 2882 (w, br), 1592 (w), 1462 (w), 1439 (m), 1203 (m, br), 1130 (m), 1113 (m), 1009 (st, br), 987 (st), 847 (m), 751 (m), 728 (st), 691 (st), 553 (st), 525 (st) 447 (m).

MS (APCI+): m/z calculated for $C_{18}H_{23}O_4P$: $[M+H]^+$ 335.14; found: $[M+H]^+$ 335.14. m/z calculated for di-substituted TMP $C_{30}H_{32}O_5P_2$: $[M+H]^+$ 535.18; found: $[M+H]^+$ 535.17. m/z calculated for tri-substituted TMP $C_{42}H_{41}O_6P_3$: $[M+H]^+$ 735.21; found: $[M+H]^+$ 735.21.

6.2.2.8. 2,2-Bis(hydroxymethyl)butyl diphenyl phosphate ($(PhO)_2PO$-TMP)

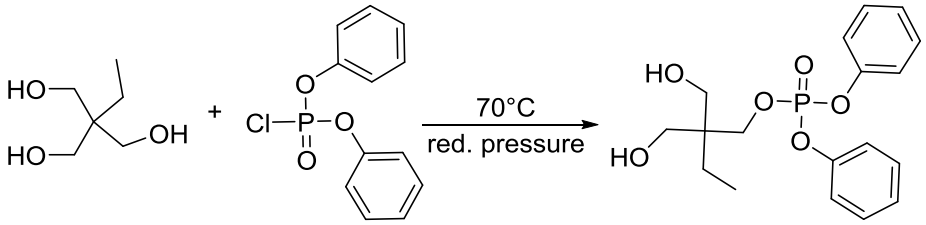

A Schlenk flask was equipped with a stir bar, an addition funnel and a gas trap and it was evacuated, heated and set under nitrogen. 140.39 g (1.046 mol) TMP were filled into the flask and dried prior use at 100 °C under vacuum for 2 h. It was allowed to cool down to 70 °C. 100.00 g (0.372 mol) $(PhO)_2PO$-Cl were filled into the addition funnel and added dropwise under reduced pressure, successively applied down to 150 mbar, over 2.25 h. It was stirred at 70 °C under vacuum until no gas was evolved anymore. The crude product was dissolved in chloroform and washed with water, sat. $NaHCO_3$ sol. and again with water. The different phases were separated, the organic phase was dried over $MgSO_4$, it was filtrated and the solvent was evaporated to yield a waxy, colorless solid.

Yield: 109.70 g ≡ 0.299 mol ≡ 81 %.

^{1}H-NMR (300 MHz, $CDCl_3$) δ = 7.40 – 7.28 (m, 4H), 7.24 – 7.09 (m, 6H), 4.29 (d, *J* = 7.6 Hz, 2H), 3.58 – 3.44 (m, 6H), 1.23 (q, *J* = 7.6 Hz, 2H), 0.79 (t, *J* = 7.6 Hz, 3H).

^{31}P-NMR (122 MHz, $CDCl_3$) δ = -10.36 (s, 84.1%), -11.21 (s, 6%, 5-ethyl-5-(hydroxymethyl)-2-phenoxy-1,3,2-dioxaphosphinane oxide), -12.85 (s, 9.9%, di-substituted TMP).

^{13}C-NMR (76 MHz, $CDCl_3$) δ = 150.44 (d, *J* = 7.4 Hz, 2C), 129.99 (d, *J* = 1.0 Hz, 4C), 125.78 (d, *J* = 1.4 Hz, 2C), 120.21 (d, *J* = 4.8 Hz, 4C), 68.93 (d, *J* = 6.4 Hz, 1C), 65.09 (s, 2C), 43.64 (d, *J* = 5.1 Hz, 1C), 22.09 (s, 1C), 7.31 (s, 1C).

IR (ATR) ν (cm^{-1}): 3351 (m, br), 2941 (w, br), 2884 (w, br), 1588 (m), 1484 (m), 1455 (w), 1385 (w), 1348 (w), 1258 (m), 1209 (w), 1178 (m), 1158 (m), 1067 (m), 1055 (m), 1008 (st, br), 947 (st, br), 910 (m), 886 (m), 860 (m), 776 (st), 740 (m), 689 (st), 616 (w), 588 (m), 540 (st), 527 (st), 504 (st), 488 (st), 458 (m), 421 (w).

MS (APCI+): m/z calculated for $C_{18}H_{23}O_6P$: $[M+H]^+$ 367.13; found: $[M+H]^+$ 367.13. m/z calculated for di-substituted TMP $C_{30}H_{32}O_9P_2$: $[M+H]^+$ 599.16; found: $[M+H]^+$ 599.15. m/z calculated for $C_{12}H_{17}O_5P$: $[M+H]^+$ 273.08; found: $[M+H]^+$ 273.09. m/z calculated for diphenyl phosphate $C_{12}H_{11}O_4P$: $[M+H]^+$ 251.04; found: $[M+H]^+$ 251.04.

6.2.2.9. Generation of P-Polyols

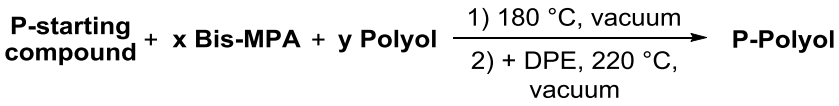

P-Polyol #	P-starting compound	x =	y =	Polyol =	One-Pot?
1	DiDOPO-PE	2	1	PE	No
2a	DOPO-TMP-d	2	1	PE	No
2b	DOPO-TMP	2	1	DPE	No
2c	DOPO-TMP	2	1	DPE	Yes
3	DOPO-TMP	1	0	-	No
4	Ph_2PO-TMP	1	0	-	Yes
5	$(PhO)_2PO$-TMP	1	0	-	Yes

A Schlenk flask was equipped with a stir bar, a nitrogen inlet and a gas trap and the whole apparatus was evacuated, heated and set under nitrogen atmosphere. The P-starting compound, x equivalents Bis-MPA and y equivalents of a polyol were added to the flask and it was heated until a homogeneous melt was formed while applying vacuum. The temperature was raised to 180 °C and the melt was stirred until no gas emerged from the reaction. Experiments **1**-**4** were executed in two consecutive steps, while experiments **5**-**7** were performed in a one-pot procedure.

Experiments **1**-**4**: The hot melt was filled into an aluminum pan and after cooling down it was crushed in a mortar to yield a fine powder. A Schlenk flask was equipped with a stir bar, a nitrogen inlet and a gas trap and the whole apparatus was evacuated, heated and set under nitrogen atmosphere. The powder from the previous step was mixed with 1 wt equivalent of DPE and the mixture was filled into the flask. It was heated to 220 °C while applying vacuum until a homogeneous melt was formed. The hot melt was filled into an aluminum pan and after cooling down it was crushed in a mortar to yield a fine powder.

Experiments **5**-**7**: 1 wt equivalent of DPE was added to the flask and the temperature was raised to 220 °C until a homogeneous melt occurred. The hot melt was poured into an aluminum pan and after cooling down it was crushed in a mortar.

Purification: The resulting powder was washed thoroughly with sat. $NaHCO_3$ sol. and water and then dried at 90 °C in a vacuum oven.

6.2.3. Synthesis and combination of P- and OH-containing Acrylates and Acrylamides

6.2.3.1. *N*-(2-((6-Oxidodibenzo[*c,e*][1,2]oxaphosphinin-6-yl)oxy)ethyl) acrylamide, (DOPO-*N*-HEAA)[186]

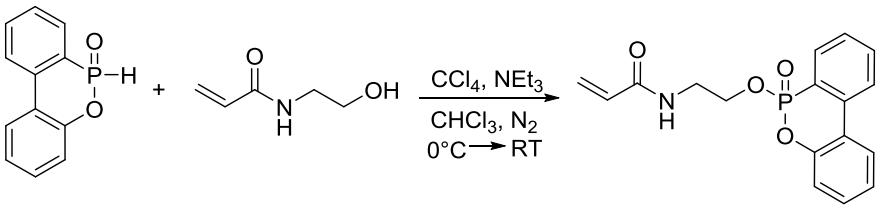

A three-necked round-bottomed flask was equipped with a stir bar, a nitrogen inlet, a condenser and a dropping funnel and the whole apparatus was evacuated, heated and set under nitrogen atmosphere three times. 5.00 g (0.023 mol) DOPO were added to the flask and dissolved in 45 mL

of dry chloroform. 7.08 g (0.046 mol) carbon tetrachloride were added and the solution was cooled down with an ice bath. A solution of 2.66 g *N*-HEAA and 2.56 g (0.025 mol) dry triethylamine in 15 mL dry chloroform was added dropwise through the addition funnel. It was stirred at room temperature for 72 h. The reaction solution was washed with sat. $NaHCO_3$ sol., brine and water. The organic phase was separated and dried over $MgSO_4$, it was filtrated and the solvent was evaporated.

Yield: 6.82 g ≡ 0.021 mol ≡ 90 %.

^{1}H-NMR (300 MHz, DMSO-d_6) δ = 7.98 – 7.80 (m, 3H), 7.71 – 7.63 (m, 1H), 7.45 (tdd, *J* = 7.5, 3.7, 1.0 Hz, 1H), 7.37 – 7.29 (m, 1H), 7.25 – 7.13 (m, 2H), 7.02 – 6.84 (m, 1H), 6.18 (dd, *J* = 17.1, 1.8 Hz, 1H), 6.03 (dd, *J* = 17.1, 10.1 Hz, 1H), 5.53 (dd, *J* = 10.1, 1.8 Hz, 1H), 4.28 – 3.99 (m, 2H), 3.51 (q, *J* = 5.1 Hz, 2H).

^{31}P-NMR (122 MHz, DMSO-d_6) δ = 11.13 (s, 1P).

^{13}C-NMR (76 MHz, $CDCl_3$) δ = 165.59 (s, 1C), 149.42 (d, *J* = 7.9 Hz, 1C), 136.80 (d, *J* = 7.1 Hz, 1C), 133.60 (d, *J* = 2.4 Hz, 1C), 130.54 (d, *J* = 6.2 Hz, 2C), 129.95 (d, *J* = 9.2 Hz, 1C), 128.21 (d, *J* = 15.5 Hz, 1C), 126.09 (s, 1C), 125.10 (d, *J* = 1.0 Hz, 1C), 124.77 (s, 1C), 123.97 (d, *J* = 12.2 Hz, 1C), 122.25 (t, *J* = 12.3 Hz, 1C), 120.02 (s, 1C), 119.90 (d, *J* = 6.7 Hz, 1C), 65.46 (d, *J* = 6.8 Hz, 1C), 39.62 (d, *J* = 5.3 Hz, 1C).

IR (ATR) ν (cm^{-1}): 3001 (w, br), 1630 (w, br), 1630 (w), 1581 (w), 1561 (w), 1476 (m), 1448 (w), 1431 (m), 1267 (m), 1237 (m), 1205 (m), 1154 (m), 1118 (m), 1095 (w), 1055 (m), 1040 (m), 1006 (w), 925 (m, br), 880 (w), 743 (st), 717 (st), 664 (m), 617 (m), 602 (w), 528 (m, br), 481 (w), 449 (w), 414 (w).

MS (APCI+): m/z calculated for $C_{17}H_{16}NO_4P$: $[M+H]^+$ 330.09; found: $[M+H]^+$ 330.09.

6.2.3.2. 2-((6-Oxidodibenzo[*c,e*][1,2]oxaphosphinin-6-yl)oxy)ethyl acrylate, (DOPO-HEA)

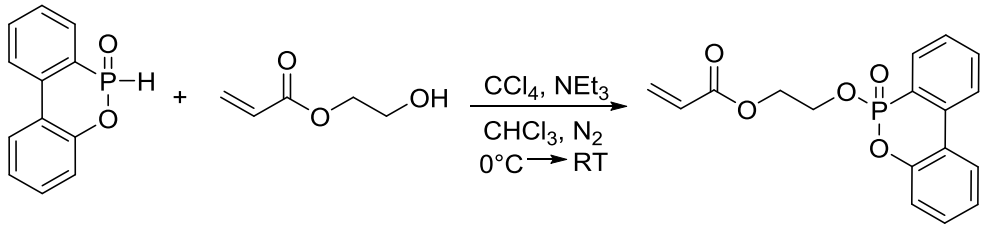

A three-necked round-bottomed flask was equipped with a stir bar, a nitrogen inlet, a condenser and a dropping funnel and the whole apparatus was evacuated, heated and set under nitrogen atmosphere three times. 10.00 g (0.046 mol) DOPO were added to the flask and dissolved in 65 mL of dry chloroform. 14.16 g (0.092 mol) carbon tetrachloride were added and the solution was cooled with an ice bath. A solution of 5.34 g (0.046 mol) HEA and 5.02 g (0.050 mol) dry triethylamine in 65 mL dry chloroform was filled into the addition funnel and added to the reaction dropwise. It was stirred at room temperature overnight. The reaction solution was washed with sat. $NaHCO_3$ sol., brine and water. The organic phase was separated and dried over $MgSO_4$, it was filtrated and the solvent was evaporated.

Yield: 11.51 g ≡ 0.035 mol ≡ 76 %.

^{1}H-NMR (300 MHz, $CDCl_3$) δ = 8.06 – 7.84 (m, 3H), 7.73 (ddt, *J* = 8.3, 7.4, 1.3 Hz, 1H), 7.52 (tdd, *J* = 7.5, 3.7, 0.9 Hz, 1H), 7.43 – 7.32 (m, 1H), 7.33 – 7.15 (m, 2H), 6.33 (dd, *J* = 17.3, 1.5 Hz, 1H), 6.01 (dd, *J* = 17.3, 10.4 Hz, 1H), 5.80 (dd, *J* = 10.4, 1.5 Hz, 1H), 4.46 – 4.33 (m, 2H), 4.33 – 4.21 (m, 2H).

^{31}P-NMR (122 MHz, $CDCl_3$) δ = 10.60 (s, 1P).

^{13}C-NMR (76 MHz, $CDCl_3$) δ = 165.08 (s, 1C), 149.20 (d, *J* = 7.9 Hz, 1C), 136.27 (d, *J* = 7.0 Hz, 1C), 134.06 (s, 1C), 131.96 (s, 1C), 130.93 (s, 1C), 129.81 (d, *J* = 9.4 Hz, 1C), 128.76 (d, *J* = 15.2 Hz, 1C), 127.76 (s, 1C), 125.86 (s, 1C), 125.09 (s, 1C), 124.69 (d, *J* = 11.8 Hz, 1C), 121.97 (d, *J* = 11.8 Hz), 121.62 (d, *J* = 179.6 Hz, 1C), 119.90 (d, *J* = 6.5 Hz, 1C), 64.38 (d, *J* = 6.2 Hz, 1C), 63.02 (d, *J* = 6.0 Hz, 1C).

IR (ATR) ν (cm^{-1}): 2956 (w), 1712 (st), 1638 (w), 1617 (w), 1597 (w), 1583 (w), 1561 (w), 1478 (m), 1448 (m), 1433 (m), 1414 (w), 1372 (w), 1251 (st), 1240 (st), 1157 (m), 1119 (m), 1080 (m), 1028 (st), 969 (st), 942 (st), 920 (st), 835 (w), 816 (m), 836 (m), 797 (m), 770 (w), 751 (st), 729 (st), 713 (st), 616 (m), 603 (m), 559 (m), 538 (m), 517 (st), 503 (m), 481 (w), 460 (w), 437 (m).

MS (APCI+): m/z calculated for $C_{17}H_{15}O_5P$: $[M+H]^+$ 331.07; found: $[M+H]^+$ 331.07.

6.2.3.3. Poly(*N*-hydroxyethyl acrylamide), (Poly(*N*-HEAA))

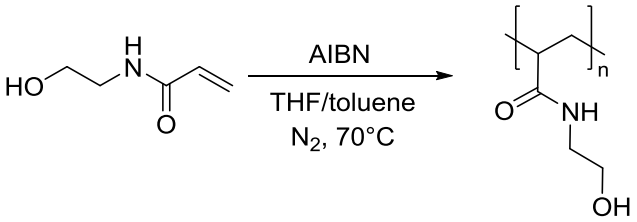

A three-necked round-bottomed flask was equipped with a mechanical stirrer, a condenser, a nitrogen inlet and a bubble counter and the whole apparatus was evacuated and set under nitrogen. 75.00 g (0.651 mol) *N*-HEAA were dissolved in 250 mL THF and filled into the flask. 250 mL of toluene were added and the temperature was raised to 70 °C under vigorous stirring. The solution was degassed with nitrogen for 90 min. 16.3 mL of an AIBN solution (0.2 M in toluene) were added dropwise and it was allowed to react for 30 min during which a white solid precipitated. The temperature was raised to 120 °C and it was stirred for 1 h. The precipitate was filtrated off and dried at 100 °C in a vacuum oven.

Yield: 65.78 g ≡ 0.571 mol ≡ 88 %.

^{1}H-NMR (300 MHz, DMSO-d_6) δ = 7.58 (s, 1H), 5.21 – 4.54 (m, 1H), 3.44 (s, 2H), 3.29 – 2.82 (m, 2H), 2.21 – 1.70 (m, 1H), 1.70 – 0.89 (m, 2H).

IR (ATR) (cm^{-1}): 3273 (m, br), 2929 (w,b), 1636 (st), 1538 (st), 1430 (m), 1357 (m, br), 1218 (m, br), 1055 (st), 871 (w, br), 522 (st, br).

T_g = 126.25 °C

6.2.3.4. Poly(hydroxyethyl acrylate), (Poly(HEA))[187]

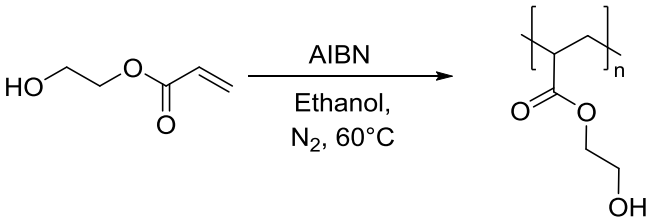

A two-necked round-bottomed flask was equipped with a stir bar, a condenser, a nitrogen inlet and a bubble counter and the whole apparatus was evacuated and set under nitrogen. 5.00 g (43 mmol) HEA were dissolved in 37 mL of ethanol and filled into the flask. The solution was degassed with nitrogen for 30 min. It was heated to 65 °C. 0.035 g (0.2 mmol) AIBN were dissolved in 3 mL of ethanol and the solution was added to the reaction flask dropwise. It was stirred at 65 °C for 5 h. The reaction solution was precipitated dropwise in diethyl ether, the filtrated polymer was redissolved in ethanol and the solvent was evaporated with rotary evaporator to yield a colorless, highly viscous liquid.

Yield: 4.36 g ≡ 0.038 mol ≡ 87 %.

^{1}H-NMR (300 MHz, DMSO-d_6) δ = 4.75 (t, br, J = 5.1 Hz, 1H), 4.19 – 3.82 (m, br, 2H), 3.55 (d, br, J = 4.9 Hz, 2H), 2.26 (s, br, 1H), 2.02 – 1.33 (m, br, 2H).

^{13}C-NMR (76 MHz, $CDCl_3$) δ = 174.15 (s, 1C), 65.75 (s, 1C), 58.87 (s, 1C), 40.85 (s, br, 1C), 34.41 (s, br, 1C).

IR (ATR) ν (cm^{-1}): 3399 (w, br), 2951 (w, br), 1723 (st), 1449 (w), 1394 (w), 1240 (m, br), 1159 (st), 889 (m), 842 (w), 503 (m, br).

T_g = 14.15 °C

6.2.3.5. Polymerization of DOPO-HEA (Poly(DOPO-HEA))

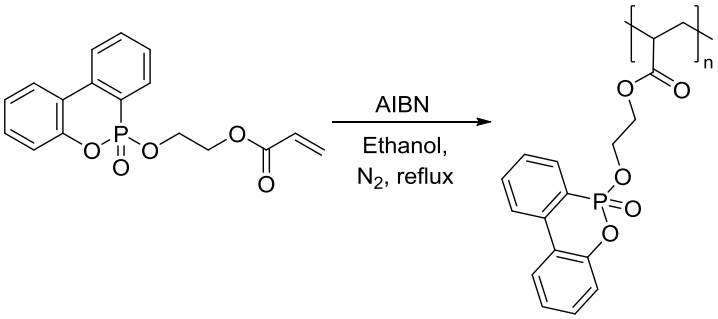

A three-necked round-bottomed flask was equipped with a stir bar, a condenser, a nitrogen inlet and a bubble counter and the whole apparatus was evacuated and set under nitrogen. 2.00 g (6.1 mmol) DOPO-HEA were dissolved in 40 mL of ethanol and filled into the flask. The solution was degassed with nitrogen for 30 min. It was heated to 65 °C. 0.005 g (0.03 mmol) AIBN were dissolved in 1 mL of ethanol and the initiator solution was added to the reaction flask dropwise. It was stirred and heated to reflux for 4.5 h. Afterwards it was stirred overnight at room temperature and then again at reflux for 9 h. A colorless highly viscous gel emerged that stuck to the wall of the

flask. The solution was decanted and the remaining gel was washed with more ethanol and dried at 80 °C in a vacuum oven to yield a colorless solid.
Yield: 1.30 g ≡ 3.9 mmol ≡ 65 %.

^{1}H-NMR (300 MHz, DMSO-d_6) δ = 8.30 – 7.90 (m, br, 2H), 7.90 – 7.58 (m, br, 2H), 7.58 – 6.99 (m, br, 4H), 4.46 – 3.58 (m, br, 4H), 2.24 – 1.68 (m, br, 1H), 1.67 – 0.68 (m, br, 2H).

^{31}P-NMR (122 MHz, DMSO-d_6) δ = 9.88 (s, br, 1P).

IR (ATR) ν (cm^{-1}): 3067 (w), 2951 (w, br), 1731 (m), 1608 (w), 1596 (w), 1583 (w), 1561 (w), 1477 (w), 1448 (w), 1431 (w), 1267 (m), 1240 (m), 1206 (m), 1153 (m), 1118 (m), 1030 (m), 917 (st, br), 751 (st), 716 (m), 687 (w), 617 (m), 542 (w), 518 (m), 445 (w), 414 (w).

6.2.3.6. Copolymerization of *N*-HEAA and DOPO-*N*-HEAA

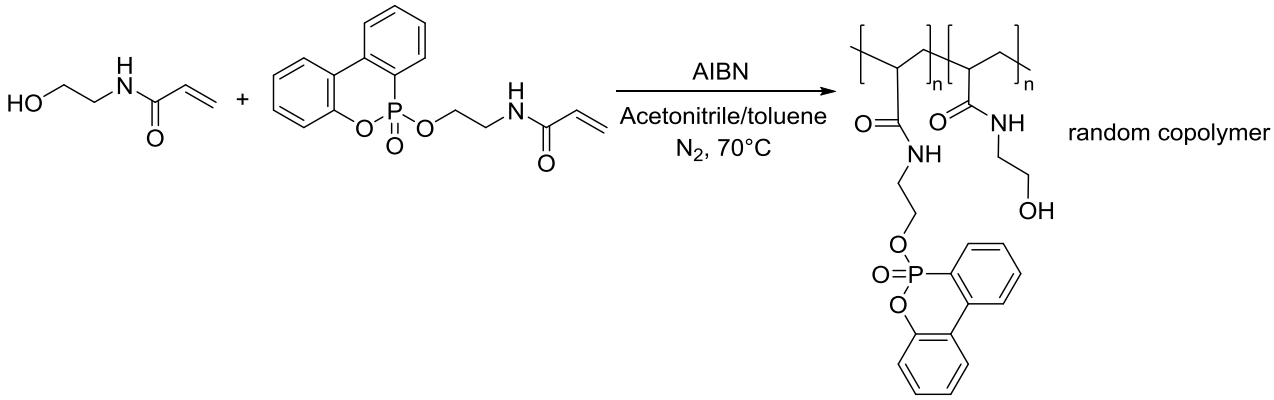

A two-necked round-bottomed flask was equipped with a stir bar, a condenser, a nitrogen inlet and a bubble counter and the whole apparatus was evacuated and set under nitrogen. 2.00 g (6.1 mmol) DOPO-*N*-HEAA were dissolved in 40 mL Acetonitrile and the solution was filled into the flask. 30 mL of toluene were added and it was stirred vigorously. It was heated to 70 °C and nitrogen was bubbled through the solution for 2 h. 0.7 g (6.1 mmol) *N*-HEAA were added and it was further degassed at 70 °C. 0.3 mL of an AIBN solution (0.2 M in toluene) were added dropwise and it was allowed to react for 2 h. The resulting precipitate was filtrated and dried at 100 °C in a vacuum oven.

Yield: 1.32 g ≡ 49 %.

IR (ATR) ν (cm^{-1}): 3271 (w, br), 2936 (w, br), 1733 (w), 1641 (m), 1552 (m), 1476 (w), 1447 (w), 1431 (m), 1204 (m), 1157 (m), 1119 (m), 1095 (m), 1054 (st), 979 (m, br), 888 (m), 784 (m), 755 (st), 718 (m), 687 (m), 616 (m), 603 (st), 528 (st).

6.2.3.7. Copolymerization of HEA and DOPO-HEA

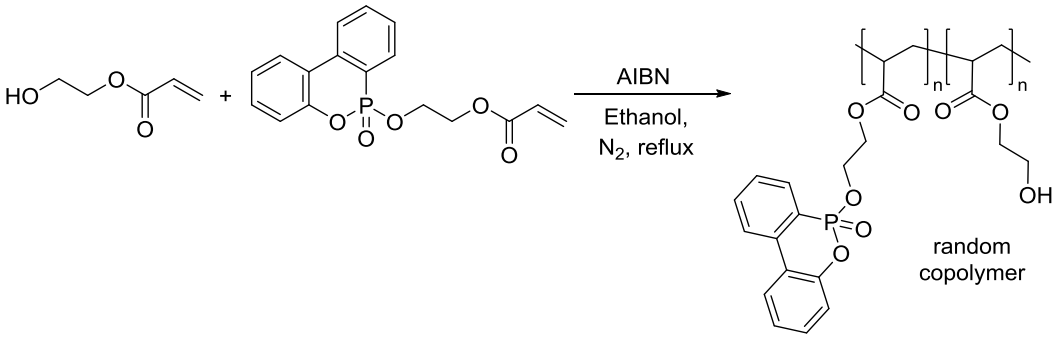

A three-necked round-bottomed flask was equipped with a stir bar, a condenser, a nitrogen inlet and a bubble counter and the whole apparatus was evacuated and set under nitrogen. 2.00 g (6.1 mmol) DOPO-HEA and 0.7 g (6.1 mmol) HEA were dissolved in 50 mL of ethanol and filled into the flask. The solution was degassed with nitrogen for 20 min. It was heated to 65 °C. 0.005 g (0.03 mmol) AIBN were dissolved in 1 mL of ethanol and the initiator solution was added to the reaction flask dropwise. It was stirred and heated to reflux for 3.8 h. Afterwards it was stirred overnight at room temperature and then again at reflux for 9 h. A colorless highly viscous gel emerged that stuck to the wall of the flask. The solution was decanted and the remaining gel was washed with more ethanol and dried at 80 °C in a vacuum oven to yield a colorless solid.

Yield: 1.10 g ≡ 41 %.

^{1}H-NMR (300 MHz, DMSO-d_6) δ = 8.29 – 7.96 (m, br, 2H), 7.96 – 7.67 (m, br, 2H), 7.64 – 7.47 (m, br, 1H), 7.47 – 7.34 (m, br, 1H), 7.34 – 7.07 (m, br, 2H), 4.91 – 4.48 (m, br, 1H), 4.44 – 3.68 (m, br, 6H), 3.66 – 3.38 (m, br, 2H), 2.38 – 1.86 (m, br, 2H), 1.86 – 0.72 (m, br, 4H).

^{31}P-NMR (122 MHz, DMSO-d_6) δ = 9.97 (s, br, 1P).

IR (ATR) ν (cm^{-1}): 3067 (w), 2950 (w, br), 1727 (m), 1608 (w), 1597 (w), 1583 (w), 1561 (w), 1478 (w), 1448 (w), 1431 (w), 1386 (w, br), 1260 (m), 1238 (m), 1201 (m), 1153 (m), 1118 (m), 1029 (m, br), 966 (m), 921, (st, br), 753 (st), 716 (m), 687 (w), 617 (w), 602 (m), 542 (w), 518 (m), 444 (w), 413 (w).

6.2.3.8. Copolymerization of *N*-HEAA and (DOPO-propionate)Zn(Acrylate)

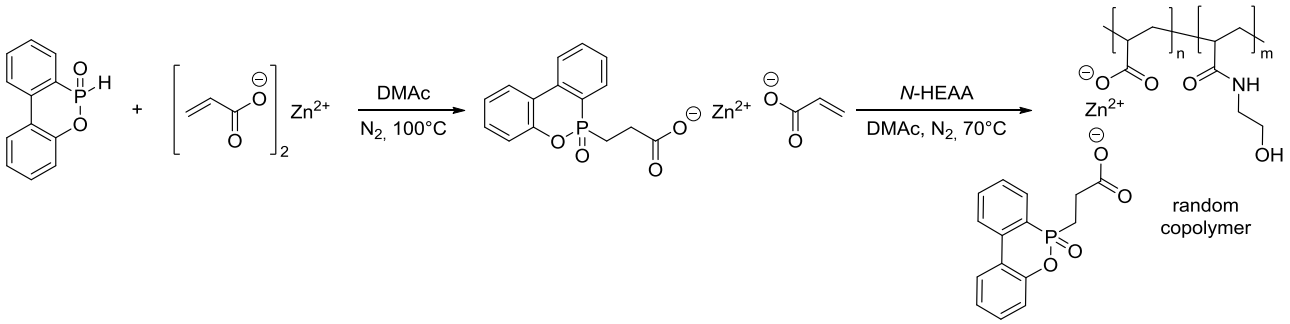

A two-necked round-bottomed flask was equipped with a stir bar, a condenser, a nitrogen inlet and a bubble counter and the whole apparatus was evacuated, heated and set under nitrogen. 5.00 g (0.023 mol) DOPO were added to the flask and dissolved in 15 mL of dry DMAc at 50-60 °C. A

second three-necked round-bottomed flask was equipped with a stir bar, a condenser, a dropping funnel, a nitrogen inlet and a bubble counter and the whole apparatus was evacuated, heated and set under nitrogen atmosphere three times. 4.80 g (0.023 mol) zinc acrylate were added to the second flask and dissolved in 15 mL DMAc. The acrylate solution was heated to 80 °C and the DOPO solution was transferred to the dropping funnel. The DOPO solution was added dropwise over 20 min while the temperature was raised to 100 °C. It was stirred at 100 °C for 30 min, then at 85 °C for 30 min. It was allowed to cool down to 70 °C and a solution of 2.65 g (0.023 mol) HEAA in 10 mL DMAc was added. 2.3 mL AIBN solution (0.2 M in toluene) were added dropwise and it was allowed to react for 2 h. When a white solid started to precipitate during the reaction time, 10 mL of DMAc were added for better stir-ability. The precipitate was gathered and washed with DMAc and THF. It was dried at 180 °C under vacuum while stirring.

Yield: 5.68 g ≡ 46 %.

IR (ATR) ν (cm^{-1}): 3278 (w, br), 2927 (w, br), 1722 (w), 1550 (st), 1412 (st), 1197 (m, br), 1119 (m), 1057 (st), 913 (m), 833 (m), 756 (st), 718 (m), 595 (m), 520 (st).

Table of Figures

Bibliography

1. **B. Rosenau**, *Kunststoffe International*, 2007, 10, 66-70.
2. **M. Scheibitz, R. Kaneko and P. Spies**, *Kunststoffe International*, 2016, 10, 40-44.
3. **R. J. Palmer**, in *Encyclopedia of Polymer Science and Technology*, 2001, pp. 618-642.
4. **GDV**, *Schäden je Gefahr*, https://www.gdv.de/de/zahlen-und-fakten/versicherungsbereiche/hausrat-24100#Schaeden, Accessed 06.06.2018.
5. **Statistisches Bundesamt**, *Todesursachen in Deutschland 2015*, 2017, 12, 4.
6. **I. f. S. u. Schadenforschung**, *Ursachenstatistik Brandschäden 2017*, https://www.ifs-ev.org/schadenverhuetung/ursachstatistiken/brandursachenstatistik/, Accessed 06.06.2018.
7. **E. D. Weil and S. V. Levchik**, in *Flame Retardants for Plastics and Textiles*, Carl Hanser Verlag GmbH & Co. KG, 2009, pp. 85-104.
8. **Umweltforschungsplan des Bundesministers für Umwelt, Naturschutz und Reaktorsicherheit**, *Erarbeitung von Bewertungsgrundlagen zur Substitution umweltrelevanter Flammschutzmittel*, 2000, Forschungsbericht 204 08 542 (alt) 297 44 542 (neu)
9. **R. J. Law, C. R. Allchin, J. de Boer, A. Covaci, D. Herzke, P. Lepom, S. Morris, J. Tronczynski and C. A. de Wit**, *Chemosphere*, 2006, 64, 187-208.
10. **C. A. de Wit**, *Chemosphere*, 2002, 46, 583-624.
11. **S. V. Levchik and E. D. Weil**, *Polym. Int.*, 2005, 54, 11-35.
12. **D. Chen, R. C. Hale and R. J. Letcher**, *Environ. Toxicol. Chem.*, 2015, 34, 687-699.
13. **P. A. Behnisch, K. Hosoe and S.-i. Sakai**, *Environment International*, 2001, 27, 495-519.
14. **P. D. Noyes, D. E. Haggard, G. D. Gonnerman and R. L. Tanguay**, *Toxicol. Sci.*, 2015, 145, 177-195.
15. **C. Hirsch, B. Striegl, S. Mathes, C. Adlhart, M. Edelmann, E. Bono, S. Gaan, K. A. Salmeia, L. Hoelting, A. Krebs, J. Nyffeler, R. Pape, A. Burkle, M. Leist, P. Wick and S. Schildknecht**, *Arch. Toxicol.*, 2017, 91, 407-425.
16. **M. Rakotomalala, S. Wagner and M. Doering**, *Materials*, 2010, 3, 4300-4327.
17. **B. Lanska, L. Matisova-Rychla and J. Rychly**, *Polym. Degrad. Stab.*, 2005, 89, 534-544.
18. **K. Marchildon**, *Macromolecular Reaction Engineering*, 2011, 5, 22-54.
19. **W. Keim**, *Kunststoffe*, Wiley-VCH, Weinheim, 2006.
20. **W. Carothers**, *DuPont*, United States, 1937, US2071253.
21. **I. n. named**, Germany, 1938, DE748253.
22. **H. Vogler**, *Chem. Unserer Zeit*, 2013, 47, 62-63.
23. **W. H. Carothers**, 1938, US2130948.
24. **G. B. Taylor**, 1944, US2361717.
25. **J. A. Carter**, 1969, GB1143258.
26. **H. Scholten and G. Marey**, 1972, DE2044105A.
27. **B. Tieke**, *Makromolekulare Chemie: Eine Einführung*, Wiley, 2012.
28. **H. G. Elias**, *Makromoleküle: Anwendungen von Polymeren*, Wiley, 2009.
29. **N. A. Jones, E. D. T. Atkins and M. J. Hill**, *Macromolecules*, 2000, 33, 2642-2650.
30. **S. V. Levchik, E. D. Weil and M. Lewin**, *Polym. Int.*, 1999, 48, 532-557.
31. **H. J. Duessel, H. Rosen and D. O. Hummel**, *Makromol. Chem.*, 1976, 177, 2343-2368.
32. **E. Braun and B. C. Levin**, *Fire Mater.*, 1987, 11, 71-88.
33. **S. V. Levchik, L. Costa and G. Camino**, *Polym. Degrad. Stab.*, 1992, 36, 229-237.
34. **D. D. Steppan, M. F. Doherty and M. F. Malone**, *J. Appl. Polym. Sci.*, 1991, 42, 1009-1021.
35. **S. V. Levchik, L. Costa and G. Camino**, *Polym. Degrad. Stab.*, 1994, 43, 43-54.
36. **F. Wiloth**, *Makromol. Chem.*, 1971, 144, 283-307.
37. **F. Wiloth and E. Schindler**, *Chem. Ber.*, 1970, 103, 757-765.
38. **Y. Yoshizawa, H. Saito and K. Nukada**, *J. Polym. Sci., Part B*, 1972, 10, 145-151.
39. **P. R. Hornsby, J. Wang, R. Rothon, G. Jackson, G. Wilkinson and K. Cossick**, *Polym. Degrad. Stab.*, 1996, 51, 235-249.
40. **K. B. Gilleo**, *Ind. Eng. Chem., Prod. Res. Develop.*, 1974, 13, 139-143.

41. **S. V. Levchik and E. D. Weil**, *Polym. Int.*, 2000, 49, 1033-1073.
42. **T. R. Hull and A. A. Stec**, in *Fire Retardancy of Polymers: New Strategies and Mechanisms*, eds. T. R. Hull and B. K. Kandola, The Royal Society of Chemistry, 2009, pp. 1-14.
43. **M. Lewin**, in *Fire Retardancy of Polymers*, eds. G. Camino, S. Bourbigot and R. Delobel, Woodhead Publishing, 1998, pp. 3-32.
44. **C. Klinkowski, B. Burk, F. Bärmann and M. Döring**, *Chemie in unserer Zeit*, 2015, n/a-n/a.
45. **S. Bourbigot and M. Le Bras**, in *Plastics Flammability Handbook*, Carl Hanser Verlag GmbH & Co. KG, 2004, pp. 133-172.
46. **J. W. Hastie**, *J. Res. Nat. Bur. Stand., Sect. A*, 1973, 77, 733-754.
47. **G. F. Levchik, S. V. Levchik, G. Camino and E. D. Weil**, in *Fire Retardancy of Polymers*, Woodhead Publishing, 1998, pp. 304-315.
48. **G. Camino and R. Delobel**, in *Fire Retardancy of Polymeric Materials*, eds. A. F. Grand and C. A. Wilkie, CRC Press, 2000, pp. 217-244.
49. **G. Camino and M. P. Luda**, in *Fire Retardancy of Polymers*, Woodhead Publishing, 1998, pp. 48-63.
50. **W. E. Horn**, in *Fire Retardancy of Polymeric Materials*, eds. A. F. Grand and C. A. Wilkie, CRC Press, 2000, pp. 285-352.
51. **B. Schartel**, *Materials*, 2010, 3, 4710-4745.
52. **U. Braun, A. I. Balabanovich, B. Schartel, U. Knoll, J. Artner, M. Ciesielski, M. Doering, R. Perez, J. K. W. Sandler, V. Altstaedt, T. Hoffmann and D. Pospiech**, *Polymer*, 2006, 47, 8495-8508.
53. **M. Lewin and E. D. Weil**, in *Fire Retardant Materials*, Woodhead Publishing, 2001, pp. 31-68.
54. **S. V. Levchik**, in *Flame Retardant Polymer Nanocomposites*, John Wiley & Sons, Inc., 2006, pp. 1-29.
55. **J. Green**, in *Fire Retardancy of Polymeric Materials*, eds. A. F. Grand and C. A. Wilkie, CRC Press, 2000, pp. 147-170.
56. **A. K. Salmeia, J. Fage, S. Liang and S. Gaan**, *Polymers*, 2015, 7.
57. **S. Bodrero**, *Makromol. Chem., Macromol. Symp.*, 1993, 74, 137-145.
58. **B. Schartel, R. Kunze and D. Neubert**, *J. Appl. Polym. Sci.*, 2002, 83, 2060-2071.
59. **U. Braun, H. Bahr and B. Schartel**, *e-Polym.*, 2010, 10, 443-456.
60. **R. V. Kasowski and M. M. Martens**, 1998, WO9845364A1.
61. **S. V. Levchik, G. F. Levchik, A. I. Balbanovich, G. Camino and L. Costa**, *Polym. Degrad. Stab.*, 1996, 54, 217-222.
62. **S. Noetzel and W. Herwig**, 1976, DE2447727A1.
63. **W. Racky, H. J. Kleiner and W. Herwig**, 1974, DE2252258A1.
64. **H.-J. Kleiner, W. Budzinsky and G. Kirsch**, 1997, EP792912A2.
65. **E. Jenewein, H.-J. Kleiner, W. Wanzke and W. Budzinsky**, 1997, DE19614424A1.
66. **H.-J. Kleiner and W. Budzinsky**, 1998, DE19708726A1.
67. **S. Costanzi and M. Leonardi**, 2005, WO2005075566A1.
68. **Q. Li, B. Li, S. Zhang and M. Lin**, *Journal of Applied Polymer Science*, 2012, 125, 1782-1789.
69. **B. Zhao, L. Chen, J.-W. Long, H.-B. Chen and Y.-Z. Wang**, *Industrial & Engineering Chemistry Research*, 2013, 52, 2875-2886.
70. **R. Borms and P. Georlette**, *Kunststoffe*, 2004, 94, 256-260.
71. **T. Koeppl, S. Brehme, D. Pospiech, O. Fischer, F. Wolff-Fabris, V. Altstaedt, B. Schartel and M. Doering**, *J. Appl. Polym. Sci.*, 2013, 128, 3315-3324.
72. **D. Pospiech, L. Haeussler, A. Korwitz, O. Fischer, S. Starke, D. Jehnichen, T. Koeppl and V. Altstaedt**, *High Perform. Polym.*, 2012, 24, 64-73.
73. **J. Troitzsch**, in *Advances in Fire Retardant Materials*, eds. A. R. Horrocks and D. Price, Woodhead Publishing, 2008, pp. 291-330.
74. in *Fire hazard testing - Part 11-10: Test flames - 50 W horizontal and vertical flame test methods*, 2004-05.

75. **Y. Wang, F. Zhang, X. Chen, Y. Jin and J. Zhang**, *Fire Mater.*, 2010, 34, 203-215.
76. **J.-L. Montchamp**, *Acc. Chem. Res.*, 2014, 47, 77-87.
77. **J. Stawinski and A. Kraszewski**, *Acc. Chem. Res.*, 2002, 35, 952-960.
78. **K. D. Troev**, in *Chemistry and Application of H-Phosphonates*, Elsevier Science Ltd, Amsterdam, 2006, pp. 11-22.
79. **R. Withnall and L. Andrews**, *The Journal of Physical Chemistry*, 1987, 91, 784-797.
80. **D. Yakhvarov, M. Caporali, L. Gonsalvi, S. Latypov, V. Mirabello, I. Rizvanov, O. Sinyashin, P. Stoppioni and M. Peruzzini**, *Angewandte Chemie International Edition*, 2011, 50, 5370-5373.
81. **K. D. Troev**, in *Chemistry and Application of H-Phosphonates*, Elsevier Science Ltd, Amsterdam, 2006, pp. 23-105.
82. **F. H. Westheimer**, *Science (Washington, D. C., 1883-)*, 1987, 235, 1173-1178.
83. **M. Diez-Castellnou, A. Martinez and F. Mancin**, in *Advances in Physical Organic Chemistry*, eds. I. H. Williams and N. H. Williams, Academic Press, 2017, pp. 129-186.
84. **W. Vogt and S. Balasubramanian**, *Die Makromolekulare Chemie*, 1973, 163, 111-134.
85. **J. Jankowska, M. Sobkowski, J. Stawiński and A. Kraszewski**, *Tetrahedron Letters*, 1994, 35, 3355-3358.
86. **F. H. Westheimer, S. Huang and F. Covitz**, *J. Am. Chem. Soc.*, 1988, 110, 181-185.
87. **P. J. Murphy**, *Organophosphorus Reagents: A Practical Approach in Chemistry*, Oxford University Press, 2004.
88. **K. D. Troev**, in *Reactivity of P-H Group of Phosphorus Based Compounds*, ed. K. D. Troev, Academic Press, 2018, pp. 291-409.
89. **D. Enders, A. Saint-Dizier, M.-I. Lannou and A. Lenzen**, *European Journal of Organic Chemistry*, 2006, 2006, 29-49.
90. **A. V. Salin**, *Phosphorus, Sulfur, and Silicon and the Related Elements*, 2016, 191, 1625-1627.
91. **A. A. Sobanov, I. V. Bakhtiyarova, M. G. Zimin and A. N. Pudovik**, *Zh. Obshch. Khim.*, 1986, 56, 711.
92. **R. K. Haynes, W. W. L. Lam and L.-L. Yeung**, *Tetrahedron Lett.*, 1996, 37, 4729-4732.
93. **W. Zhao, J. Li and Q. Yan**, 2013, CN103044485A.
94. **S. Chai, J. Li, G. Xu and J. Han**, 2011, CN102050835A.
95. **N. Qi, N. Zhang, S. R. Allu, J. Gao, J. Guo and Y. He**, *Organic Letters*, 2016, 18, 6204-6207.
96. **F. Wang, R. Tang, J. L. F. Kao, S. D. Dingman and W. E. Buhro**, *Journal of the American Chemical Society*, 2009, 131, 4983-4994.
97. **W.-L. Lee, L.-C. Liu, C.-M. Chen and J.-S. Lin**, *Polym. Adv. Technol.*, 2014, 25, 36-40.
98. **É. Záhonyi-Budó and L. I. Simándi**, *Inorganica Chimica Acta*, 1993, 205, 207-212.
99. **F. R. Atherton, H. T. Openshaw and A. R. Todd**, *Journal of the Chemical Society (Resumed)*, 1945, 660-663.
100. **S. S. Le Corre, M. Berchel, H. Couthon-Gourvès, J.-P. Haelters and P.-A. Jaffrès**, *Beilstein Journal of Organic Chemistry*, 2014, 10, 1166-1196.
101. **G. M. Steinberg**, *The Journal of Organic Chemistry*, 1950, 15, 637-647.
102. **V. I. Krutikov, A. V. Erkin and V. V. Krutikova**, *Russian Journal of General Chemistry*, 2012, 82, 822-826.
103. **K. Anne and E. Robert**, *Bulletin of the Chemical Society of Japan*, 1985, 58, 3671-3672.
104. **L. P. Reiff and H. S. Aaron**, *Journal of the American Chemical Society*, 1970, 92, 5275-5276.
105. **W. Stec and M. Mikołajczyk**, *Tetrahedron*, 1973, 29, 539-546.
106. **Y. Zhou, G. Wang, Y. Saga, R. Shen, M. Goto, Y. Zhao and L.-B. Han**, *The Journal of Organic Chemistry*, 2010, 75, 7924-7927.
107. **G. Wang, R. Shen, Q. Xu, M. Goto, Y. Zhao and L.-B. Han**, *The Journal of Organic Chemistry*, 2010, 75, 3890-3892.
108. **B. Kaboudin, A. Donyavi and F. Kazemi**, *Synthesis*, 2018, 50, 170-174.

109. **B. A. Trofimov, N. K. Gusarova, P. A. Volkov, N. I. Ivanova and K. O. Khrapova**, *Heteroatom Chemistry*, 2016, 27, 44-47.
110. **E. S. Blake, W. C. Hammann, J. W. Edwards, T. E. Reichard and M. R. Ort**, *J. Chem. Eng. Data*, 1961, 6, 87-98.
111. **B. Schartel, A. I. Balabanovich, U. Braun, U. Knoll, J. Artner, M. Ciesielski, M. Doering, R. Perez, J. K. W. Sandler, V. Altstaedt, T. Hoffmann and D. Pospiech**, *J. Appl. Polym. Sci.*, 2007, 104, 2260-2269.
112. **R. M. Perez, J. K. W. Sandler, V. Altstädt, T. Hoffmann, D. Pospiech, M. Ciesielski and M. Döring**, *Journal of Materials Science*, 2006, 41, 341-353.
113. **C. Klinkowski, L. Zang and M. Döring**, *Materials China*, 2013, 32, 144-158.
114. **K. A. Salmeia and S. Gaan**, *Polym. Degrad. Stab.*, 2015, 113, 119-134.
115. **T. Saito**, 1972, US3702878A.
116. **Y. Bykov, S. Wagner, O. Walter, M. Doering, O. Fischer, D. Pospiech, T. Koeppl and V. Altstaedt**, *Heteroat. Chem.*, 2012, 23, 146-153.
117. **B. Burk**, *Entwicklung neuer Flammschutzmittel basierend auf Derivaten des 9,10-Dihydro-10-oxaphosphaphenanthren-10-oxids*, Ruprecht-Karls-University Heidelberg, PhD, 2016.
118. **M. Ciesielski, J. Diederichs, M. Döring and A. Schäfer**, in *Fire and Polymers V Materials and Concepts for Fire Retardancy*, eds. C. A. Wilkie, G. L. Nelson and A. B. Morgan, ACS, Washington, DC, USA, 2009, pp. 174-190.
119. **A. Schaefer, S. Seibold, W. Lohstroh, O. Walter and M. Doering**, *J. Appl. Polym. Sci.*, 2007, 105, 685-696.
120. **A. Schäfer**, *Gasphasenaktive phosphacyclische Flammschutzmittel und deren Wirkmechanismen*, Ruprecht-Karls-University Heidelberg, PhD, 2008.
121. **M. Doering, C. Kollann, U. Storzer, M. Ciesielski, U. Dittrich, B. Just, H. Keller, K. Heinemann and E. Meusel**, *Proc. Conf. Recent Adv. Flame Retard. Polym. Mater.*, 2005, 16, 83-92.
122. **H. Kamata, H. Li, H. Kofune, K. Takahashi and T. Okabe**, 2009, JP2009035597A.
123. **M. Moreno, G. Lligadas, J. C. Ronda, M. Galia and V. Caldiz**, *J. Polym. Sci., Part A: Polym. Chem.*, 2012, 50, 3206-3213.
124. **O. Fischer, D. Pospiech, A. Korwitz, K. Sahre, L. Haeussler, P. Friedel, D. Fischer, C. Harnisch, Y. Bykov and M. Doering**, *Polym. Degrad. Stab.*, 2011, 96, 2198-2208.
125. **H. C. Fisher, L. Prost and J. L. Montchamp**, *European Journal of Organic Chemistry*, 2013, 2013, 7973-7978.
126. **J.-L. Montchamp and H. C. Fisher**, 2014, US20140303394A1.
127. **S. Carroccio, C. Puglisi, G. Scaltro, T. Ferreri and G. Montaudo**, *Eur. J. Mass Spectrom.*, 2007, 13, 397-408.
128. **C. H. Do, E. M. Pearce, B. J. Bulkin and H. K. Reimschuessel**, *J. Polym. Sci., Part A: Polym. Chem.*, 1987, 25, 2409-2424.
129. **T. Karstens and V. Rossbach**, *Makromol. Chem.*, 1989, 190, 3033-3053.
130. **B. Lanska**, *Polym. Degrad. Stab.*, 1996, 53, 89-98.
131. **B. Lanska and J. Hauer**, *Polym. Degrad. Stab.*, 1997, 56, 149-155.
132. **P. Cerruti, J. Rychly, L. Matisova-Rychla and C. Carfagna**, *Polym. Degrad. Stab.*, 2004, 84, 199-206.
133. **K. Janssen, P. Gijsman and D. Tummers**, *Polym. Degrad. Stab.*, 1995, 49, 127-133.
134. **P. Cerruti and C. Carfagna**, *Polymer Degradation and Stability*, 2010, 95, 2405-2412.
135. **S. Jeol and T. Badel**, 2012, FR2974095A1.
136. **R. J. Palmer and M. M. Martens**, 2010, WO2010014810A1.
137. **U. Zucchelli**, 2013, WO2013045966A1.
138. **R. J. Palmer and T. Kobayashi**, 2016, EP2307480B1.
139. **R. J. Palmer, J. A. Peacock and G. Topoulos**, 2010, WO2010014801A1.
140. **T. Yu**, 2012, WO2012064965A2.
141. **J. Endtner and M. Bienmüller**, *L. D. GmbH*, Germany, 2016, EO3034553A1.

142. **M. Wang, J. Xu, H. Wu and S. Guo**, *Polymer Degradation and Stability*, 2006, 91, 2101-2109.
143. **M. Wang, X. Song, J. Jiang, J. Xia, S. Li and M. Li**, *Thermochim. Acta*, 2017, 658, 84-92.
144. **S. Xu, D. Li, X. Yu, Y. Zhang, Y. Yu, M. Zhou and S. Tang**, *Journal of Applied Polymer Science*, 2012, 126, 569-574.
145. **L. Xie, D. Li, M. Fu, J. Zhang, L. Zhang, Y. Zhang and P. Zhao**, *Journal of Vinyl and Additive Technology*, 2017, 23, 55-61.
146. **P. Cazuc**, *Reinforced Plastics*, 2016, 60, 376-379.
147. **G. P. Kozielski, C. Y. Lee, J. L. Thompson and S. Mok**, *Annu. Tech. Conf. Soc. Plast. Eng.*, 2011, 69th, 170-175.
148. **M. Sicken, N. Weferling and H.-P. Schmitz**, *Clariant*, 2003, US20030216533.
149. **M. Sicken, W. Krause, N. Weferling and H.-P. Schmitz**, Germany, 2004, DE10309570B3.
150. **L. Wang, T. Zhang, H. Yan, M. Peng and Z. Fang**, *J. Appl. Polym. Sci.*, 2013, 129, 2986-2997.
151. **B. Just, U. Dittrich, H. Keller, M. Doering, M. Ahlmann and U. Storzer**, 2006, DE102004049614A1.
152. **S. V. Levchik and E. D. Weil**, *J. Fire Sci.*, 2006, 24, 345-364.
153. **M. Roth, K. Uske and C. Minges**, 2014, WO2014170148A1.
154. **T. Saito and H. Ohishi**, 1981, US4280951A.
155. **S. Inoue, M. Kobayashi and T. Tozuka**, *J. Organomet. Chem.*, 1974, 81, 17-21.
156. **J. Skorsepa, E. Godocikova and J. Cernak**, *J. Therm. Anal. Calorim.*, 2004, 75, 773-780.
157. **Z. Zhang, H. Suo, L. Ma, M. Liu, T. Zhang and M. Zhou**, *IEEE Trans. Appl. Supercond.*, 2010, 20, 1605-1609.
158. **M. Leistner**, *Phosphorhaltige Triazinverbindungen als Flammschutzmittel für Thermoplaste*, Technichal University Darmstadt, PhD, 2013.
159. **E. Schlosser, B. Nass and W. Wanzke**, 2001, EP1070754A2.
160. **U. Zucchelli**, 2013, WO2013045965A1.
161. **H. Fan, P. Zhang, Y. Chen, J. Yan, S. Tian and B. Shi**, 2015, CN105085575A.
162. **T. C. Chang, W. Y. Shen, Y. S. Chiu, H. B. Chen and S. Y. Ho**, *Journal of Polymer Research*, 1994, 1, 353-359.
163. **J. Paul and T. M. Svetlana**, *Polymers for Advanced Technologies*, 2011, 22, 395-406.
164. **L. Qiang‐Lin, W. Xiu‐Li, W. De‐Yi, X. Wei‐Cheng, Z. Guang‐Hong and W. Yu‐Zhong**, *Journal of Applied Polymer Science*, 2010, 117, 3066-3074.
165. **P. Müller**, *Mehrfunktionelle phosphorhaltige Flammschutzmittel für Epoxidharze*, Ruprecht-Karls-University Heidelberg, PhD, 2013.
166. **B. M. Trost**, *Science*, 1991, 254, 1471.
167. **R. A. Sheldon, I. Arends and U. Hanefeld**, *Green Chemistry and Catalysis*, Wiley-VCH, Weinheim, 2007.
168. **C. D. Schmiedl**, *Atomefficient Phosphorylation of Alcohols*, Technische Universität Darmstadt, Master, 2016.
169. **K. Ogemark and K. Sörensen**, 1996, WO1996034042A1.
170. **M. Vannini, P. Marchese, A. Celli, C. Marega, A. Marigo and C. Lorenzetti**, *Journal of Applied Polymer Science*, 2015, 132, n/a-n/a.
171. **L. Ree, M. A. Kelland, D. Haddleton and F. Alsubaie**, *Energy Fuels*, 2017, 31, 1355-1361.
172. **A. Gomez-Valdemoro, M. Trigo, S. Ibeas, F. C. Garcia, F. Serna and J. M. Garcia**, *J. Polym. Sci., Part A: Polym. Chem.*, 2011, 49, 3817-3825.
173. **M. Xiao, E. Gonzalez, A. M. Monterroza and M. Frey**, *Carbohydr. Polym.*, 2017, 174, 626-632.
174. **Y. Nishikawa and T. Matsumoto**, 2018, JP2018009137A.
175. **Y. Zhang, D. Chu, M. Zheng, T. Kissel and S. Agarwal**, *Polymer Chemistry*, 2012, 3, 2752-2759.
176. **J. Kizhakkedathu, D. Lange, J. Lo, Y. Mei and K. Yu**, 2016, WO2016187698A1.

177. **D. Zhang, Y. Fu, L. Huang, Y. Zhang, B. Ren, M. Zhong, J. Yang and J. Zheng**, *J. Mater. Chem. B*, 2018, 6, 950-960.
178. **X. Qin, K. Chen, L. Cao, Y. Zhang, L. Li and X. Guo**, *Colloids Surf., B*, 2017, 155, 408-414.
179. **S. B. Rodrigues, F. M. Collares, V. C. B. Leitune, L. F. J. Schneider, F. A. Ogliari, C. L. Petzhold and S. M. W. Samuel**, *Dental Materials*, 2015, 31, 1579-1586.
180. **K. Mahdhaoui, B. Fournier and M. A. Derbanne**, *Dental Materials*, 2017, 33, 743-751.
181. **A. Alli and A. Guzman**, 2018, US20180009922A1.
182. **H. Chen, Y. Liu, B. Ren, Y. Zhang, J. Ma, L. Xu, Q. Chen and J. Zheng**, *Adv. Funct. Mater.*, 2017, 27, n/a.
183. **P. Pissis and A. Kyritsis**, *J. Polym. Sci., Part B: Polym. Phys.*, 2013, 51, 159-175.
184. **M. R. Romero, A. Wolfel and C. I. Alvarez Igarzabal**, *Sens. Actuators, B*, 2016, 234, 53-62.
185. **J. Kopecek**, *Journal of Polymer Science Part A: Polymer Chemistry*, 2009, 47, 5929-5946.
186. **D. Goedderz**, *Synthesis of P- and S-containing flame retardants for PET applications*, Technische Universität Darmstadt, Master, 2016.
187. **S. N. Guntari, A. C. H. Khin, E. H. H. Wong, T. K. Goh, A. Blencowe, F. Caruso and G. G. Qiao**, *Adv. Funct. Mater.*, 2013, 23, 5159-5166.
188. **B. Plage, H. R. Schulten, J. Schneider and H. Ringsdorf**, *Macromolecules*, 1990, 23, 3417-3422.
189. **S. Chen, T. Hu, Y. Tian, L. Chen and J. A. Pojman**, *Journal of Polymer Science Part A: Polymer Chemistry*, 2007, 45, 873-881.
190. **E. Vargün and A. Usanmaz**, *Journal of Polymer Science Part A: Polymer Chemistry*, 2005, 43, 3957-3965.
191. **A. Buczko, T. Stelzig, L. Bommer, D. Rentsch, M. Heneczkowski and S. Gaan**, *Polym. Degrad. Stab.*, 2014, 107, 158-165.
192. **S. Huo, J. Wang, S. Yang, J. Wang, B. Zhang, B. Zhang, X. Chen and Y. Tang**, *Polym. Degrad. Stab.*, 2016, 131, 106-113.
193. **S. Yang, J. Wang, S. Huo, M. Wang and L. Cheng**, *Ind. Eng. Chem. Res.*, 2015, 54, 7777-7786.
194. **H. Mispreuve, R. Näscher, S. Gaan, M. Neisius, P. Mercoli and S. Liang**, 2014, EP2557085 B1.
195. **V. Lehr**, *Dehydratisierung von Glycerol zu Acrolein*, Technische Universität Darmstadt, PhD, 2008.
196. **L. Liu, H.-m. Chang, H. Jameel, J.-Y. Park and S. Park**, *Ind. Eng. Chem. Res.*, 2017, 56, 14447-14453.
197. **X.-n. Ye, Q. Lu, X. Wang, H.-q. Guo, M.-s. Cui, C.-q. Dong and Y.-p. Yang**, *ACS Sustainable Chem. Eng.*, 2017, 5, 10815-10825.
198. **S. Eminov, P. Filippousi, A. Brandt, J. D. E. T. Wilton-Ely and J. P. Hallett**, *Inorganics*, 2016, 4, 32/31-32/15.
199. **O. Pamies and J. E. Baeckvall**, *J. Org. Chem.*, 2003, 68, 4815-4818.
200. **V. I. Volodina, A. I. Tarasov and S. S. Spasskii**, *Russian Chemical Reviews*, 1970, 39, 140-155.
201. **R. C. Laible**, *Chem. Rev. (Washington, DC, U. S.)*, 1958, 58, 807-843.
202. **O. Berger, L. Gavara and J.-L. Montchamp**, *Org. Lett.*, 2012, 14, 3404-3407.
203. **X. Wang, Y. Hu, L. Song, H. Yang, W. Xing and H. Lu**, *Prog. Org. Coat.*, 2011, 71, 72-82.
204. **G. Piancatelli, M. D'Auria and F. D'Onofrio**, *Synthesis*, 1994, 1994, 867-889.
205. **C. H. Issidorides and R. Gulen**, *Organic Syntheses*, 1958, 38, 65.

16.12.2019

Erklärung

Ich erkläre hiermit, dass ich meine Dissertation selbstständig und nur mit den angegebenen Hilfsmitteln angefertigt und noch keinen Promotionsversuch unternommen habe.

Kim Garth

16.12.2019

Erklärung der Übereinstimmung

Ich erkläre hiermit, dass die elektronische Version der Doktorarbeit mit der schriftlichen Version übereinstimmt. Die elektronische Version liegt dem Prüfungssekretariat vor.

Kim Garth